THE UNIVERSITY OF ALBERTA

THE POSSIBILITY OF USING ELECTROMAGNETIC ANGULAR MOMENTUM TO STABILIZE A SPACE VEHICLE

by

FREDERICK STEPHEN CHUTE

A THESIS

SUBMITTED TO THE FACULTY OF GRADUATE STUDIES

IN PARTIAL FULFILMENT OF THE REQUIREMENTS FOR THE DEGREE

OF DOCTOR OF PHILOSOPHY

DEPARTMENT OF ELECTRICAL ENGINEERING

EDMONTON, ALBERTA

DATE...14..Jan..66.

UNIVERSITY OF ALBERTA

FACULTY OF GRADUATE STUDIES

The undersigned certify that they have read, and recommend to the Faculty of Graduate Studies for acceptance, a thesis entitled "The Possibility of Using Electromagnetic Angular Momentum to Stabilize a Space Vehicle" submitted by Frederick Stephen Chute in partial fulfilment of the requirements for the degree of Doctor of Philosophy.

ABSTRACT

A brief review of the conservation of momentum in electromagnetic theory is given. It is shown that a reaction torque exists on an antenna that radiates a net angular momentum, and that this torque can be large enough to provide a means of applying controlling torques to a space vehicle. A number of antenna configurations are considered and it is shown that a turnstile type of antenna is most appropriate for a space application.

The reaction torque was successfully demonstrated using a form of loop antenna suspended over a large artificial earth system. The antenna consisted of two loops at right angles fed in phase quadrature. The loop diameter was 2 meters and the operating frequency, 14 Mc/s. The torque was measured by means of a calibrated suspension and agreement with theory was obtained to within experimental error.

ACKNOWLEDGEMENT

I wish to express my deep appreciation to Dr. G. B. Walker for his constant encouragement and support and for all his efforts on my behalf throughout the course of this work.

I would also like to thank Mr. L. Bice, Mr. E. Buck, Mr. N. Burtch, and the technical staff of the Electrical Engineering Department, University of Alberta for their unfailing cooperation. Special thanks is due Mr. S. Hardy for his able assistance during the experimental work associated with this project.

In addition I would like to acknowledge the special equipment made available for the project by the Royal Canadian Air Force, The Department of Transport, Cowley Brothers Electronics, The Alberta Research Council, and the City of Edmonton Electrical Distribution System.

To my wife,Dianne, my most sincere thanks for her patience and moral support during my postgraduate years.

I should like to express grateful acknowledgement to the National Research Council for Studentships awarded in 1963, 1964, and 1965

TABLE OF CONTENTS

LIST OF ILLUSTRATIONS

LIST OF SYMBOLS

ψ ..... density of stored electromagnetic energy

η ..... characteristic impedance of free space

ω ..... angular frequency

λ ..... wavelength

ε ..... permittivity of free space

μ ..... permeability of free space

ρ ..... density of free charge

J ..... current density

$\mu\mu$fd ..... micromicrofarads

μh ..... microhenries

k ..... wave number $2\pi/\lambda$

$\vec{i}_r, \vec{i}_\theta, \vec{i}_\phi$ ... unit vectors of a system of spherical coordinates

$\vec{E}$ ..... electric field intensity

$\vec{H}$ ..... magnetic field intensity

$\vec{D}$ ..... electric displacement

$\vec{B}$ ..... magnetic induction

$\vec{a} \times \vec{b}$ ..... vector cross product

$\vec{a} \cdot \vec{b}$ ..... vector dot product

$\vec{a}^*$ ..... complex conjugate of a

Re ..... real part of

T ..... torque

I ..... current

P ..... power

THE POSSIBILITY OF USING ELECTROMAGNETIC ANGULAR MOMENTUM TO STABILIZE A SPACE VEHICLE

1. INTRODUCTION

1.1 Historical Development of the Concept of Electromagnetic Momentum.

Nearly two centuries prior to the development of classical electromagnetism men of science had associated momentum with radiant energy. Light, they maintained, was a corpuscular phenomenum and must possess mechanical momentum. They believed that a powerful beam of light would cause a delicately suspended body to move. In 1708, Homberg[1] claimed to have observed this motion but in view of later experiments it is likely the force he measured resulted from heating effects in the surrounding air rather than from an actual transfer of momentum from the light beam.

Several unsuccessful attempts to establish the existence of this radiation pressure followed. In 1746, J. J. deMairan[2], essentially repeating Homberg's work, was unable to measure any force. A. Bennet[3], in 1792, focused light on a piece of writing paper suspended in an evacuated chamber but could not establish an effect distinguishable from that produced by heating.

Eighty-one years later J. C. Maxwell showed, from his electromagnetic theory of light, that a beam of radiation falling normally on a flat surface would give rise to a pressure equal in magnitude to the electromagnetic energy density at the surface. Then, Peter Lebedew[4], in 1899, and E. F. Nichols and G. F. Hull[5], in 1901, in a series of delicate experiments gave the first reliable demonstrations of the reality of the pressure of radiation, and were able to verify quantitatively Maxwell's theoretical result.

N. Carrara and P. Lombardini[6], in 1949, demonstrated the existence of radiation pressure at microwave frequencies. The first practical use of radiation pressure was made by A. L. Cullen[7], in 1952. He and his associates developed an instrument that measured the power in a wave-guide system by measuring the force on a suitably placed metallic vane.

Early workers felt that, using a beam of circularly polarized radiation, it should be possible to produce a torque, as well as a pressure of radiation, on a material body. The existence of such a torque was first predicted by A. Sadowsky,[8] in 1899, and later by J. H. Poynting[9] and Epstein[10]. In 1935, R. A. Beth[11] succeeded in measuring this torque by passing a beam of light through a doubly refracting plate which changed the state of polarization of the radiation.

At this point it is appropriate to note that these mechanical reactions had been predicted without ever associating momentum properties with the electromagnetic field. Momentum effects were first linked with electromagnetic phenomena when, in 1891, J. J. Thomson[12] adopted the view that the aether was the vehicle of mechanical momentum of amount S/c^2 per unit volume, where S is Poyntings vector and c is the velocity of light in a vacuum. In the years immediately following, he developed the momentum concept and showed that Newton's Third Law and the Conservation of Momentum applied to electromagnetic problems only if proper account was taken of this aetheral momentum.

In 1900, Poincaré[13], referring to Thomson's momentum expression, suggested that electromagnetic energy might possess mass density such that $E = Mc^2$ where E is the energy, M the mass and c the velocity of light. He remarked that if this were so then a Hertz oscillator radiating predominately in one direction should recoil in the opposite direction, as does a gun when fired.

Gradually the idea of a material aether was abandoned, largely on the results of the Michelson-Morley experiment, and Thomson's aetheral momentum came to be thought of as an intrinsic property of the field itself. Unfortunately this field momentum cannot be subjected to direct measurement and this may be the reason that it is often regarded as a somewhat dubious concept.

1.2 Maxwell's Stress Tensor and the Conservation of Momentum in Vacuum Electrodynamics.

Two of the basic laws in classical physics are; the conservation of energy and the conservation of momentum. The conservation of energy in an electromagnetic system leads to the familiar Poynting relationship.

$$-\int (\vec{E}\times\vec{H})\cdot\vec{n}\, dS = \int \vec{J}\cdot\vec{E}\, dv + \frac{\partial}{\partial t}\int \frac{1}{2}(\vec{E}\cdot\vec{D} + \vec{H}\cdot\vec{B})\, dv \qquad ...1.1$$

The first term on the right hand side represents the Joule heating or the rate at which electromagnetic energy is being converted to heat. The second term is recognized as the rate of increase of the stored energy within the volume. The left hand side may then be interpreted as the total flux of energy, or the power, passing through the closed surface, S.

An analogous relationship can be obtained for the momentum balance in an electromagnetic system. Consider the volume force on a finite but otherwise arbitrary distribution of charge and current in free space.

$$\vec{f} = \rho\vec{E} + \vec{J}\times\vec{B}$$

$$= \vec{E}\,\mathrm{div}\vec{D} - \vec{B}\times\mathrm{curl}\vec{H} - \frac{\partial}{\partial t}(\vec{D}\times\vec{B}) \qquad ...1.2$$

since $\mathrm{curl}\vec{H} = \vec{J} + \frac{\partial\vec{D}}{\partial t}$ and $\mathrm{div}\vec{D} = \rho$,

Now add $\frac{\partial}{\partial t}(\vec{D}\times\vec{B})$ to both sides of equation 1.2.

$$\vec{f} + \frac{\partial}{\partial t}(\vec{D}\times\vec{B}) = \vec{E}\,\mathrm{div}\vec{D} - \vec{B}\times\mathrm{curl}\vec{H} - \vec{D}\times\mathrm{curl}\vec{E} \qquad \ldots 1.3$$

since $\mathrm{curl}\vec{E} = -\frac{\partial}{\partial t}\vec{B}$.

In Appendix I it is shown that:

$$\mathrm{div}M = \vec{E}\,\mathrm{div}\vec{D} - \vec{B}\times\mathrm{curl}\vec{H} - \vec{D}\times\mathrm{curl}\vec{E} \qquad \ldots 1.4$$

where divM is defined as $\frac{\partial M}{\partial x_k}jk\ \vec{i}_j$. M is known as Maxwell's stress tensor and is, in dyadic form,

$$M = \vec{H}\vec{B} + \vec{E}\vec{D} - \frac{1}{2}(\vec{E}\cdot\vec{D} + \vec{H}\cdot\vec{B})U \qquad \ldots 1.5$$

where U is the fundamental tensor whose components are δ_{ik}, the Kronecker delta.

Substituting equation 1.4 in 1.3 gives:

$$\mathrm{div}M = \vec{f} + \frac{\partial}{\partial t}(\vec{D}\times\vec{B}) \qquad \ldots 1.6$$

Integrating both sides of this equation over a volume, v, and converting the divergence integral to the equivalent integral over the closed surface surrounding the volume gives:

$$\int M\cdot\vec{n}\ dS = \int \vec{f}\ dv + \frac{\partial}{\partial t}\int (\vec{D}\times\vec{B})\ dv \qquad \ldots 1.7$$

The similarity between equations 1.7 and 1.1 is readily apparent.

Now let the surface tend to infinity so that it encloses the entire field. The left hand side goes to zero and equation 1.7 becomes,

$$0 = \int \vec{f}\, dv + \frac{\partial}{\partial t} \int (\vec{D}\times\vec{B})\, dv$$

Writing $\vec{f}$ as the time rate of change of mechanical momentum, $\vec{Q}$, gives,

$$0 = \frac{\partial}{\partial t}\left(\int \vec{Q}\, dv + \int (\vec{D}\times\vec{B})\, dv \right) \quad \ldots 1.8$$

Therefore,

$$K = \int \vec{Q}\, dv + \int \vec{D}\times\vec{B}\, dv$$

where K is a constant which may be taken as zero.

The sum, therefore, of the mechanical momentum of the system and this extra term,

$$\int \vec{D}\times\vec{B}\, dv$$

is a quantity that is conserved. This term is interpreted as the electromagnetic momentum stored in the field, on which basis, $\vec{D}\times\vec{B}$ is taken as the momentum density distributed throughout the field. The sum, then, of mechanical and electromagnetic momentum is conserved -- the mechanical momentum itself is not necessarily

conserved. For example, consider the case of two electrons moving at right angles to each other. The forces on the two particles are not equal and opposite, thus seemingly violating Newton's law of action and reaction. However, from above, whenever the total ponderomotive force on a electromagnetic system is not zero, it is equal to the volume integral of $-\frac{\partial}{\partial t}(\vec{D}\times\vec{B})$ over the entire volume where $\vec{D}$ and $\vec{B}$ exist; in other words it is equal to the negative time rate of change of the electromagnetic momentum stored in the system. Newton's Third Law and the Conservation of Momentum are satisfied only when we take into account the mass of the electromagnetic field energy.

Equation 1.7 may now be intepreted in the following manner. The right hand side is the mechanical force, or the rate at which electromagnetic momentum is being converted to mechanical momentum, plus the rate at which electromagnetic momentum is increasing within the volume. The left hand side is then the total inward flux of momentum through the closed surface, S.

The angular momentum with respect to a fixed point, O, of a system of charges and currents can be determined in a similar fashion. Consider the relationship,

$$\vec{r}\times\text{divM} = \vec{r}\times\vec{f} + \frac{\partial}{\partial t}\,\vec{r}\times(\vec{D}\times\vec{B}) \qquad \ldots 1.9$$

where $\vec{r}$ is the radius vector from the origin to the point of interest. Integrating both sides of this expression yields:

$$\int \vec{r}\times\text{divM}\, dv = \int \vec{r}\times\vec{f}\, dv + \frac{\partial}{\partial t}\int \vec{r}\times(\vec{D}\times\vec{B})\, dv$$

However, in Appendix 2 it is shown that,

$$\int \vec{r}\times \mathrm{div}\vec{M}\, dv = \int \vec{r}\times\vec{M}\cdot\vec{n}\, dS \qquad \ldots 1.10$$

where S is the closed surface surrounding the volume in question. Hence

$$\int \vec{r}\times\vec{M}\cdot\vec{n}\, dS = \int \vec{r}\times\vec{f}\, dv + \frac{\partial}{\partial t}\int \vec{r}\times(\vec{D}\times\vec{B})\, dv \qquad \ldots 1.11$$

Equation 1.11 expresses the conservation of angular momentum in an electromagnetic system. The interpretation of this equation is similar to that of equation 1.7. The left hand side is the total inward flux of angular momentum through the closed surface and the term $\vec{r}\times(\vec{D}\times\vec{B})$ is taken as the density of electromagnetic angular momentum in the field.

The evaluation of the angular momentum of an arbitrary system of charges and currents is not as simple as the case of the linear momentum. For example, consider a circularly polarized plane wave. From the expression for the angular momentum of the system,

$$\vec{m} = \int \vec{r}\times(\vec{D}\times\vec{B})\, dv \qquad \ldots 1.12$$

it would seem that this wave could not possess any net angular momentum about the direction of propagation, when $\vec{D}\times\vec{B}$ is parallel to $\vec{r}$. It is, however, an experimental fact that such a wave can exert a torque on a material plate perpendicular to $\vec{r}$.

This apparent paradox may be resolved in the case of a plane wave by accounting for the finite extension of this plate[14]. For a spherical wave, the small radial fields present in the wave zone must be considered in order to obtain a proper accounting of the system's angular momentum. Electromagnetic angular momentum is

perhaps a more subtle effect than electromagnetic linear momentum because it involves second order fields.

Equations 1.7 and 1.11 are most useful in the calculation of forces and torques on arbitrary distributions of charge and current. Since, for steady state conditions the time averages of

$$\frac{\partial}{\partial t}\int (\vec{D}\times\vec{B})\ dv \text{ and } \frac{\partial}{\partial t}\int \vec{r}\times(\vec{D}\times\vec{B})\ dv$$

are zero, the steady state mechanical reactions on the sources within a volume enclosed by the surface, S are given by:

$$\vec{F} = \frac{Re}{2}\int M^{*}\cdot\vec{n}\,dS \qquad \ldots 1.13$$

and

$$\vec{T} = \frac{Re}{2}\int \vec{r}\times M^{*}\cdot\vec{n}\ dS \qquad \ldots 1.14$$

where M^{*} is obtained from M by replacing H by H^{*} and E by E^{*}.

In Appendix 3 it is shown that

$$-M\cdot\vec{i}_r = \frac{\vec{E}\times\vec{H}}{c} + O(r^{-4}) \qquad \ldots 1.15$$

where $O(r^{-n})$ refers to terms vanishing as $1/r^{n}$, $1/r^{n+1}$, $1/r^{n+2}$ ... as r goes to infinity. Integrating both sides of equation 1.15 over a spherical surface yields:

$$\int \mathbf{M}\cdot\vec{n}\, dS = -\frac{1}{c} \int (\vec{E}\times\vec{H})\, dS + O(r^{-2})$$

since $\vec{i}_r = \vec{n}$. As the surface approaches infinity,

$$\int \mathbf{M}\cdot\vec{n}\, dS = -\frac{1}{c} \int (\vec{E}\times\vec{H})\, dS \qquad \ldots 1.16$$

Similarly,

$$\int \vec{r}\times\mathbf{M}\cdot\vec{n}\, dS = -\frac{1}{c} \int \vec{r}\times(\vec{E}\times\vec{H})\, dS \qquad \ldots 1.17$$

Therefore, equations 1.13 and 1.14 for the time average force and the time average torque can be reduced to the following simple expressions:

$$\vec{F} = \frac{-Re}{2c} \int (\vec{E}\times\vec{H}^*)\, dS \qquad \ldots 1.18$$

and

$$\vec{T} = \frac{-Re}{2c} \int \vec{r}\times(\vec{E}\times\vec{H}^*)\, dS \qquad \ldots 1.19$$

where S is a spherical surface tending to infinity.

1.3 The Production of Mechanical Reactions by Radiating Electromagnetic Fields.

Once it has been accepted that momentum may be associated

with electromagnetic fields it becomes obvious that there can be mechanical reactions on a source producing such radiation. Likewise, if this momentum is absorbed or reflected by a material body a mechanical force will result, the magnitude being proportional to the time rate of change of the elctromagnetic momentum.

Consider for example a device producing a collimated beam of radiation. The momentum density associated with this wave is $\vec{D}\times\vec{B}$. Assuming that momentum propagates at the velocity of light, as does the energy associated with the beam, the momentum crossing unit area per second is simply $c\,\vec{D}\times\vec{B}$. The pressure, then, on a material body that perfectly absorbs this radiation is equal in magnitude to this flux of momentum. In other words the pressure is $c\vec{D}\times\vec{B} = \frac{\vec{E}\times\vec{H}}{c}$. The force per unit area on the absorber is the power absorbed per unit area divided by the velocity of light in a vacuum. The magnitude of the force acting on the device producing this radiation is $Ac(\vec{D}\times\vec{B})$, where A is the area of the beam. Hence, the force is equal to the total power radiated from the source divided by the velocity of light. In general a radiator does not produce a true beam and the force is some constant times the ratio of the radiated power and the velocity of light. The forces involved are of course extremely small, of the order of a few dynes for several hundred watts of power radiated.

In an analogous fashion a device radiating circularly polarized waves will be subjected to a mechanical torque. The most direct way to obtain the magnitude of this torque is to consider the radiation as being composed of a beam of photons whose spins are aligned in one direction. Each photon has an angular momentum whose magnitude is $h/2\pi$, where h is Planck's constant. The energy of each photon is hf, where f is the frequency of the radiation. Hence, if E is the total energy per unit volume in the field, the number of photons per unit volume is E/hf. Since E = P/c, where P is the power flow per unit area of the beam, the number of photons becomes P/hcf. Hence, the total angular momentum per unit volume is given by $P/hcf\cdot h/2\pi = P/\omega c$, where ω is the angular frequency of the radiation. Assuming

the angular momentum is carried at the velocity of light, the resultant flux of angular momentum crossing a unit surface perpendicular to the direction of propagation is $P/\omega c \cdot c = P/\omega$. Therefore, the magnitude of the mechanical torque, per unit area, on the device producing the beam or on a material body absorbing this radiation is P/ω. The total torque on the radiating device is of course this value multiplied by the beam area. In other words it is equal to the total power radiated divided by the angular frequency. This simple expression is quite general and applies to a wide variety of radiating systems.

2. THE TORQUE - ANTENNA

2.1 Introduction

A mechanical torque will be exerted on any antenna radiating eletromagnetic angular momentum. For example, the helix, the planar spiral, and the turnstile antennas, which produce mainly circularly polarized waves, will experience a torque.

In the following Sections a few simple antennas will be analyzed. All of the antennas discussed produce travelling waves of the form $\cos(\omega t - kr \pm \phi)$. The field spirals away from the antenna and a torque is exerted on the antenna in a sense opposite to that of the spiralling wave.

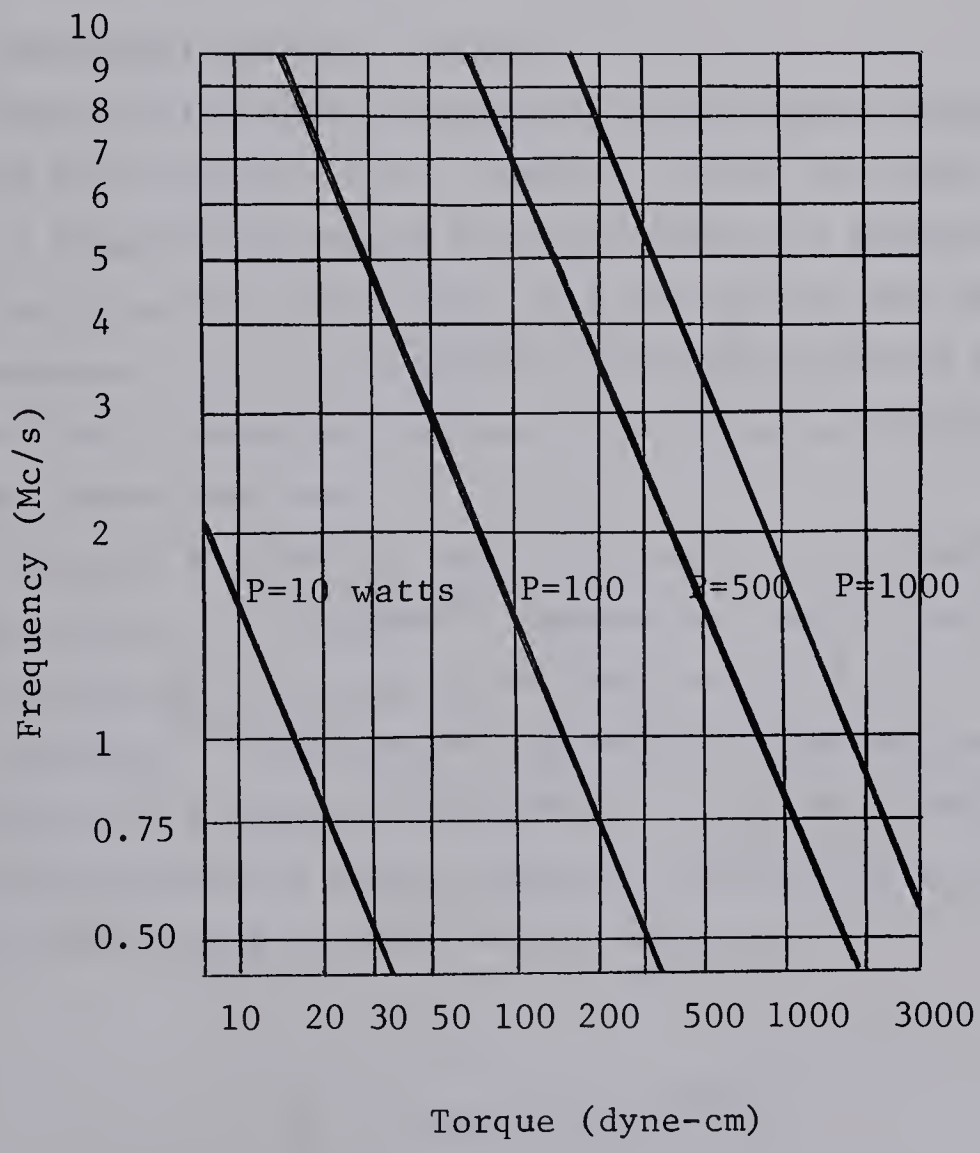

Fig. 2.1 Electromagnetic Torque ($T=\frac{P}{\omega}$)

The magnitude of the torque applied to these antennas is given by the fundamental relationship,

$$T = \frac{P}{\omega}$$

where P is the total power radiated. At high frequencies the actual torque is extremely small, however, if the frequency is reduced to the low megacycle region, moderate amounts of power can produce useable torques. For example at one megacycle the resultant torque is approximately 1.6 dyne - cm per watt. Figure 2.1 shows the order of magnitude of torque that can be produced by radiating electromagnetic angular momentum.

2.2 The Spherical Torque - Antenna

The reaction torque acting on a particular antenna can be calculated from equation 1.19, once the fields are known. By choosing a spherical geometry for the antenna, a mathematically rigorous solution for the fields, and the torque, can be obtained. Such an antenna, while not entirely practical, permits an investigation of the parameters involved in a torque-antenna without introducing any approximations.

Consider a spherical shell of radius, a, supporting a current sheet, varying as $I = I_0 \sin\theta e^{j\omega t}$ amperes per meter, and flowing on the surface in the direction of the unit vector $\vec{i}_\phi$.

Stratton[15] derives the general solution of the vector wave equation in a spherical geometry. It can be shown from this general solution that a vector magnetic potential suitable for describing the fields of this current sheet is:

$$\vec{A} = A \sin\theta Z_1(kr) e^{j\omega t} \vec{i}_\phi \qquad \ldots 2.1$$

where $Z_1 = j_1(kr)$ (inside the sphere)

and $$Z_1 = h_1(kr) = j_1(kr) - jn_1(kr)$$

(outside the sphere)

$j_1(kr)$ and $n_1(kr)$ are spherical Bessel functions of the first and second kind. Now,

$$\left.\begin{aligned} \vec{B} &= \text{curl}\vec{A} \\ \text{and} \\ \vec{E} &= -\frac{\partial}{\partial t}\vec{A} \end{aligned}\right\} \ldots 2.2$$

since $\text{div}\vec{A} = 0$. Hence,

$$E_\theta = -j\omega A \sin\theta Z_1(kr) e^{j\omega t}$$

$$\left.\begin{aligned} B_r &= 2A\cos\theta Z_1(kr)\frac{e}{r}^{j\omega t} \\ B_\theta &= -A\sin\theta\frac{\partial}{\partial r}\left(rZ_1(kr)\right)\frac{e}{r}^{j\omega t} \end{aligned}\right\} \ldots 2.3$$

The solution for the fields is completed by matching the interior and exterior fields at the spherical surface, r = a. The boundary conditions are:

B_r is continuous

and $I = H_{\theta\text{external}} - H_{\theta\text{internal}}$.

Therefore, with $A = A_0$ inside the sphere and $A = A_1$ outside the sphere,

$$A_0 j_1(ka) = A_1\left(j_1(ka) - jn_1(ka)\right) \qquad \ldots 2.4$$

and since,

$$\frac{\partial}{\partial r}\left(rZ_1(kr)\right) = krZ_0(kr) - Z_1(kr)$$

$$I_0 \sin\theta = -A_1 \frac{\sin\theta}{\mu a}\left\{ka\left(j_0(ka) - jn_0(ka)\right) - \left(j_1(ka) - jn_1(ka)\right)\right\}$$

$$+ A_0\left(kaj_0(ka) - j_1(ka)\right) \qquad \ldots 2.5$$

Using equation 2.4 and substituting for the spherical Bessel functions equation 2.5 reduces to:

$$j_1(ka) I_0 \mu a = j\frac{A_1}{ka}$$

Hence,

$$\left.\begin{aligned} A_1 &= -j\mu a^2 k I_0 j_1(ka) \\ A_0 &= -j\mu a^2 k I_0 h_1(ka) \end{aligned}\right\} \ldots 2.6$$

Substituting A_0 and A_1 for A in equations 2.3 gives the complete field solution inside and outside the sphere.

Consider now two current sheets of the above form. Superimpose these currents on the surface of a sphere of radius, a, in such a manner that one current flows about the y - axis, the other about the x - axis. Let there be a phase difference of $\frac{\pi}{2}$

between the two currents. Referring to Figure 2.2, the fields due to the y - axis current sheet are identical to equations 2.3 when expressed with respect to the primed coordinate system. Likewise the fields of the x - axis current sheet are identical to equation 2.3 when expressed with respect to the doubly primed coordinate system. The total field can now be obtained by substituting first

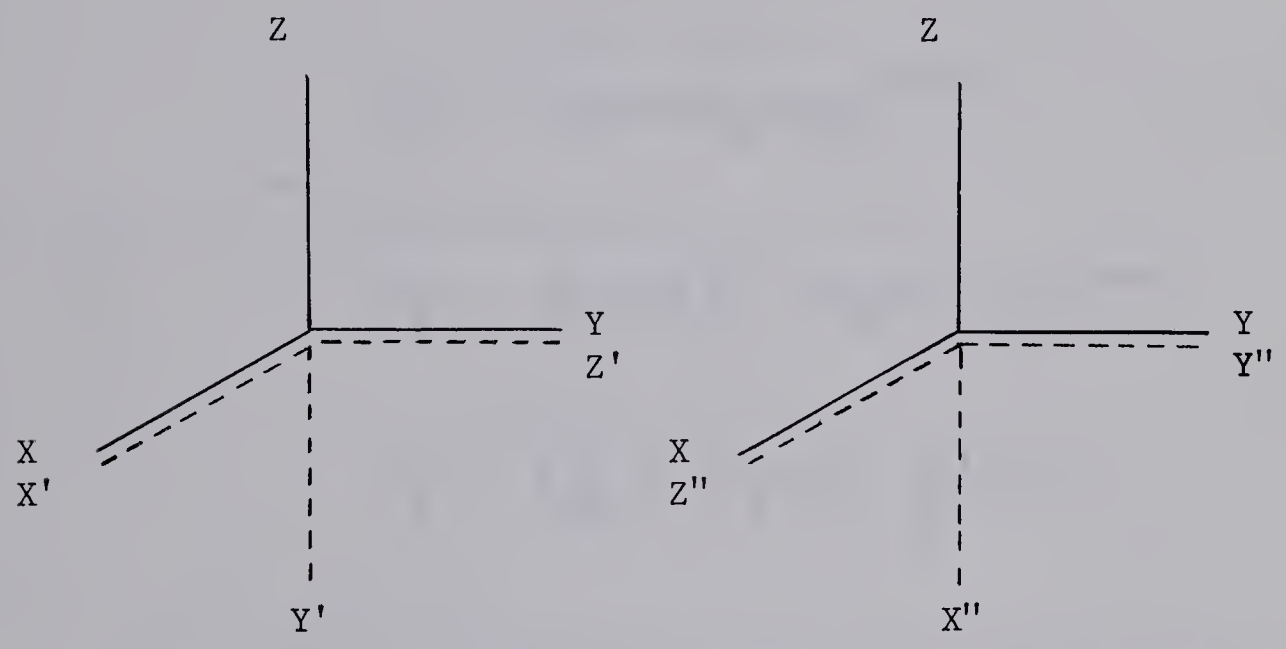

Fig. 2.2 Current Coordinates

the primed then the doubly primed parameters into the field expression given by equations 2.3 and adding the resulting set of fields. Hence,

$$\vec{E} = E_{\phi'}\vec{i}_{\phi'} + jE_{\phi''}\vec{i}_{\phi''}$$

$$\vec{B} = B_{r'}\vec{i}_{r'} + jB_{r''}\vec{i}_{r''} + B_{\theta}\vec{i}_{\theta} + jB_{\theta''}\vec{i}_{\theta''}$$

}...2.7

The relationships of Appendix 4 permit these field equations to be expressed with respect to the unprimed coordinates, r, θ and ϕ. The resulting fields external to the sphere are:

$$\left.\begin{aligned} E_\theta &= -j\omega A_1 h_1(kr) e^{j(\omega t-\phi)} \\ E_\phi &= -\omega A_1 \cos\theta h_1(kr) e^{j(\omega t-\phi)} \\ Br &= j2A_1 \sin\theta h_1(kr) \frac{e}{r}^{j(\omega t-\phi)} \\ B_\theta &= jA_1 \cos\theta \frac{\partial}{\partial r}\left(rh_1(kr) \right) \frac{e}{r}^{j(\omega t-\phi)} \\ B_\phi &= A_1 \frac{\partial}{\partial r}\left(rh_1(kr) \right) \frac{e}{r}^{j(\omega t-\phi)} \end{aligned}\right\} \ldots 2.8$$

These fields are spiralling waves progressing in the positive ϕ direction. It is to be expected then that a mechanical torque will be exerted on the sphere. The magnitude of this torque can be calculated from equation 1.19.

$$\begin{aligned} \vec{T} &= -\frac{Re}{2c} \int \vec{r}\times(\vec{E}\times\vec{H}^*)\, dS \\ &= -\frac{Re}{2c} \int (\vec{r}\times\vec{i}_\theta E_\phi H_r^* - \vec{r}\times\vec{i}_\phi E_\theta H_r^*)\, dS \\ &= \frac{1}{2c} \int \vec{r}\times\vec{i}_\phi E_\theta H_r^*\, dS \end{aligned} \qquad \ldots 2.9$$

since $E_\phi H_r^*$ is imaginary and $E_r=0$. Substituting for $E_\theta H_r^*$,

$$\vec{T} = -\int \vec{r}\times\vec{i}_\phi A_1 A_1^* \frac{\sin\theta}{\mu k r^3}\, dS \qquad \ldots 2.10$$

The only non-zero component is T_z, hence the torque acting on the sphere is,

$$T_z = \frac{8}{3}\pi\mu a^4 k I_o^2 j_1^2(ka) \qquad \ldots 2.11$$

The total power radiated can be calculated from

$$P = \frac{Re}{2}\int (\vec{E}\times\vec{H}^*)\cdot\vec{n}\, dS$$

and it is easily shown that

$$T = \frac{P}{\omega} \qquad \ldots 2.12$$

It is interesting to note that the fields of the spherical torque-antenna are the same fields that would be obtained by spinning a uniformly magnetized sphere about its axis with angular velocity ω. The mechanical power necessary to spin the sphere against the reaction torque is given by T , and this quantity is just equal to the total power radiated.

2.3 The Loop Torque-Antenna

The spherical antenna described in Section 2.2 would be extremely difficult to realize in practice. A more practical antenna can be made by taking the limiting case of the sphere - two crossed loops driven in phase quadrature with equal currents.

In Appendix 5 it is shown that for a loop, centered at the origin and lying in the x-y plane, whose diameter is much less than a wavelength, the vector magnetic potential is

$$\vec{A} = \frac{\mu I S \sin\theta}{4\pi} \left(\frac{jk}{r} + \frac{1}{r^2}\right) e^{j(\omega t - kr)} \qquad \ldots 2.13$$

where S is the area of the loop. Since,

$$\vec{B} = \text{curl}\vec{A}$$

and

$$\vec{E} = -\frac{\partial}{\partial t}\vec{A}$$

the field of this single loop becomes:

$$B_r = \frac{\mu I S \cos\theta}{2\pi} \left(\frac{jk}{r^2} + \frac{1}{r^3}\right) e^{j(\omega t - kr)}$$

$$B_\theta = \frac{\mu I S \sin\theta}{4\pi} \left(-\frac{k^2}{r} + \frac{jk}{r^2} + \frac{1}{r^3}\right) e^{j(\omega t - kr)} \} \ldots 2.14$$

$$E_\phi = \frac{\eta I S \sin\theta}{4\pi} \left(\frac{k^2}{r} - \frac{jk}{r^2}\right) e^{j(\omega t - kr)}$$

Now consider two loops oriented as shown in Figure 2.3.

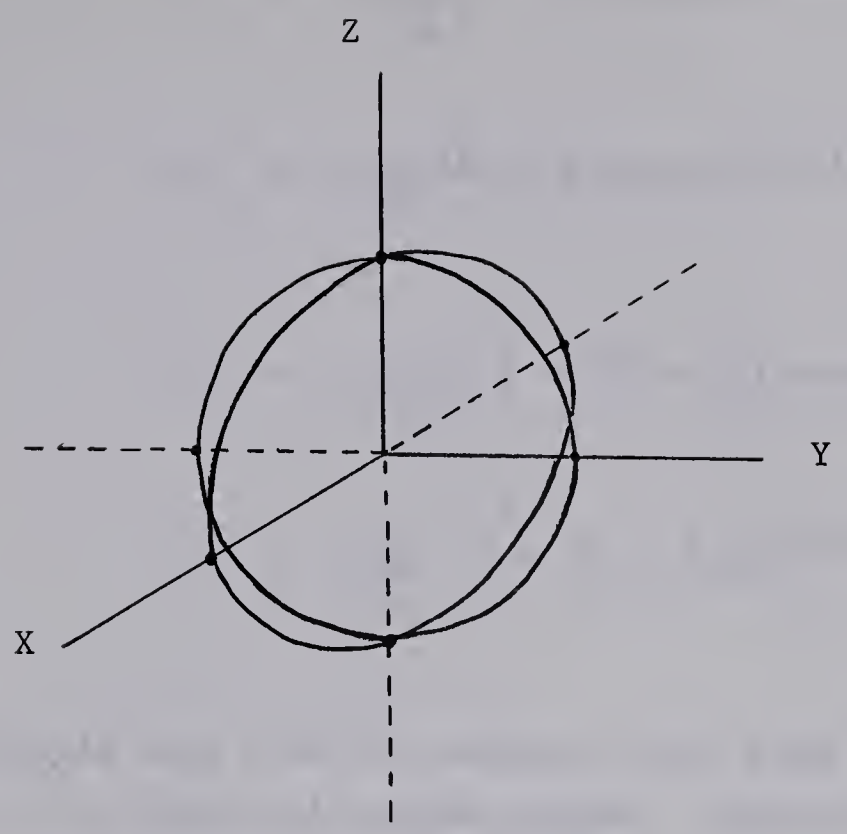

Fig. 2.3 Crossed Loops

The loop whose axis is parallel to the y-axis is assumed to lead in phase by $\pi/2$. The total field of the two loops can be found in a manner exactly analogous to that used in Section 2.2. Hence,

$$\vec{E} = E_{\phi}\vec{i}_{\phi} + jE_{\phi'}\vec{i}_{\phi'}$$

$$\vec{B} = B_{r'}\vec{i}_{r'} + jB_{r'}\vec{i}_{r'} + B_{\theta}\vec{i}_{\theta} + jB_{\theta'}\vec{i}_{\theta'} \qquad \ldots 2.15$$

Using the relationships given in Appendix 4, the fields of the crossed loops are:

$$E_{\theta} = \frac{\eta IS}{4\pi}\left(\frac{k^2}{r} - \frac{jk}{r}2\right)e^{j(\omega t - kr - \phi)}$$

$$E_\phi = -j\eta\frac{IS}{4\pi}\left(\frac{k^2}{r} - j\frac{k}{r^2}\right)\cos\theta e^{j(\omega t-kr-\phi)}$$

$$B_r = j\mu\frac{IS}{2\pi}\left(j\frac{k}{r^2} + \frac{1}{r^3}\right)\sin\theta e^{j(\omega t-kr-\phi)} \quad \}...2.16$$

$$B_\theta = -j\mu\frac{IS}{4\pi}\left(-\frac{k^2}{r} + j\frac{k}{r^2} + \frac{1}{r^3}\right)\cos\theta e^{j(\omega t-kr-\phi)}$$

$$B_\phi = -\mu\frac{IS}{4\pi}\left(-\frac{k^2}{r} + j\frac{k}{r^2} + \frac{1}{r^3}\right)e^{j(\omega t-kr-\phi)}$$

The field spirals away from the antenna in the same fashion as the fields of the spherical torque-antenna. Equation 1.19 for the time average torque reduces to

$$\vec{T} = \frac{1}{2c}\int \vec{r}\times\vec{i}_\phi E_\theta H_r^* \, dS \qquad ...2.17$$

from which the torque is readily calculated to be

$$T_z = \frac{\mu S^2 k^3 I^2}{6\pi} \qquad ...2.18$$

As in the spherical case it is easily shown that the total radiated power is related to the torque as

$$T = \frac{P}{\omega}$$

At this point it is worth noting that the torque on a small loop antenna is independent of the shape of the loop -- only the area

is of importance.

The spherical antenna may be compared to the circular loop antenna by setting equal the total current in the two antennas. The current flowing across the sphere due to the current sheet $I_o \sin\theta$ is

$$I = \int_o^{\pi} I_o a \sin\theta \, d\theta = 2I_o a \qquad \ldots 2.19$$

Hence,

$$T_{sphere} = \frac{2\pi\mu a^4 k^3 I^2}{27} \qquad \ldots 2.20$$

since $j_1^2(ka) \rightarrow \frac{ka}{3}$ for $ka \ll 1$

and

$$T_{loop} = \frac{\pi\mu a^4 k^3 I^2}{6} \qquad \ldots 2.21$$

since $S = \pi a^2$.

Comparing equations 2.20 and 2.21 shows that the circular loop produces more torque, for the same current, than a sphere of the same radius. This result should not be surprising since in the loop case the current is confined to where it does the most good, as it were. For the sphere the same current is spread out over the entire spherical surface.

2.4 Turnstile Torque-Antenna

Consider two linear current elements of length, 1, small compared to a wavelength, situated as shown in Figure 2.4 with respect to a system of rectilinear coordinates. The element

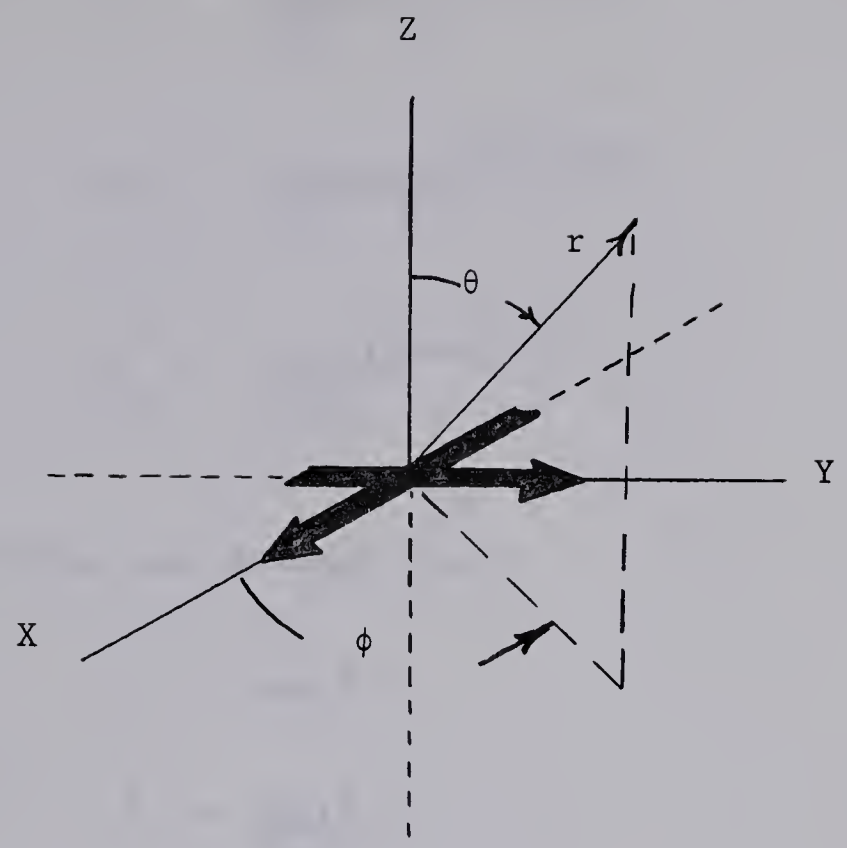

Fig. 2.4 Crossed Electric Dipoles

lying on the y-axis is assumed to lead in phase by $\pi/2$.

The magnetic vector potential is

$$\vec{A} = \frac{\mu I l e^{j(\omega t - kr)}}{4\pi r}\vec{i}_x + j\frac{\mu I l e^{j(\omega t - kr)}}{4\pi r}\vec{i}_y \quad ...2.22$$

But,

$$\left.\begin{aligned} A_r &= A_x \sin\theta\cos\phi + A_y \sin\theta\sin\phi + A_z \cos\theta \\ A_\theta &= A_x \cos\theta\cos\phi + A_y \cos\theta\sin\phi - A_z \sin\theta \\ A_\phi &= -A_x \sin\phi + A_y \cos\phi \end{aligned}\right\} \quad ...2.23$$

Hence,

$$A_r = \frac{\mu I l \sin\theta}{4\pi r} e^{j(\omega t - kr + \phi)}$$

$$A_\theta = \frac{\mu I l \cos\theta}{4\pi r} e^{j(\omega t - kr + \phi)} \quad \}...2.24$$

$$A_\phi = j\frac{\mu I l}{4\pi r} e^{j(\omega t - kr + \phi)}$$

The field quantities are obtained from

$$\vec{B} = \text{curl}\vec{A}$$

$$\vec{D} = \frac{\text{curl}\vec{B}}{j\omega\mu} \quad \}...2.25$$

and are given by:

$$B_\theta = j\frac{\mu I l}{4\pi}\left(\frac{jk}{r} + \frac{1}{r^2}\right) e^{j(\omega t - kr + \phi)}$$

$$B_\phi = -\frac{\mu I l}{4\pi}\left(\frac{jk}{r} + \frac{1}{r^2}\right)\cos\theta e^{j(\omega t - kr + \phi)}$$

$$D_r = \frac{I l}{2\pi\omega}\left(\frac{k}{r^2} - \frac{j}{r^3}\right)\sin\theta e^{j(\omega t - kr + \phi)} \quad \}...2.26$$

$$D_\theta = \frac{I l}{4\pi\omega}\left(-\frac{jk^2}{r} - \frac{k}{r^2} + \frac{j}{r^3}\right)\cos\theta e^{j(\omega t - kr + \phi)}$$

$$D_\phi = \frac{I l}{4\pi\omega}\left(\frac{k^2}{r} - \frac{jk}{r^2} - \frac{1}{r^3}\right) e^{j(\omega t - kr + \phi)}$$

Substituting these fields in equation 1.19 the time average torque is

$$\vec{T} = -\frac{1}{2c}\int \vec{r}\times\vec{i}_{\phi} E_r H_{\theta}^{*}\, dS \qquad \ldots 2.27$$

The only non-zero component of $\vec{T}$ is

$$T_z = \frac{\mu l^2 k I^2}{6\pi} \qquad \ldots 2.28$$

The power radiated is given by

$$P = \frac{Re}{2}\int (\vec{E}\times\vec{H}^{*})\cdot\vec{n}\, dS$$

$$= \frac{\mu l^2 k I^2 \omega}{6\pi}$$

and again

$$T = \frac{P}{\omega}$$

2.5 An Alternate Method For Producing A Reaction Torque

The torque exerted on all the antennas described above resulted from the radiation of electromagnetic angular momentum by these antennas. The torque-antenna described in this Section utilizes the linear momentum produced by a beam radiator.

Consider two beam radiators rigidly fixed to a common arm of length, d — radiating equal power in opposite directions. There must be a reaction force on each radiator thereby exerting a torque on the overall structure. Referring to Section 1.3, if each antenna produced a true beam, the torque would be $T = P/c\cdot d$. The torque is independent of frequency which marks a fundamental difference between this torque-antenna and those discussed in

Sections 2.2 to 2.4. In order to obtain an idea of the torque to be expected in a practical case, where the radiators do not produce ideal beams, consider the reaction force on the simple antenna shown in Figure 2.5. The antenna consists of two Hertz elements separated by $\lambda/4$ meters. The element shown on the negative x-axis in Figure 2.5 leads in phase by $\pi/2$.

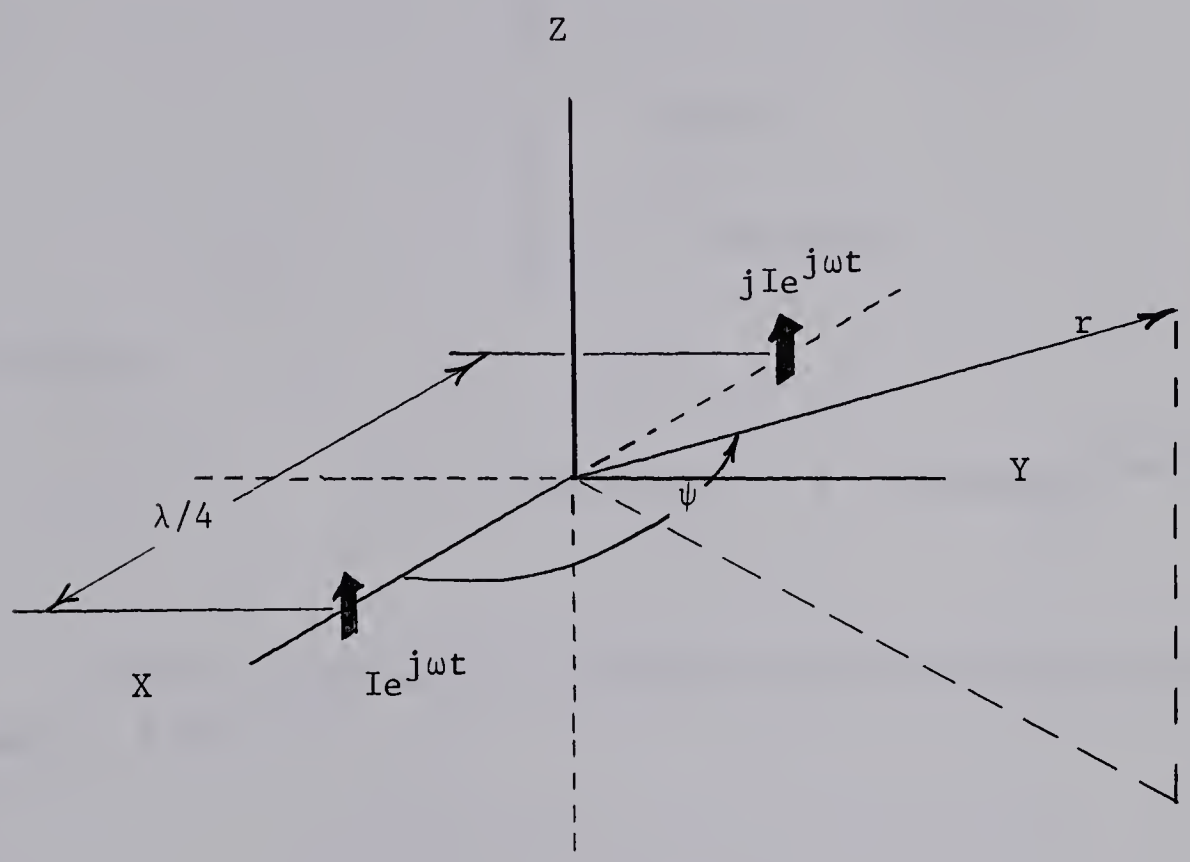

Fig. 2.5 A Beam Radiator

At some point a large distance from the source the field vectors resulting from each element are equal in magnitude and parallel, but they are out of time phase by $\alpha = \pi/2 + 2\pi/\lambda \cdot \Delta r$, where Δr is the path difference from each element to the point in question. The total field at that point can be found by adding the field vectors of the two elements as phasors separated by the angle α. Hence, the total field will be proportional to $2\cos\alpha/2$.

The only fields at large distances from a Hertz element parallel to the z-axis are E_θ and H_ϕ. E_θ and H_ϕ vary as $\sin\theta/r \cdot e^{j(\omega t-kr)}$ and are independent of the ϕ coordinate. The total field becomes:

$$\left.\begin{aligned} E_\theta &= A\sin\theta\cos\frac{\alpha}{2}\,\frac{e}{r}^{j(\omega t-kr)} \\ H_\phi &= \frac{E}{\eta}\theta \end{aligned}\right\} \ldots 2.29$$

Now,

$$\alpha = \frac{\pi}{2} + \frac{2\pi}{\lambda}\cdot\frac{\lambda}{4}\cos\psi$$

$$= \frac{\pi}{2}(1 + \sin\theta\cos\phi) \qquad \ldots 2.30$$

Therefore,

$$E_\theta = A\sin\theta\cos\frac{\pi}{4}(1 + \sin\theta\cos\phi)\frac{e}{r}^{j(\omega t-kr)} \qquad \ldots 2.31$$

The force acting on the antenna can be calculated from equation 1.18.

$$\vec{F} = -\frac{Re}{2c}\int \vec{E}\times\vec{H}^* \, dS$$

$$= -\frac{Re}{2c}\int \vec{i}_r \frac{E}{\eta}\theta E_\theta^* \, dS$$

$$= -\frac{A^2}{2c\eta}\int \vec{i}_r \sin^2\theta\frac{\cos^2}{r^2}\left\{\frac{\pi}{4}(1 + \sin\theta\cos\phi)\right\} dS \qquad \ldots 2.32$$

The only non-zero component of $\vec{F}$ is:

$$F_x = -\frac{A^2}{2c\eta}\int_0^{2\pi}\int_0^{\pi} \sin^4\theta\cos\phi\cos^2\{\frac{\pi}{4}(1+\sin\theta\cos\phi)\}\,d\theta d\phi \qquad ...2.33$$

Now,

$$\cos(\frac{\pi}{4}+\frac{\pi}{4}\sin\theta\cos\phi) = \cos\frac{\pi}{4}\cos\beta - \sin\frac{\pi}{4}\sin\beta, \beta = \frac{\pi}{4}\sin\theta\cos\phi$$

$$\cos^2(\frac{\pi}{4}+\frac{\pi}{4}\sin\theta\cos\phi) = \frac{1}{2}\cos^2\beta + \frac{1}{2}\sin^2\beta - \cos\beta\sin\beta$$

$$= \frac{1}{2} - \frac{1}{2}\sin^2\beta$$

$$= \frac{1}{2} - \frac{1}{2}\sin(\frac{\pi}{2}\sin\theta\cos\phi)$$

Therefore,

$$F_x = -\frac{A^2}{2c\eta}\int_0^{2\pi}\int_0^{\pi} \sin^4\theta\cos\phi\,\{\frac{1}{2} - \frac{1}{2}\sin(\frac{\pi}{2}\sin\theta\cos\phi)\}\,d\theta d\phi$$

$$= \frac{A^2}{4c\eta}\int_0^{2\pi}\int_0^{\pi} \sin^4\theta\cos\phi\sin(\frac{\pi}{2}\sin\theta\cos\phi)\,d\theta d\phi \qquad ...2.34$$

The total radiated power can be calculated as:

$$P = \frac{Re}{2}\int (\vec{E}\times\vec{H}^*)\cdot\vec{n}\,dS$$

$$= \frac{1}{2}\int \frac{E_\theta}{\eta}E_\theta^*\,dS$$

$$= \frac{2\pi A^2}{3\eta} \qquad ...2.35$$

Hence,

$$F_x = \frac{P}{c}\cdot\frac{3}{8\pi}\int_0^{2\pi}\int_0^{\pi}\sin^4\theta\cos\phi\sin(\frac{\pi}{2}\sin\theta\cos\phi)\ d\theta d\phi \qquad ...2.36$$

Now,

$$B = \int_0^{2\pi}\int_0^{\pi}\sin^4\theta\cos\phi\sin(\frac{\pi}{2}\sin\theta\cos\phi)\ d\theta d\phi$$

can be integrated by expanding $\sin(\frac{\pi}{2}\sin\theta\cos\phi)$ in an infinite series and integrating term by term. Since,

$$\sin\delta = \delta - \frac{\delta^3}{3!} + \frac{\delta^5}{5!} - \frac{\delta^7}{7!} + ...$$

the first term becomes:

$$\frac{8\pi^2}{15} = \int_0^{2\pi}\int_0^{\frac{\pi}{2}}\sin^5\theta\cos^2\phi\ d\theta d\phi \qquad ...2.37$$

It is easily demonstrated that the remaining terms are related as

$$\frac{a_n}{a_{n-1}} = -\frac{\pi^2}{4}\frac{(2n+2)}{(2n-2)(2n+3)2n} \qquad ...2.38$$

where n runs from two to infinity. Hence,

$$B = \frac{8\pi^2}{15} - \frac{\pi^4}{70} + \frac{\pi^6}{7560} - .....$$

The sum of the first six terms gives B as approximately 3.9905.

Therefore equation 2.36 becomes:

$$F_x \simeq 0.476\frac{P}{c} \qquad \ldots 2.39$$

The torque produced using two of these beam radiators then, is

$$T \simeq 0.476d\frac{P}{c} \qquad \ldots 2.40$$

2.6 A Comparison of the Loop Torque-Antenna and the Turnstile Torque-Antenna.

The question arises as to which antenna, the loop antenna (circular loops will be considered for convenience) or the turnstile antenna, is the better torque producer. Since both antennas experience identical torques if each radiates the same power, the problem of finding which antenna produces the most torque reduces to determining which one radiates the most power at the lowest frequency for a given power supplied to the terminals.

Power is fed to the loop antenna by tuning out the inductive reactance of the loop. This matching can be accomplished in an essentially lossless fashion by using an air capacitor. The turnstile antenna presents a capacitive reactance at the terminals and an inductive reactance of equal magnitude must be provided in order to feed power to this antenna. Unfortunately a large amount of the terminal power will now go into heating this inductance(usually a large air-core coil).

In comparing the two torque-antennas the required matching networks will be included. The antennas will have identical overall extension(the length of the turnstile,l, equal to the diameter of the loop,a) and will be constructed of identical materials. So that realistic figures will be obtained, the following dimensions are selected:

Material - aluminum tubing 3/8 inch diameter

Size - $l=2a=d=6$ meters

The comparison will be made by obtaining, for each antenna, a graph of the torque versus frequency for a constant power of 300

watts at the terminals of each antenna matching network.

(i) The Loop Antenna

The graphs for the loop antenna are obtained in the following manner:

(a) select a frequency

(b) calculate the radiation resistance, R_r

(c) calculate the ohmic loss, R_Ω

(d) calculate the radiated power

$$P_r = 300 \frac{R_r}{R_\Omega} \cdot \frac{1}{1 + \frac{R_r}{R_\Omega}}$$

(e) calculate the torque from $T=P/\omega$

(f) plot T versus f

Since the matching in this case is essentially lossless it is not necessary to know the reactive component of the input impedance of the loop antenna. The ohmic loss, then, is simply the ohmic loss of the aluminum tubing used.

The real part of the input impedance, the radiation resistance, is easily determined since the two loops forming the torque-antenna do not couple to one another. The radiation resistance for the circular loop is simply,

$$R_r = 3.075 \times 10^5 \left(\frac{a}{\lambda}\right)^4$$

The resulting graphs are shown in Figure 2.6.

(ii) The Turnstile Antenna

The procedure for plotting the graphs in this case is identical to that used for the loop antenna.

The radiation resistance of the turnstile is given by:

$$R_r = 20\pi^2 \left(\frac{1}{\lambda}\right)^2$$

The required inductive reactance to match the antenna is given by[16]:

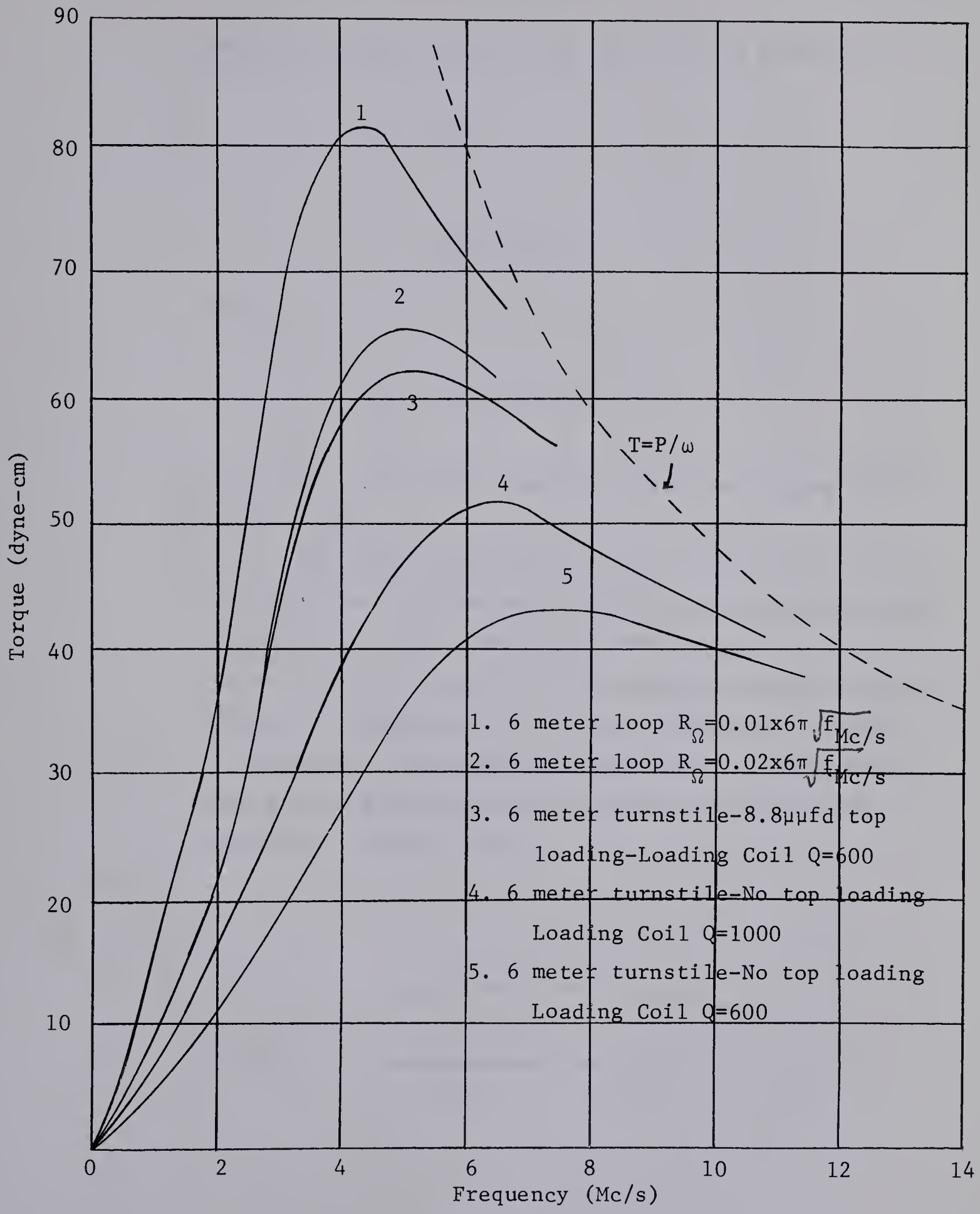

Fig. 2.6 Torque-Frequency Curves

$$X_L = Z_o \cot\left(\frac{\pi l}{\lambda}\right)$$

Hence, the ohmic loss of the coil will be given as:

$$R_{coil} = \frac{X_L}{Q}$$

$$= \frac{Z_o}{Q} \cot\left(\frac{\pi l}{\lambda}\right)$$

where,

$$Z_o = 120\{\ln\left(\frac{1}{a}\right) - 1\}$$

The ohmic loss of the aluminum tubing can be neglected in this case.

The radiating efficiency of a linear antenna can be significantly improved by providing capacitive loading at the ends. This loading can take many forms, such as spheres, discs or spirals. The added capacitance has the effect of lengthening the antenna electrically thereby increasing the radiation resistance while at the same time reducing the capacitive reactance at the input terminals. (Figure 2.7)

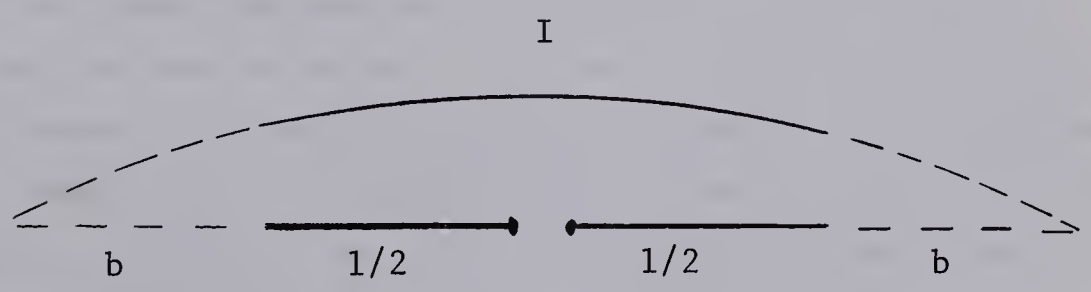

Fig. 2.7 Current Distribution on Loaded Antenna

The increase in electrical length, b, can be determined from,

$$\frac{1}{\omega c} = Z_o \cot\left(\frac{2\pi b}{\lambda}\right)$$

where C is the amount of capacitive loading. In this case the ohmic loss is

$$R_{coil} = \frac{Z_o}{Q} \cot\left(\frac{2\pi(b + 1/2)}{\lambda}\right)$$

The radiation resistance can be taken from graphs given in the Antenna Engineering Handbook, H. Jasik, McGraw Hill, 1961. Figure 2.6 shows the results for both loaded and unloaded turnstile antennas.

Obviously from Figure 2.6 an antenna of given dimensions has an optimum frequency for the production of torque. At high frequencies when the radiating efficiency of the antenna is high the torque is related to the supplied power by $T = P_s/\omega$. As the frequency is decreased the radiation efficiency decreases but $1/\omega$ increases more rapidly until some optimum frequency is reached. At lower frequencies the radiated power decreases faster than $1/\omega$ can increase. In effect radiation efficiency has been traded for torque producing efficiency. This optimum frequency occurs when the characteristic dimensions of the radiator are a small fraction of the total wavelength (in the examples shown the overall dimensions were between 0.08λ and 0.14λ).

The Q of the loading coil makes a significant difference as does the conductivity of the material forming the loop. Capacitive loading also provides a marked improvement on the

unloaded turnstile. The amount of torque that can be obtained is increased by reducing the ohmic loss in the antenna and associated matching networks.

It is apparent from Figure 2.6 that both antennas are capable of producing torques of the same order of magnitude for the same power. There appears to be no clear cut choice as to which antenna is the better torque producer. The loop with the largest ohmic loss is practically identical with the turnstile using a loading coil of Q = 600 with 8.8 pf of capacitive loading. Factors arising from the manner in which it is proposed to use such a torque-antenna will dictate the final choice.

For example, in a particular application, the time taken to turn through a given angle may be important. This response time is proportional to $\sqrt{I/T}$, where T is the reaction torque and I is the moment of inertia of the antenna. Obviously if rapid responses are desired the moment of inertia must be small. The moments of inertia of the loop and turnstile torque-antennas are:

$$I_{loop} = 2\pi\rho a^3$$

$$I_{turnstile} = \frac{\rho l^3}{6}$$

where ρ is the mass per unit length of the material forming the antennas. The ratio of the response times for the loop and turnstile antennas is,

$$\frac{\tau_{turnstile}}{\tau_{loop}} = \sqrt{\frac{l^3}{12\pi a^3}\frac{T_{loop}}{T_{turnstile}}}$$

When the two antennas have the same physical extent ($l = 2a$), the ratio of the torques can be nearly unity, and

$$\frac{\tau_{turnstile}}{\tau_{loop}} = \frac{1}{2.17}$$

In other words the turnstile antenna responds to an applied torque in approximately half the time of the loop antenna. The response time of the turnstile arrangement can be made even faster by tapering the antenna arms. In an application where moment of inertia is important, then, it appears that the turnstile torque-antenna should be selected.

An interesting comparison can be made between the linear-force torque-antenna and the loop or turnstile arrangement in the following manner:

$$T_1 = 0.476d\frac{P}{c} \quad \text{....equation 2.40}$$

$$T_c = \frac{\lambda}{2\pi}\frac{P}{c} \quad \text{....conventional torque-antenna}$$

where λ is the wavelength of the radiation produced by the conventional torque-antenna. Now, if both antennas have the same physical extent $d \simeq 0.14\lambda$ (from Figure 2.6)

$$T_1 \simeq 0.476d\frac{P}{c}$$

$$T_c \simeq 1.07d\frac{P}{c}$$

The linear force torque-antenna produces less than half the torque of the conventional torque-antenna. The 1-f torque-antenna is at a further disadvantage in that it must operate at a much higher frequency than the loop or turnstile antennas to ensure the independent operation of each beam radiator. Moreover, the 1-f torque-antenna is more complicated and has a larger moment of inertia than a conventional torque-antenna. The beam antennas

must be supported on arms, thus placing a relatively large mass at the end of the moment arms and giving a large moment of inertia. The moment of inertia of the supporting arms alone is of the same order of magnitude as for the turnstile torque-antenna. An alternate scheme would be to beam radiation from the axis to mirrors supported on the ends of the moment arms and inclined at 45 degrees. In this case, however, the supporting arms would be quite massive in order to provide the rigidity required to ensure the beam striking the mirror, and the moment of inertia would again be significantly larger than for the conventional type of torque-antenna. In the light of these factors it seems that the linear-force torque-antenna cannot compete with the loop and turnstile configurations.

3. THE APPLICATION OF A TORQUE-ANTENNA TO THE ATTITUDE CONTROL OF A SPACE VEHICLE

3.1 Introduction

Generally speaking, most space vehicles require some form of attitude control, perhaps to align suitably some measuring device, or to permit the use of highly directive communications antennas.

Many methods have been used [17 - 21] to apply control torques to spacecraft. For short-lived satellites, the almost universal method has been to remove unwanted angular momentum by exhausting mass through a gas-jet nozzle. Liquid propane is frequently used because of its low latent heat of evaporation and low freezing point. The life of such a control device is clearly limited by the amount of gas or vapor carried aboard the spacecraft. Gas-jets are used extensively in present attitude control schemes mainly because of the very large control torques that may be produced. For long-lived satellites, studies have been made of the possibility of using the earth's magnetic field to dump momentum, by controlling the current in a set of mutually perpendicular coils aboard the spacecraft. This scheme has proved to be light weight and reliable, and requires only small amounts of electrical power. The very serious disadvantage of such a system is that its application is restricted to vehicles whose missions do not carry them beyond the range of the earth's magnetic field. Inertia wheels, the effect of gravitational gradients, plasma emissions, and maneuverable solar sails and paddles also find applications in attitude control.

What is needed, or will be needed in future space applications, is a reliable, long-life device, capable of dumping unwanted momentum about any specified axis. The control device should be independent of any mechanism external to the spacecraft, such as solar radiation or the earth's magnetic field. It is the purpose of this Section to show that it is possible for the torque-antenna to meet these requirements.

3.2 The Practicability of Electromagnetic Torque Control

The success of an attitude control system using a torque-antenna, to provide reaction torques on the space vehicle, depends upon the magnitude of the disturbing torques acting on the vehicle. The magnitude of these disturbing torques depends greatly upon the vehicle design and mission. Briefly the most important of these torques are:

(i) Gravitational Gradient Torques

A torque is exerted on a spacecraft in the presence of a large mass, such as the earth, when the vehicle has an unsymmetric mass distribution. The axis of minimum moment of inertia tends to be aligned with the direction of the gravitational attraction. This effect can be used to stabilize spacecraft but more often it is present as a disturbing influence on a stabilized satellite. Typically this torque may range from 0 - 20 dyne-cm, depending of course on the particular vehicle design.

(ii) Torques Arising from Interaction With The Earth's Magnetic Field

Current elements and magnetic material in the circuitry of the space vehicle will interact with the earth's magnetic field and may result in a net torque. As already mentioned in Section 3.1 specially designed current carrying coils can use this effect to control the attitude of the vehicle.

Another type of interaction occurs between the space vehicle and the earth's magnetic field. Any rotating, conducting body experiences a torque, opposing the rotation, resulting from the interaction of the induced currents with the magnetic field.

The torques of magnetic nature are usually of the order of several hundred dyne-cm for satellites whose orbits fall below 1000 Km. Magnetic torques experienced by vehicles travelling between planets can be expected to

be extremely small since the magnetic field in outer space has been estimated to be of the order of 10^{-5} gauss.

(iii) Solar Pressure Torques

The pressure exerted on a vehicle by solar radiation can give rise to a torque if the centres of pressure and mass do not coincide. The radiation pressure can reach as high as 4.5×10^{-4} dynes/cm^2. The resulting torque using specially designed paddles can reach as high as several hundred dyne-cm. However, for nearly symmetric vehicles solar torques are negligible.

(iv) Atmospheric Drag Torques

For low altitude satellites the motion through the atmosphere gives a resultant torque when the centre of pressure and mass do not coincide in the direction of motion. Such torques are usually negligible above about 500 Km.

(v) Torques Resulting from Internal Momentum Changes

Space vehicles with many moving parts, such as hydraulic flaps, switches, relays, and rotating machinery, experience torques arising from the momentum changes associated with the motion of these parts. Such torques are generally very small with the exception of the gyroscopic torques resulting from a change in the attitude of a space vehicle carrying massive, high speed, rotating devices.

It should also be noted that when a vehicle is injected into orbit the separation from the final stage usually generates tumbling rates, which must be reduced to zero prior to establishing the vehicle in its final position. Large momentum changes are involved and correspondingly large control torques are required to stabilize the craft initially in a reasonable time. It is quite probable the torque requirements in these instances are of the order of newton-meters instead of dyne-centimeters.

Comparing these above torques with those obtainable from a torque-antenna (Figure 2.1) shows that, with the exception of the initial detumbling, electromagnetic control is a feasible solution to the problem of stabilizing a space vehicle, especially if care is taken to minimize the disturbance torques.

The practicability of electromagnetic control in a given instance depends upon whether or not the required torque can be obtained with existing limitations on available power and on permissible size of antenna. To date only relatively small powers have been used in space work but in the future much higher powers will be required. Manned space stations and large maneuverable vehicles will conceivably require many hundreds of kilowatts. Much research at the present time is concentrated on achieving these high power levels. More than 500 watts of continuous power can be supplied for periods up to 5 years with combinations of solar cells and storage batteries, and it is hoped that before long nuclear power sources will be able to produce satellite powers of as much as 0.5 Mw.

The torque-power relationship of the torque-antenna indicates that, for the maximum possible torque for a given power, the largest possible antenna should be used. Antennas of more than a few meters have, until recently, presented difficult technical problems in construction and launching procedure. However, the advent of the telescoping antennas designed for the Canadian Satellite, Alouette, have made it possible to launch spacecraft having antennas well in excess of 100 feet. In the near future it should be possible to launch much longer antennas. Moreover, such telescoping antennas, known collectively as STEM devices (storeable-tubular-extendible-member), are ideally suited for constructing the turnstile torque-antenna described in Section 2.4.

Such a torque-antenna, 100 meters in length, radiating 10 Kw could produce a torque in excess of 35,000 dyne-cm.

It would seem that, when care is taken to minimize disturbance

torques and a supply of gas is carried to accomplish the initial detumbling and alignment, an electromagnetic torque-antenna can provide a means of controlling the attitude of a space vehicle. Producing the controlling torque in an electromagnetic fashion has several distinct advantages. It has a long-life in that no expendible materials, such as bottled gas, are required. There are no moving parts to wear out, thus increasing the systems reliability. The operation is independent of external phenomena such as interaction with earth's magnetic field. The system is relatively simple consisting only of the antennas and a radio frequency generator. Lastly, as will be shown in the following Section, it is possible to obtain a torque about an arbitrary axis. As increasingly greater power becomes available the torque-antenna may provide an attractive alternative to the present stabilization schemes.

3.3 Three Turnstile Antennas For Attitude Control About An Arbitrary Axis.

The turnstile torque-antenna described in Section 2.4 can be modified to provide 3-axis control by simply adding an additional antenna at right angles to the first two antennas. Essentially any pair of antennas may be used as a turnstile antenna. When the currents and phases of the three antennas are varied suitably, it is possible to obtain a torque about an arbitrary axis. It is the purpose of this Section to obtain simple expressions for the direction cosines of the resulting torque axis in terms of the currents flowing in the antennas and the relative phases between them.

Consider the three current elements shown in Figure 3.1:

Now, the vector magnetic potential is,

$$A_x = \frac{\mu I}{4\pi} x \frac{le}{r} e^{j(\omega t - kr)}$$

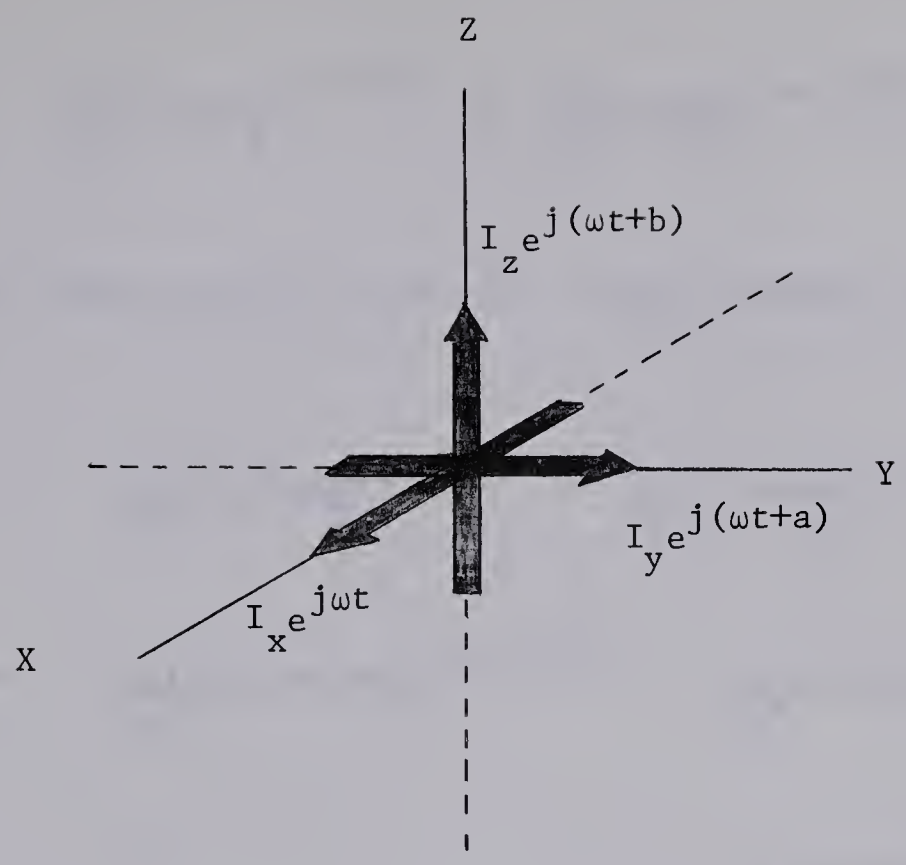

Fig. 3.1 Three-Axis Torque Control

$$A_y = \frac{\mu I_y}{4\pi} l \frac{e}{r}^{j(\omega t-kr+a)} \quad \}...3.1$$

$$A_z = \frac{\mu I_z}{4\pi} l \frac{e}{r}^{j(\omega t-kr+b)}$$

Hence,

$$A_r = \frac{\mu I_x}{4\pi} l\sin\theta\cos\phi \frac{e}{r}^{j(\omega t-kr)} + \frac{\mu I_y}{4\pi} l\sin\theta\sin\phi \frac{e}{r}^{j(\omega t-kr+a)}$$

$$+ \frac{\mu I_z}{4\pi} l\cos\theta \frac{e}{r}^{j(\omega t-kr+b)}$$

$$A_\theta = \frac{\mu I_x}{4\pi} l\cos\theta\cos\phi \frac{e}{r}^{j(\omega t-kr)} + \frac{\mu I_y}{4\pi} l\cos\theta\sin\phi \frac{e}{r}^{j(\omega t-kr+a)}$$

$$- \frac{\mu I_z}{4\pi} l\sin\theta \frac{e}{r}^{j(\omega t-kr+b)} \quad \}...3.2$$

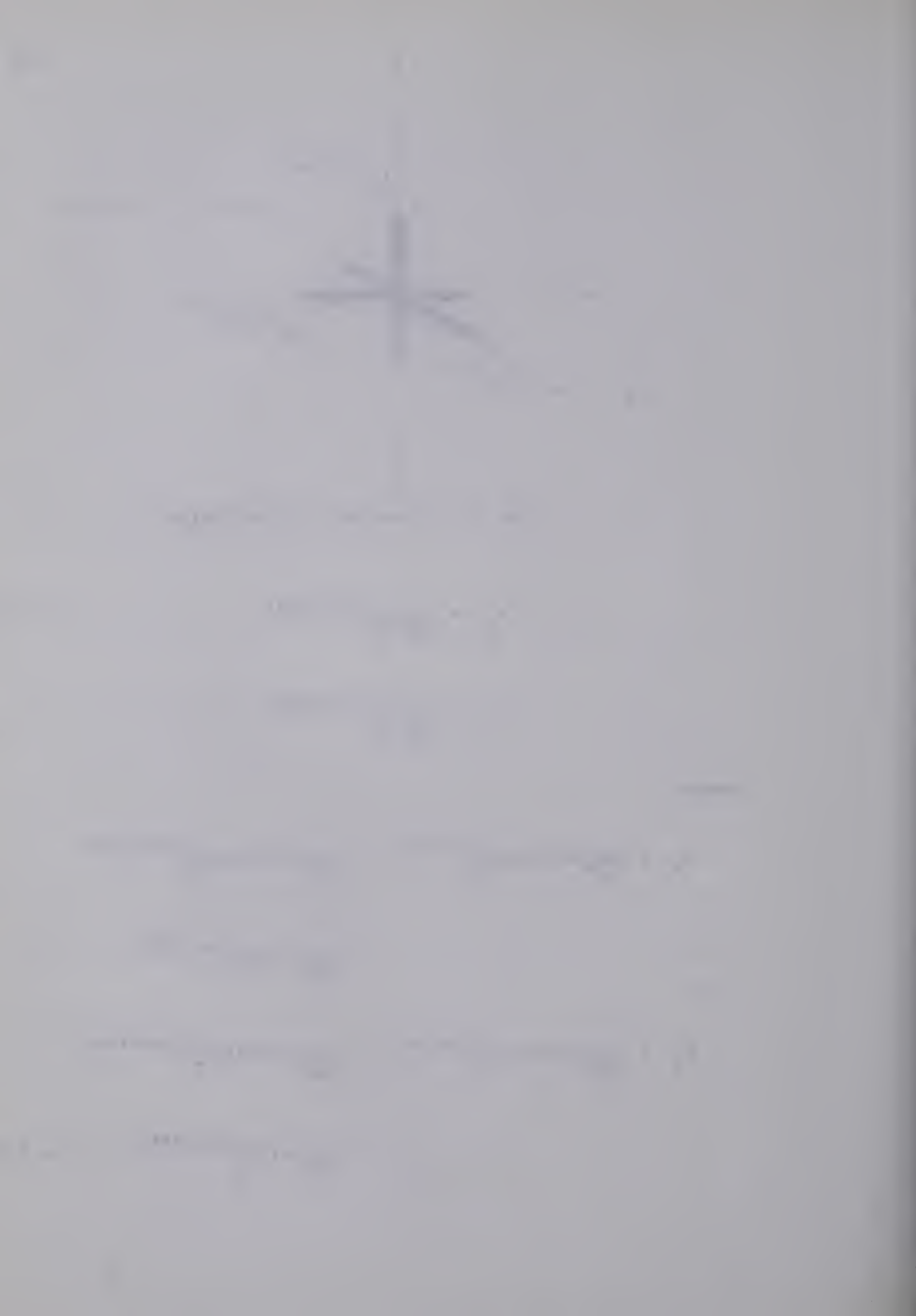

$$A_\phi = -\frac{\mu I}{4\pi}{}_x l\sin\phi\frac{e}{r}^{j(\omega t-kr)} + \frac{\mu I}{4\pi}{}_y l\cos\phi\frac{e}{r}^{j(\omega t-kr+a)}$$

Therefore, the resulting field at a large distance from the antenna is,

$$B_\theta = -\frac{j\mu I}{4\pi}{}_x kl\sin\phi\frac{e}{r}^{j(\omega t-kr)} + \frac{j\mu I}{4\pi}{}_y kl\cos\phi\frac{e}{r}^{j(\omega t-kr+a)}$$

$$B_\phi = -\frac{j\mu I}{4\pi}{}_x kl\cos\theta\cos\phi\frac{e}{r}^{j(\omega t-kr)} - \frac{j\mu I}{4\pi}{}_y kl\cos\theta\sin\phi\frac{e}{r}^{j(\omega t-kr+a)}$$

$$+ \frac{j\mu I}{4\pi}{}_z kl\sin\theta\frac{e}{r}^{j(\omega t-kr+b)}$$

$$D_r = \frac{I}{2}{}_x\frac{kl}{\pi\omega}\sin\theta\cos\phi\frac{e}{2}^{j(\omega t-kr)} + \frac{I}{2}{}_y\frac{kl}{\pi\omega}\sin\theta\sin\phi\frac{e}{2}^{j(\omega t-kr+a)}$$

$$+ \frac{I}{2}{}_z\frac{kl}{\pi\omega}\cos\theta\frac{e}{r^2}^{j(\omega t-kr+b)} \quad \}...3.3$$

$$D_\theta = -jI_x\frac{k^2 l}{4\pi\omega}\cos\theta\cos\phi\frac{e}{r}^{j(\omega t-kr)} - jI_y\frac{k^2 l}{4\pi\omega}\cos\theta\cos\phi\frac{e}{r}^{j(\omega t-kr+a)}$$

$$- jI_z\frac{k^2 l}{4\pi\omega}\sin\theta\frac{e}{r}^{j(\omega t-kr+b)}$$

$$D_\phi = jI_x\frac{k^2 l}{4\pi\omega}\sin\phi\frac{e}{r}^{j(\omega t-kr)} - jI_y\frac{k^2 l}{4\pi\omega}\cos\phi\frac{e}{r}^{j(\omega t-kr+a)}$$

The resulting torque can be calculated from equation 1.19

$$\vec{T} = -\frac{Re}{2c}\int \vec{r}\times(\vec{E}\times\vec{H}^*)\, dS$$

$$= -\frac{Re}{2c}\int \vec{r}\times(E_r H_\theta^{*}\vec{i}_\phi - E_r H_\phi^{*}\vec{i}_\theta)\, dS \qquad \ldots 3.4$$

But,

$$\frac{Re}{2}E_r H_\theta^{*} = \left(\frac{I_x I_y k^2 l^2 \sin\theta\sin a}{16\pi^2\omega\varepsilon r^3} + \frac{I_x I_z k^2 l^2 \sin\phi\cos\theta\sin b}{16\pi^2\omega\varepsilon r^3} \right.$$

$$\left. + \frac{I_y I_z k^2 l^2 \cos\phi\cos\theta\sin(a-b)}{16\pi^2\omega\varepsilon r^3} \right) \qquad \ldots 3.5$$

and

$$\frac{Re}{2}E_r H_\phi^{*} = \left(\frac{I_x I_z k^2 l^2 \cos\phi\sin b}{16\pi^2\omega\varepsilon r^3} - \frac{I_y I_z k^2 l^2 \sin\phi\sin(a-b)}{16\pi^2\omega\varepsilon r^3} \right) \qquad \ldots 3.6$$

Hence, the torque can be shown to be,

$$\left.\begin{aligned} T_x &= \frac{\mu k l^2}{6\pi} I_y I_z \sin(a-b) \\ T_y &= \frac{\mu k l^2}{6\pi} I_x I_z \sin b \\ T_z &= -\frac{\mu k l^2}{6\pi} I_x I_y \sin a \end{aligned}\right\} \ldots 3.7$$

One possible simplification of equations 3.7 results if the phases are fixed at a=120° and b=240°. Then, a torque can be obtained about an arbitrary axis by adjusting only the three antenna currents.

The direction cosines of the resulting torque axis are defined by

$$\cos\alpha = \frac{T_x}{(T_x^2 + T_y^2 + T_z^2)^{1/2}}$$

$$\cos\beta = \frac{T_y}{(T_x^2 + T_y^2 + T_z^2)^{1/2}} \quad \}...3.8$$

$$\cos\gamma = \frac{T_z}{(T_x^2 + T_y^2 + T_z^2)^{1/2}}$$

Substituting equations 3.7 in equations 3.8 with a=120° and b=240°, the expressions for the direction cosines of the torque axis become:

$$\cos\alpha = \frac{-I_{yz}}{(I_y^2 I_z^2 + I_x^2 I_z^2 + I_y^2 I_x^2)^{1/2}}$$

$$\cos\beta = \frac{-I_{xz}}{(I_y^2 I_z^2 + I_x^2 I_z^2 + I_y^2 I_x^2)^{1/2}} \quad \}...3.9$$

$$\cos\gamma = \frac{-I_{xy}}{(I_y^2 I_z^2 + I_x^2 I_z^2 + I_y^2 I_x^2)^{1/2}}$$

It is worthwhile noting that with the addition of the third antenna element the moment of inertia about any axis is the same, and is equal to the moment of inertia of the original turnstile configuration.

4. AN EXPERIMENTAL DEMONSTRATION OF THE REACTION-TORQUE

4.1 Introduction

Initially the possibility of an airborne experiment to demonstrate the reaction-torque was considered. Conceptually, the experiment consisted of supporting a torque-antenna, complete with a source of radio frequency power, with a balloon. The balloon was to rise to some fixed altitude where it would then establish itself in equilibrium with the air stream. The torque was to be measured by making remote observations of the rotational motion of the balloon antenna. However, the problems associated with designing a suitable power source and of then remotely controlling it from a ground station made this scheme quite impractical. The remaining possibility was to perform an experiment on the ground.

The experiment described in the following Sections essentially consisted of observing the rotation of a loop torque-antenna suspended, from a form of quadra-pod, directly over a large artificial earth system. This earth system effectively simulated a perfectly conducting ground plane. Since it was necessary for the torque-antenna to operate as if it were in empty space, the experiment was conducted in a large open area. Practically speaking, if an antenna is several wavelengths from any trees, power poles, buildings, or other obstructions, and if the earth is highly conducting, the operation of the antenna is essentially the same as in free space.

The artificial ground system consisted of approximately 5000 square feet of galvanized iron mesh. The mesh was supplied in 2 feet by 8 feet sheets, weighing about 3 pounds apiece. The system was constructed by first spot-welding the individual sheets end to end to form strips 72 feet long. These strips were then placed side by side, overlapped about one inch, and stapled together to lengths of 1 inch by 2 inch spruce lumber. No attempt was made to electrically insulate the screen from the actual earth.

In order to demonstrate the reaction-torque, it was

necessary for the antenna to be free to turn against the suspension. The antenna, then, could not be rigidly connected to the source of power. This difficulty was overcome by feeding power to the two loops forming the torque-antenna through a mercury switch arrangement. The ends of each loop dipped into small pools of mercury which were connected to the remainder of the electrical system. The torque-antenna made no contact other than with the mercury, leaving it completely free to rotate under the influence of even very small torques.

The basic electrical system is pictured schematically in Figure 4.1.

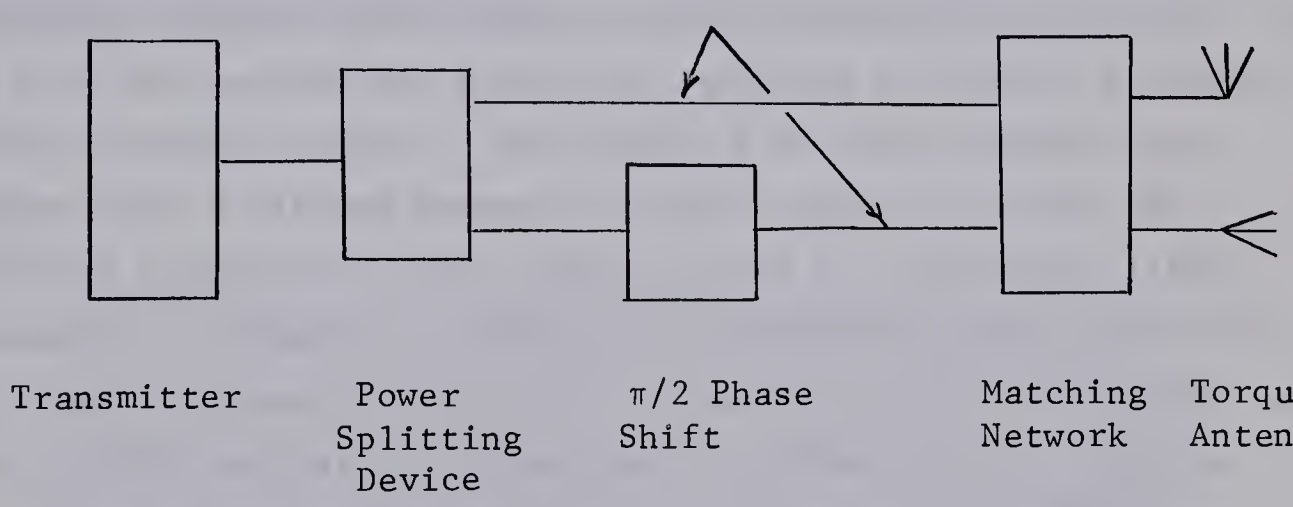

Fig. 4.1 Basic Electrical System

Power from the transmitter was divided equally to each of the loops forming the torque-antenna. The required $\pi/2$ phase shift between the loops was provided by inserting a suitable lumped element T-section in series with one line. In order to obtain maximum power transfer to the antenna, the input impedance of each loop was matched to the coaxial feed line.

The power source was an AN/FRT-501 radio frequency transmitter operating at 14.0055 megacycles. The transmitter was manufactured in 1952 by the Canadian Marconi Company for the Royal Canadian Airforce and is capable of delivering in excess of 500 watts to a 50 ohm load at any frequency between 1.5 and 15 megacycles. In practice it was found that 570 watts could be obtained easily. An input power of 2.5 Kw (115 volt, 60 cps, single phase) was required to operate the transmitter. See Figure 4.2.

The experiment was set up in a field on the University of Alberta Experimental Farm, 2 miles west of Ellerslie, Alberta. The particular field was selected because it was a low lying, swampy area. It was felt that the conductivity of this field would be somewhat higher than that of adjacent areas because the natural soil salts in the surrounding region would tend to be carried by run-off water to this lower area.

Since relatively small torques were to be measured it was absolutely essential that the antenna be suspended in still air. To this end, the antenna was housed in a plywood structure, shielding it from any wind currents. See Figure 4.3. The structure was designed with a minimum number of wooden supports so that the electrical properties of the antenna would be affected as little as possible. Mechanical rigidity was obtained by guying the four top corners as shown in Figure 4.3. The roof of this structure was made of 0.004 inch plastic sheeting to provide natural lighting within the antenna enclosure. Initially the entire shelter was made of plastic sheeting supported on a wooden framework. However, it was found that such a structure could not withstand the frequent, strong winds encountered during the course of the experiment.

The electrical equipment was housed in a small canvas tent located about eighty feet from the antenna shelter - far enough away to have negligible effect on the radiating properties of the antenna. Electrical power to run this equipment was brought to the tent by a two-wire line from an existing facility in one of the major farm

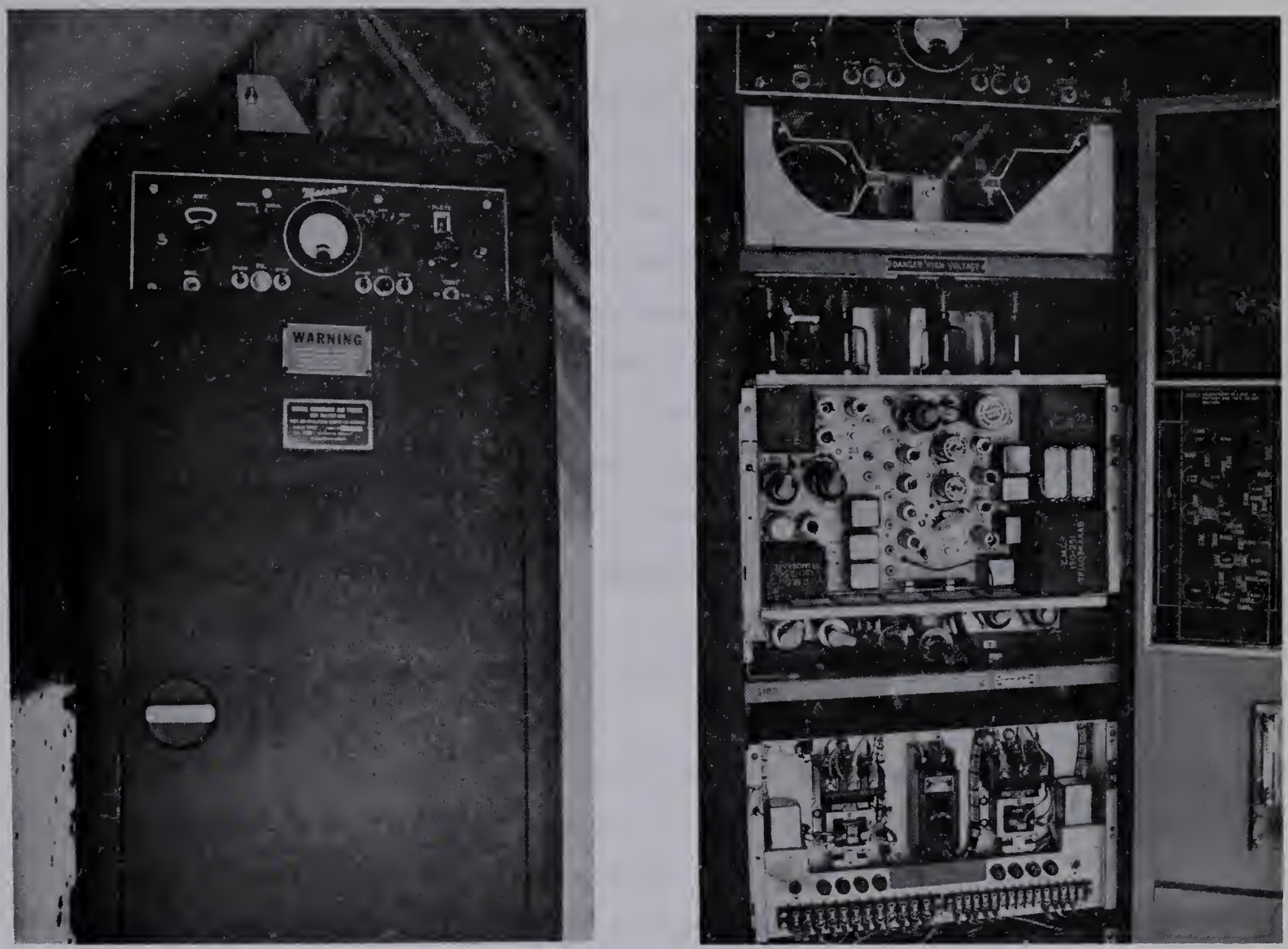

Fig. 4.2 AN/FRT 501 Transmitter

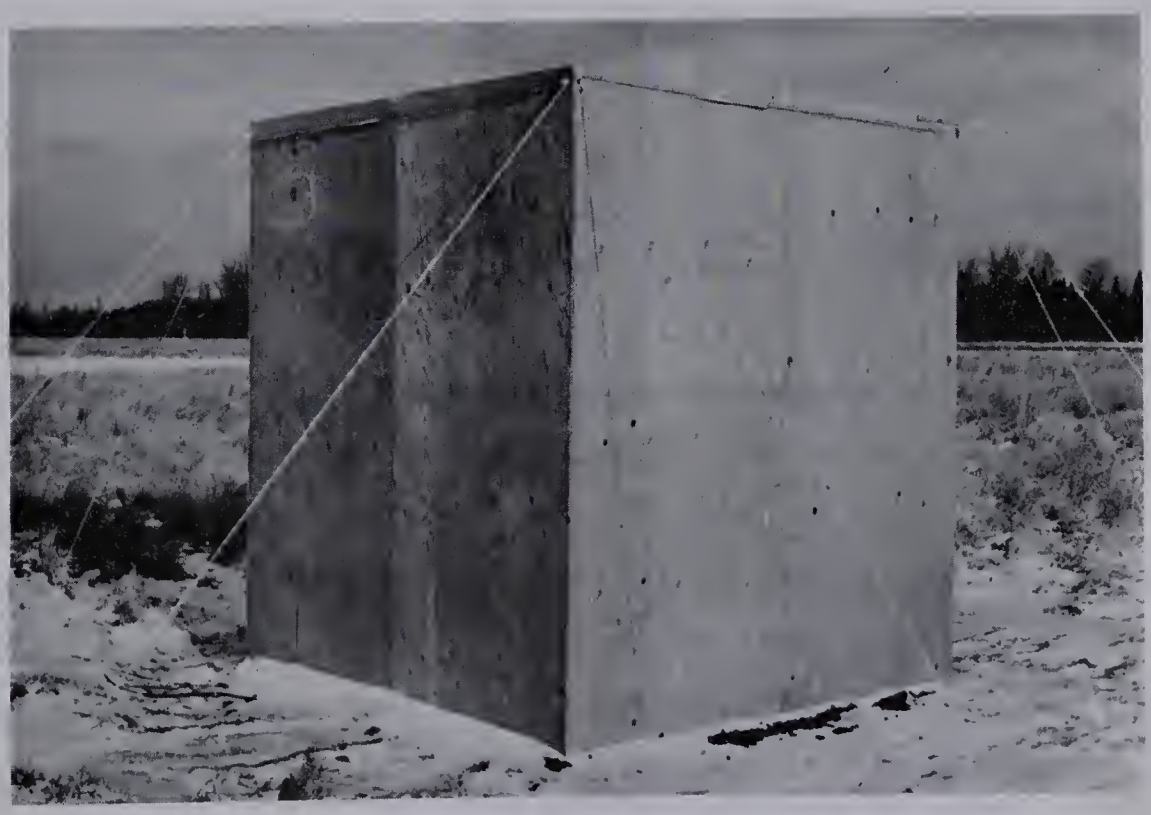

Fig. 4.3 Plywood Wind Shelter

buildings. The line consisted of No.6 weatherproofed solid copper wire supported on wooden stakes approximately 2.5 feet above the ground. The line was about 450 feet long and was capable of delivering in excess of 3Kw with negligible voltage drop at the terminals. Figure 4.4 shows the general layout of the site.

The following Sections describe in detail the development of each phase of the experiment. The major purpose of the experiment was to demonstrate that an antenna can be turned by radiating electromagnetic angular momentum, and to verify, at least qualitatively, the theoretical predictions of the amount of torque produced.

4.2 Design of the Loop Torque-Antenna and the Mercury Switch

(i) The Loop Torque-Antenna

The loop antenna configuration was chosen because the fields of the image antenna, produced by the currents flowing in the ground system, add in phase with the fields of the actual antenna. Even though the relationship between torque and power is unchanged, a given current flowing in a loop antenna over a perfectly conducting ground produces twice as much torque as that same current flowing in the antenna in free space. Effectively the radiation resistance of the antenna is doubled. For the turnstile torque-antenna, however, the radiation resistance approachs zero as the distance above the ground plane is reduced.

The design of a suitable loop torque-antenna is a compromise of many factors. Since $T = P/\omega$, it is obvious that choosing the lowest possible operating frequency will give the maximum torque for a given power. In other words a large antenna is desirable. However, a large antenna is difficult to construct and suspend. In addition the cost and complexity of the windshelter increases with increased antenna size. Another factor affecting the choice of antenna dimensions is the cost of the required ground screen. An adequate ground system must be approximately one wavelength in diameter. The cost of the screen, then, varies as the square of

Fig. 4.4 The Experimental Site

the wavelength and a low frequency ground system is very expensive.

Since the moment of inertia of the antenna system should be small, to permit the antenna to respond quickly to an applied torque, a small antenna, made of a light weight material such as aluminum, is indicated. Decreasing the antenna diameter, however, increases the operating frequency and therefore decreases the amount of torque that can be obtained with the available power. If the antenna is too small the resulting reaction torque will not be demonstrable in the presence of such disturbing torques as would result from stray wind currents.

Considering all of the above factors a diameter of 2 meters was selected for the torque-antenna. It was fabricated with aluminum tubing, 3/16 inches in diameter with a wall thickness of 0.035 inches. The optimum operating frequency was determined by plotting torque versus frequency for a fixed input power. The resulting graph is shown in Figure 4.5.

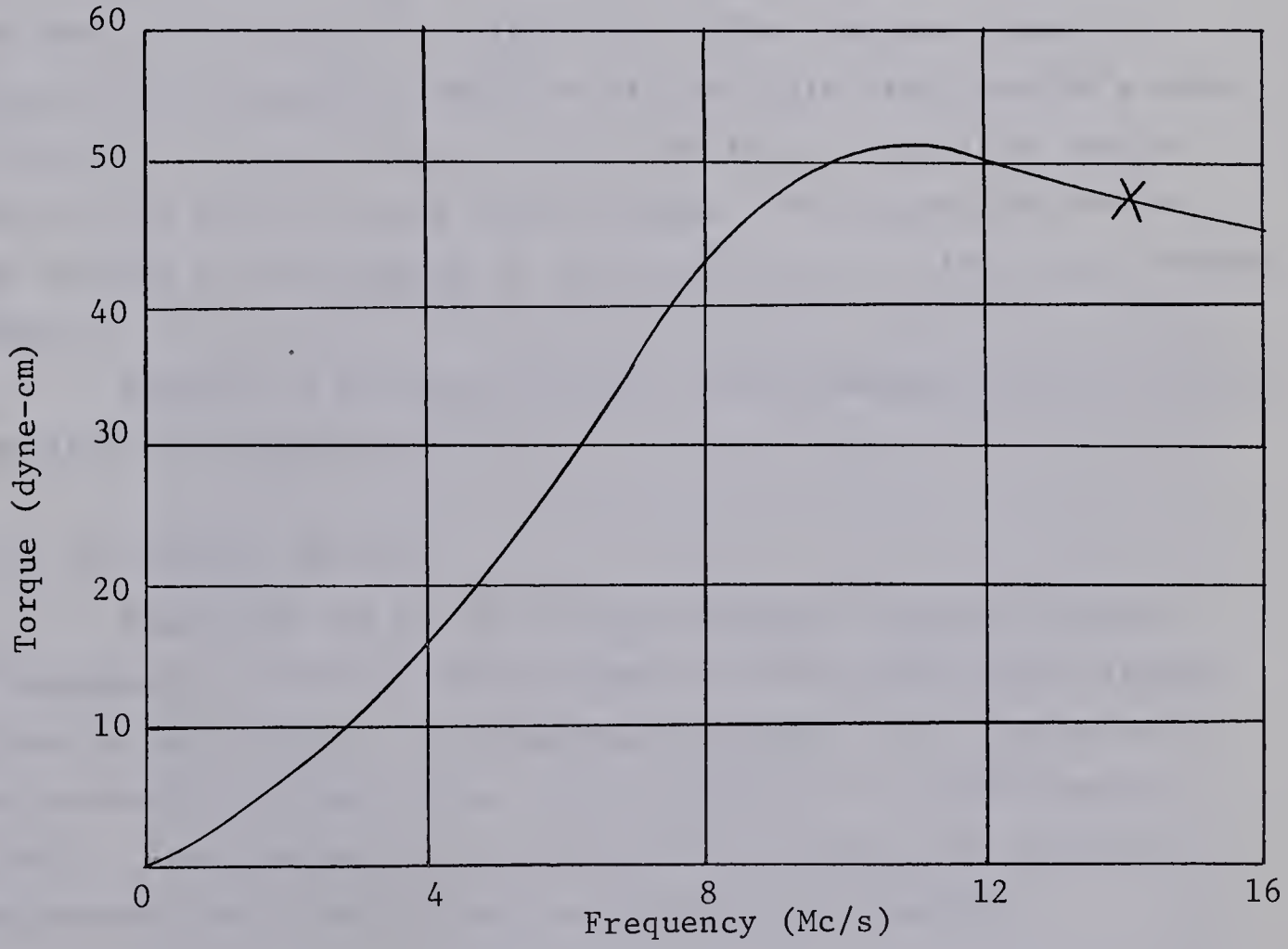

Fig. 4.5 Optimum Operating Frequency

The optimum operating frequency was approximately 11 Mcs. but to comply with Department of Transport frequency allocation regulations the actual operating frequency was taken as 14.0055 Mcs.

Each loop was formed in two half circles bent from 12 foot lengths of aluminum tubing. The antenna was held at the top by a clamping device made of lucite. The lucite clamp held two 4 inch copper tubes at right angles to one another. The ends of each loop were inserted in the copper tubes and tightened in position with small split clamps. See Figure 4.6. The feed end of the antenna was supported by a 4 inch diameter lucite cross, as shown in Figure 4.7. When suspended the antenna would not maintain its circular shape and it was necessary to fasten a nylon line of appropriate length between the upper and lower supports.

In order to measure the angular rotation of the antenna a 12 inch diameter ring, calibrated in degrees, was placed on the top of the antenna. (Figure 4.6) The ring was formed by mounting a photographic negative of the scale divisions on a strip of lucite, 1/2 inch wide and 1/16 inch thick, bent in a circle and held in place by four lucite spokes. This measuring device was mounted on the antenna as an integral part of the upper antenna support.

Figure 4.8 pictures the loop torque-antenna suspended within the plywood windshelter.

(ii) The Mercury Switch

Power was fed to the antenna through a mercury switch arrangement. Initially the feed ends of the loops simply dipped directly into mercury, as diagramed in Figure 4.9. The mercury was contained in four copper cups mounted on a 4 inch diameter circle. Each cup was 1 inch wide by 1 inch deep and permitted the antenna to rotate through approximately 55 degrees.

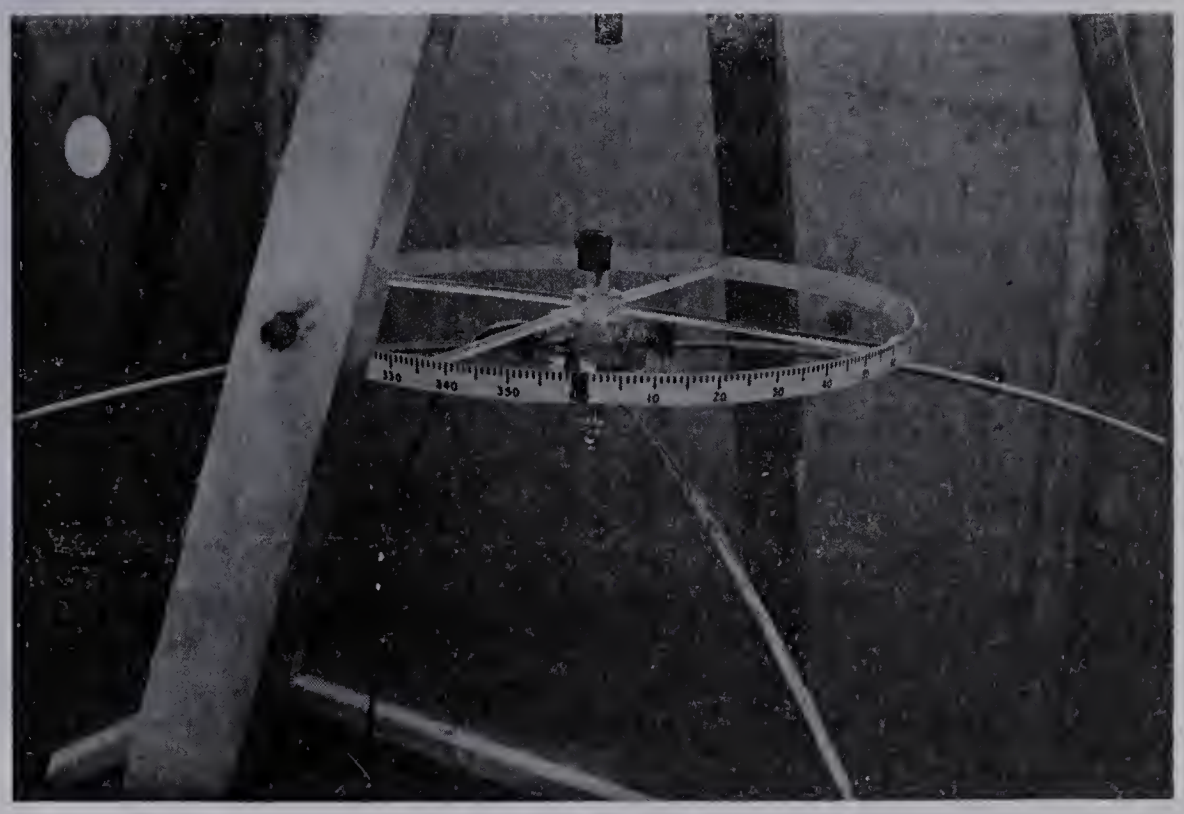

Fig. 4.6 Upper Support and Calibrated Ring

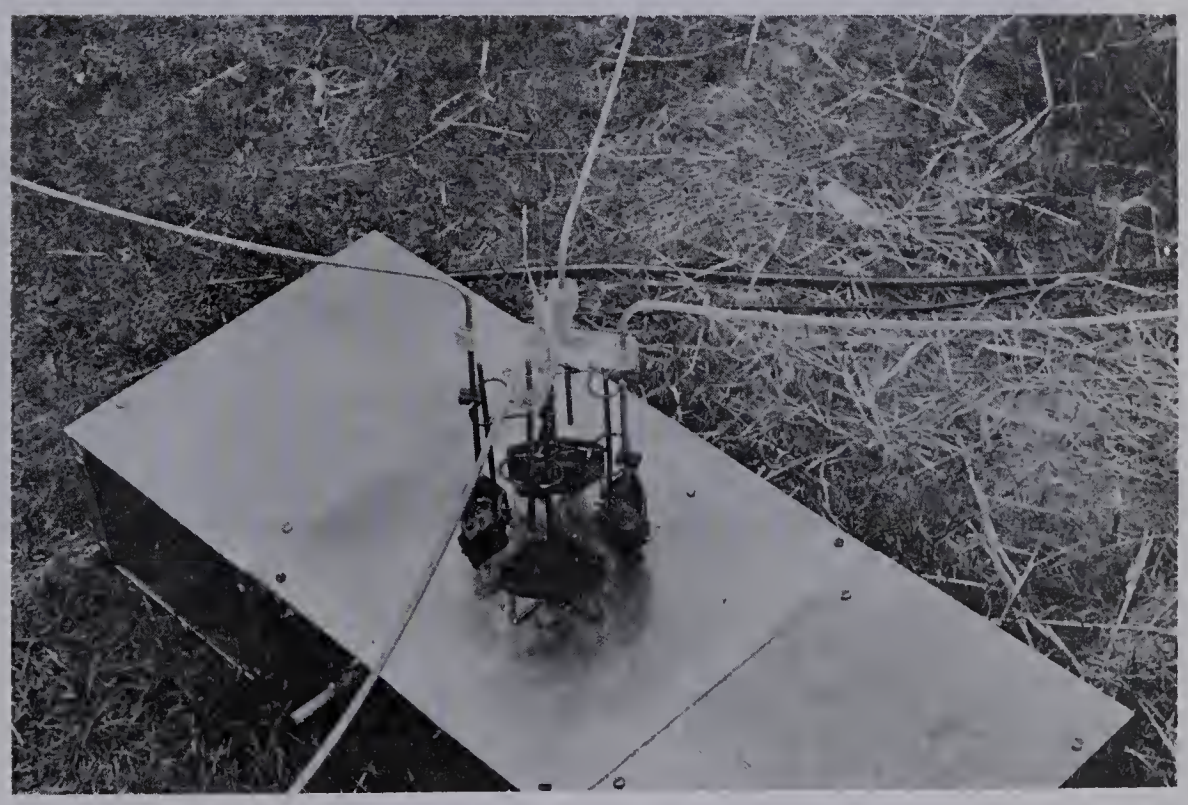

Fig. 4.7 Lower Support and Mercury Feed Assembly

Fig. 4.8 Loop Torque-Antenna

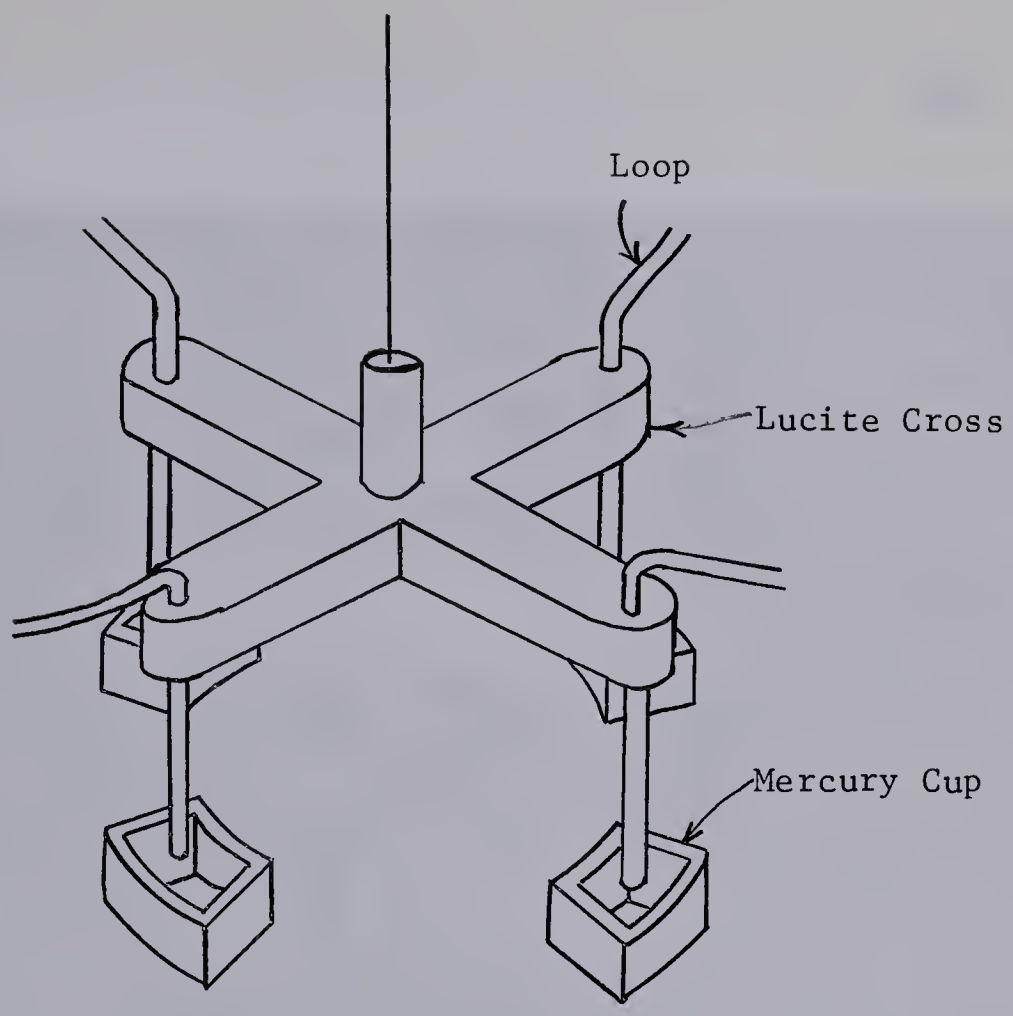

Fig. 4.9 Initial Mercury Switch

During the course of the experiment it was discovered that some static torque was being exerted on the antenna by the mercury. Instead of oscillating freely through the mercury, the antenna would remain at rest at any position within the mercury cups. Varying the diameter and the depth of penetration, in the mercury, of the ends of the loops had no noticeable effect on this static phenomenum. The static torque was not of electrical origin because the effect was the same for open and short circuit conditions. The most probable cause for this torque was surface contamination of the mercury. To circumvent this problem, the mercury cups were made much smaller and were placed on the axis of the antenna. With the cups on the axis, the ends of the loops dipping in the mercury did not actually move through the mercury but merely rotated in it. As expected the static torque of this configuration was completely negligible.

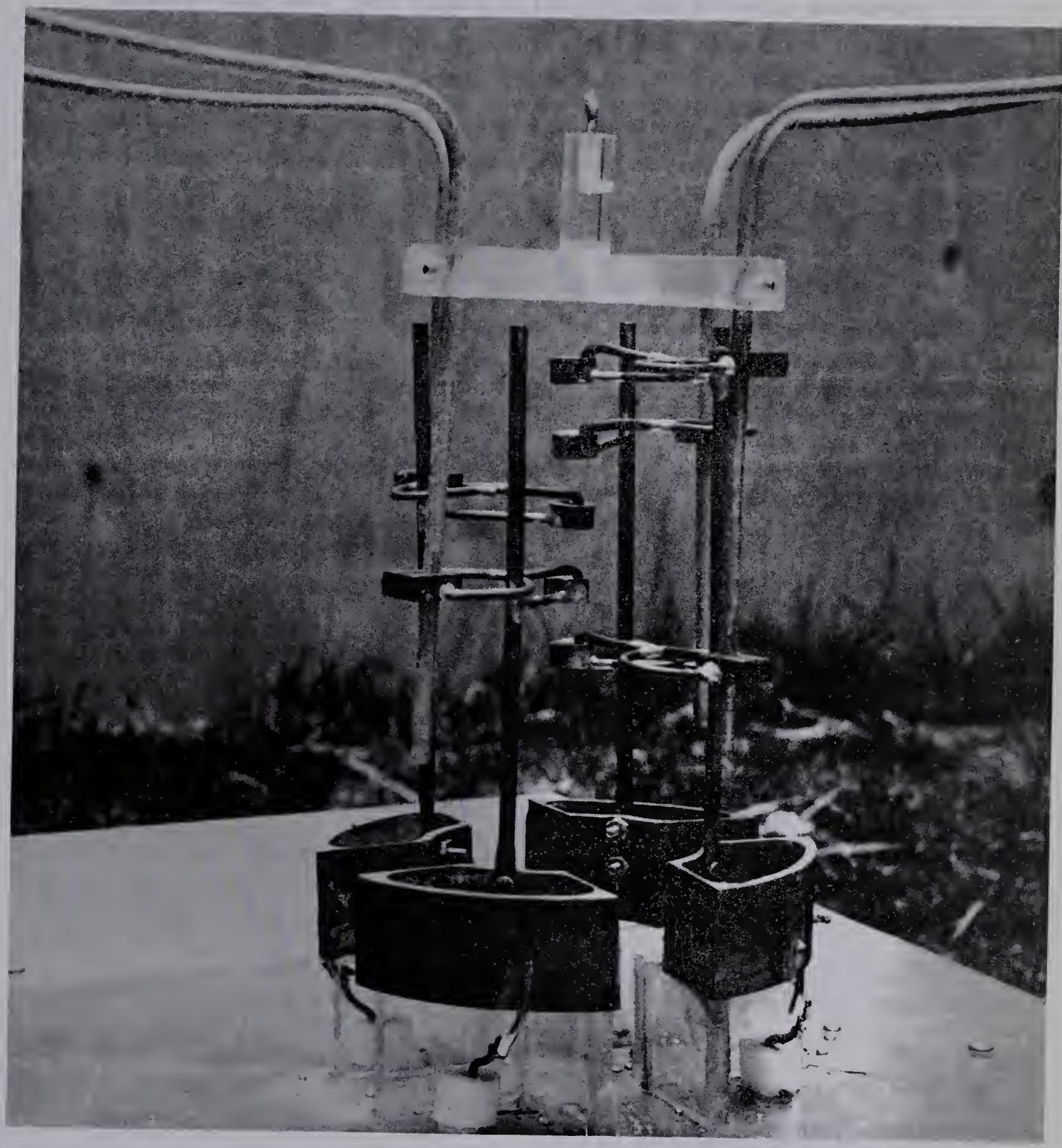

Fig. 4.10 Final Mercury Switch

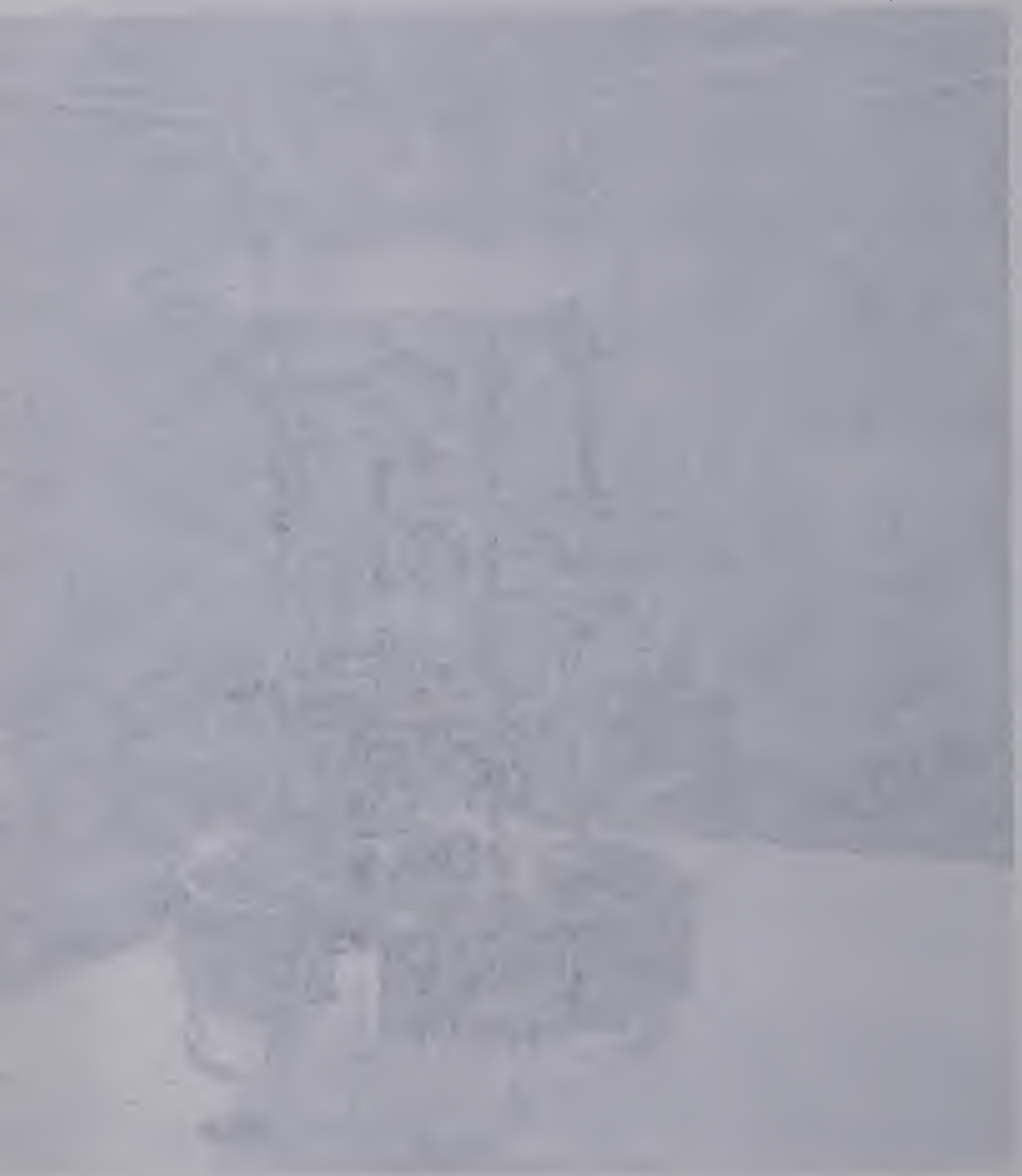

Each cup was circular in shape; 1/2 inch in diameter and 1/4 inch deep. They were mounted vertically with a 1/2 inch space between each one. See Figure 4.10. It was actually necessary to mount five cups in order to preserve the capacitive balance between the two loops forming the antenna. Any unbalance is extremely undesirable because it couples the two loops, and the input impedance becomes dependent not only on the amount of coupling but also on the relative phases of the currents flowing in the loops.

The inner surface of each cup was plated with gold. The gold permitted the mercury to wet the side of the cup resulting in a concave meniscus as shown in Figure 4.11.

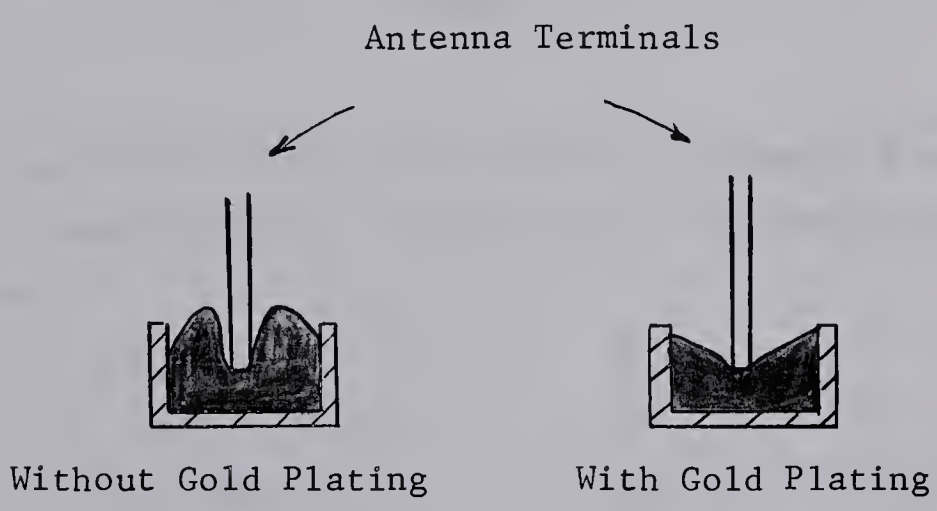

Fig. 4.11 Axial Mercury Cups

This concave meniscus helped to keep the antenna terminals centered on the axis. Without the gold plating the antenna terminals tended to rest against the side of the mercury cup.

4.3 The Fields of the Experimental Loop Torque-Antenna

In the analysis of preceding sections the loop torque-antenna has been assumed to have a uniform current distribution. Actually, at frequencies above the optimum operating frequency the distribution is no longer uniform. The torque-power relationship is unaltered and the so called radiation resistance remains approximately the same. However, the input resistance can change significantly as will be seen in a following section. In order to calculate this input resistance and the relationship between the field strengths and the radiated power, for the experimental antenna, the fields of a loop torque-antenna, with a non-uniform current distribution, over a perfectly conducting ground, must be calculated.

The current distribution of a loop whose perimeter is less than half a wavelength is adequately given by,

$$I = I_o \cos\frac{2\pi x}{\lambda} \qquad \ldots 4.1$$

where x is the distance measured along the perimeter from a point opposite the feed terminals. Figure 4.12 illustrates this current distribution.

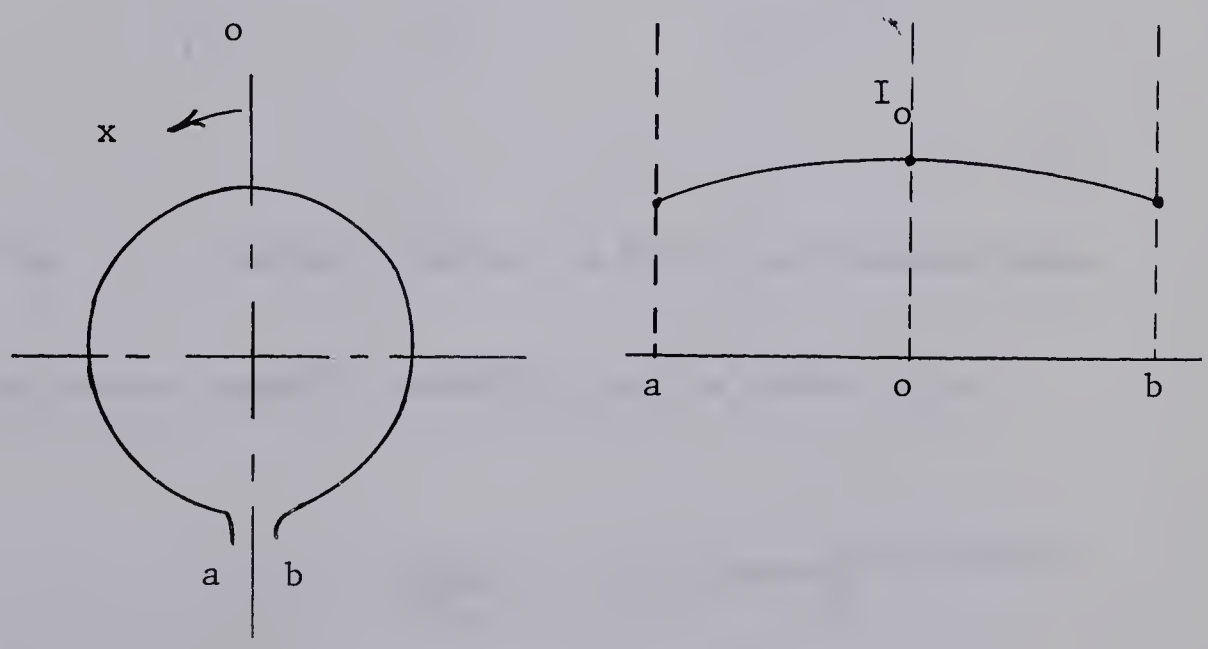

Fig. 4.12 The Current Distribution on a Loop Antenna

The mathematics can be greatly simplified, without significantly effecting the accuracy of the results, by replacing the circular loop with a square loop of the same area. The average current flowing in each side (I_b, I_s, I_f as shown in Figure 4.13) can be calculated from the current distribution in Figure 4.12. Notice that the current, I_f, contributes nothing to the radiation of a square loop over a perfectly conducting ground. The fields of the torque-antenna shown in Figure 4.13b are to be calculated.

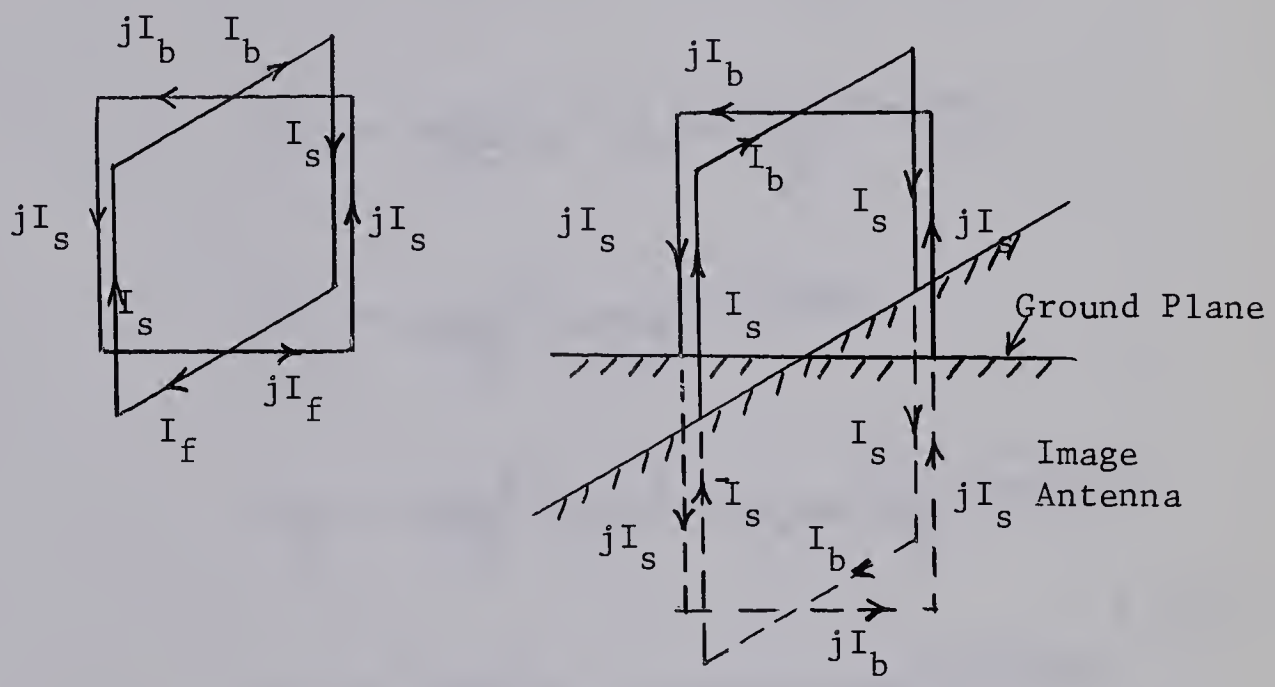

(a) (b)

Fig. 4.13 Current Flowing in Equivalent Square Loops

The vector magnetic potential can be shown to be:

$$A_r = j\mu\frac{Sk}{2\pi}(I_s - I_b)\sin\theta\cos\theta\frac{e}{r}^{j(\omega t-kr+\phi)}$$

$$A_\theta = -j\mu\frac{Sk}{2\pi}(I_s\sin^2\theta + I_b\cos^2\theta)\frac{e}{r}^{j(\omega t-kr+\phi)} \quad \}...4.2$$

$$A_\phi = \mu \frac{SkI_b}{2\pi} \cos\theta \frac{e}{r}^{j(\omega t - kr + \phi)}$$

where S is the area of one loop. From,

$$\begin{aligned} \text{curl } \vec{A} &= \vec{B} \\ \text{curl } \vec{B} &= j\omega\mu\vec{D} \end{aligned} \quad \}...4.3$$

the fields become:

$$B_r = -\mu \frac{Sk}{2\pi}(I_s + I_b)\sin\theta \frac{e}{r^2}^{j(\omega t - kr + \phi)}$$

$$B_\theta = j\mu \frac{Sk^2}{2\pi} I_b \cos\theta \frac{e}{r}^{j(\omega t - kr + \phi)}$$

$$B_\phi = -\mu \frac{Sk^2}{2\pi}(I_s \sin^2\theta + I_b \cos^2\theta) \frac{e}{r}^{j(\omega t - kr + \phi)}$$

$$\}...4.4$$

$$D_r = j \frac{3Sk^2}{2\pi\omega}(I_s - I_b)\sin\theta\cos\theta \frac{e}{r^2}^{j(\omega t - kr + \phi)}$$

$$D_\theta = -\frac{Sk^3}{2\pi\omega}(I_s \sin^2\theta + I_b \cos^2\theta) \frac{e}{r}^{j(\omega t - kr + \phi)}$$

$$D_\phi = -j \frac{Sk^3}{2\pi\omega} I_b \cos\theta \frac{e}{r}^{j(\omega t - kr + \phi)}$$

Comparing equations 4.4 with equations 2.16 shows that if the areas of the loops are equal and $I_b = I_s$, the above fields are just twice the free space fields of a circular loop torque-antenna.

The torque as given by equation 1.19 reduces to,

$$\vec{T} = -\frac{Re}{2c}\int \vec{r}\times\vec{i}_{\phi}(E_r H_{\theta}^{*} - E_{\theta}H_r^{*})\, dS \qquad ...4.5$$

Substituting equations 4.4 in equation 4.5 gives for the torque,

$$T_z = \frac{\mu S^2 k^3}{16\pi^2}\left(I_s^2\frac{32\pi}{15} + I_s I_b\frac{16\pi}{15} + I_b^2\frac{32\pi}{15}\right) \qquad ...4.6$$

This torque is just twice the torque of a circular loop torque-antenna in free space when $I_s = I_b$. It is easily shown that $T = P/\omega$.

However, if the current distribution does not have its maximum opposite the feed terminals, as would be the case if the ends of the loops were not capacitively balanced with respect to the ground plane, this simple relationship between torque and power would no longer hold. In that case only a portion of the power is radiated in a fashion that would exert a torque on the antenna. An approximate idea of the magnitude of the torque acting on an unbalanced antenna can be obtained by superimposing the fields of equation 2.16 and the fields of a z-directed current element whose vector magnetic potential is given as:

$$A_z = (1 + j)\mu\frac{I'_1 e}{4\pi r}e^{j(\omega t - kr)} \qquad ...4.7$$

where I'1 is a measure of the unbalance in the system. It is easily shown that for this case the torque is related to the power as:

$$T = \frac{1}{\left(1 + \left(\frac{I'1}{I}\right)^2 \frac{1}{k^2S^2}\right)} \cdot \frac{P}{\omega} \qquad \ldots 4.8$$

For example, if the experimental torque antenna is unbalanced such that $I'1 = 0.2I_o a$ and $I = 0.8I_o$, where I_o is the current flowing in the balanced antenna,

$$T \simeq 0.93\frac{P}{\omega} \qquad \ldots 4.9$$

The importance of ensuring the balanced operation of the torque antenna is readily apparent.

4.4 The Input Impedance of a Loop Torque-Antenna

The input impedance of the antenna must be known before the matching network, which will provide efficient coupling between the transmitter and the antenna, can be designed. The impedance of each loop forming the antenna will be the same and, since there is no mutual coupling between the two loops, it will be independent of the currents flowing in the loops.

The resistive component of the input impedance of one loop can be calculated from the radiated power as

$$I_t^2 R_a = P \qquad \ldots 4.10$$

where $P = T\omega$ and T is given by equation 4.6 and I_t is the terminal current in the loop. Therefore,

$$R_a = \omega\mu\frac{S^2k^3}{16\pi^2}\left(I_s^2\frac{32\pi}{15} + I_sI_b\frac{16\pi}{15} + I_b^2\frac{32\pi}{15}\right)\frac{1}{I_t^2} \qquad \ldots 4.11$$

Referring to Figure 4.12 the currents I_b and I_s can be approximated as

$$I_b = \frac{4}{p}\int_{-p/8}^{p/8} I_o \cos\frac{2\pi x}{\lambda}\, dx$$

$$= 0.991 I_o \qquad \ldots 4.12$$

and

$$I_s = \frac{4}{p}\int_{p/8}^{3p/8} I_o \cos\frac{2\pi x}{\lambda}\, dx$$

$$= 0.893 I_o \qquad \ldots 4.13$$

where p is the perimeter of the loop torque-antenna. I_t is calculated from equation 4.1,

$$I_t = I_o \cos\frac{\pi p}{\lambda}$$

$$= 0.604 I_o \qquad \ldots 4.14$$

Hence,

$$R_a = 2.58 \left(\frac{I_o}{I_t}\right)^2$$

$$R_a = 7.08 \text{ ohms} \qquad \ldots 4.15$$

The reactive component of a loop in free space can be adequately represented by replacing the loop with a suitable section of short-circuited transmission line.[22] Figure 4.14 diagrams a loop and its equivalent transmission line.

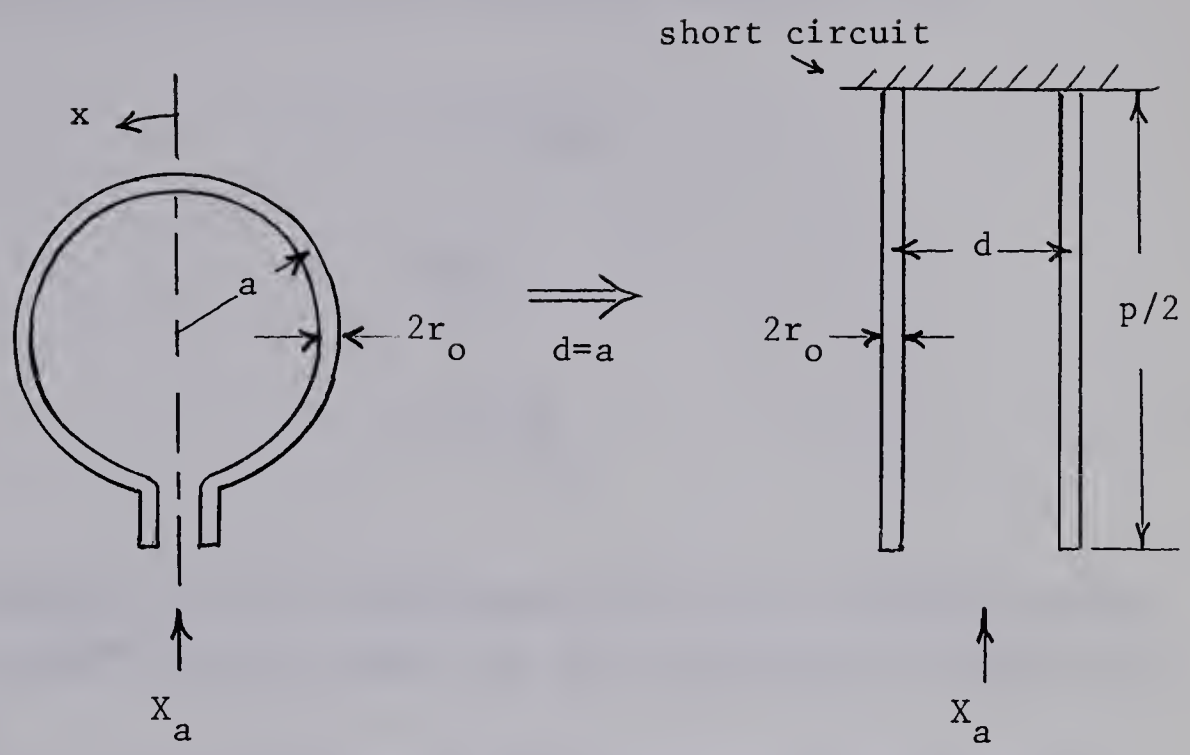

Fig. 4.14 The Transmission Line Equivalent of a Loop-Antenna

The characteristic impedance of this transmission line is given by

$$Z_o = 120 \ln \frac{a}{r_o} \qquad \ldots 4.16$$

Then, from transmission line theory

$$X_a = jZ_o \tan \frac{\pi p}{\lambda}$$

$$= j953 \qquad \ldots 4.17$$

The inductive reactance of a loop over a perfectly conducting ground can be approximated accurately enough to design the matching network by doubling the above value. It is only necessary to know the reactive component to within an order of magnitude since it will be resonated with a variable capacitor in the matching network.

The transmission line approach can be justified in the following manner. Consider the low frequency approximation of the expression for the inductive reactance (equation 4.17).

$$L = Z_o\left(\frac{2\pi}{\lambda}\right)\left(\frac{p}{2}\right)$$

$$L = \pi\frac{a}{c}Z_o$$

$$L = \mu a \ln\frac{a}{r_o} \qquad \ldots 4.18$$

This expression for the inductance of the loop is exactly equal to the commonly quoted result for the inductance of a small loop of wire.

The input impedance of the experimental loop antenna is given approximately by

$$Z_a = 7.08 + j1900 \text{ ohms} \qquad \ldots 4.19$$

4.5 The Matching Network

The matching network consisted of two identical inductive-coupling circuits, one for each loop. Schematically the circuit for a single loop is shown in Figure 4.15.

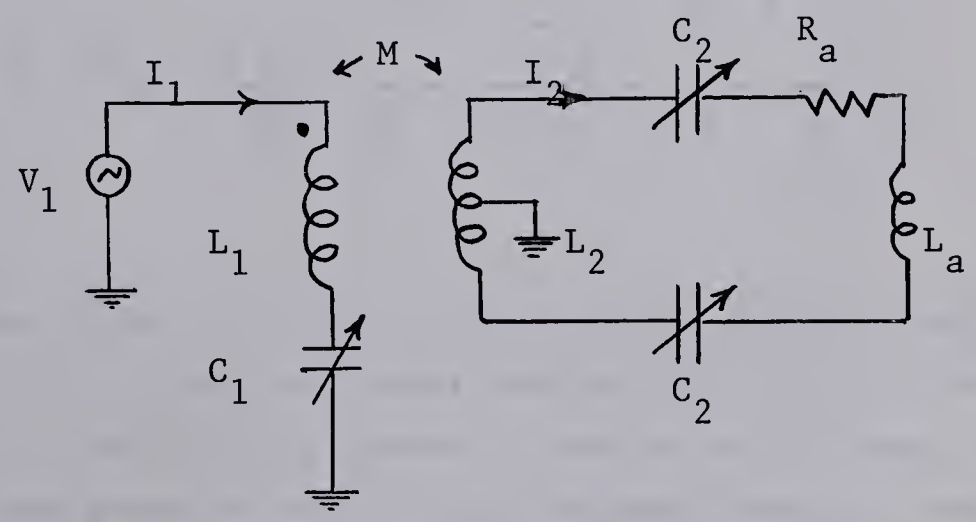

Fig. 4.15 Inductive-Coupling Network

R_a and L_a represent the loop input impedance. M is the mutual inductance.

The equation relating the voltages and currents in this circuit are:

$$\left.\begin{aligned} V_1 &= (j\omega L_1 - j\frac{1}{\omega C_1})I_1 + j\omega M I_2 \\ 0 &= j\omega M I_1 + \left(R_a + j\omega(L_a + L_2) - j\frac{2}{\omega C_2}\right)I_2 \end{aligned}\right\} \ldots 4.20$$

Solving equations 4.20 for the impedance, Z_i, seen at the input of the matching network, gives:

$$Z_i = \frac{V_1}{I_1} = j\omega L_1 - j\frac{1}{\omega C_1} + \frac{\omega^2 M^2}{R_a + j\omega(L_a + L_2) - \frac{j2}{\omega C_2}} \quad \ldots 4.21$$

Therefore,

$$R_i = \frac{\omega^2 M^2 R_a}{R_a^2 + \left(\omega(L_a + L_2) - \frac{2}{\omega C_2}\right)^2} \quad \ldots 4.22$$

and

$$X_i = j\omega L_1 - j\frac{1}{\omega C_1} + \frac{j\omega^2 M^2 \left(\frac{2}{\omega C_2} - (L_a + L_2)\right)}{R_a^2 + \left(\omega(L_a + L_2) - \frac{2}{\omega C_2}\right)^2} \quad \ldots 4.23$$

It can be seen that a wide range of R_i can be obtained with this type of matching circuit by proper choice of M, L_a, L_2, and C_2. When L_1 and C_1 are properly chosen X_i can be set to zero. To provide maximum power transfer to the antenna from the coaxial

feed line, the matching network must present a resistive termination equal to the characteristic impedance of the line. In this case,

$$Z_i = 53 + j0.0$$

The design was simplified by choosing C_2 to resonate with the inductance of the secondary $(L_a + L_2)$. Then,

$$R_i = \frac{\omega^2 M^2}{R_a}$$

$$X_i = j\omega L_1 - j\frac{1}{\omega C_1} \quad \}...4.24$$

ωL_1 was chosen to be about twice the Z_o of the line at 14 Mcs, and C_1 was a variable capacitance chosen to resonate $L_1/2$ at maximum capacitance. Hence,

$$C_1 = 250\mu\mu fd \quad \text{(maximum)}$$

$$L_1 = 1.14\mu h$$

The coil, L_1, consisted of 5 turns of No. 12 solid copper wire wound, on a 2 inch diameter form, with a pitch of 4 turns per inch. The mutual inductance calculated from equation 4.24 was about 0.22μh. Approximately the correct value of M was obtained with a secondary winding consisting of 5 turns of 1/8 inch diameter copper tubing wound, on a 2 1/8 inch diameter form, with a pitch of 4 turns per inch. C_2 was a variable capacitor with a maximum capacitance approximately double the capacitance necessary to resonate the loop. Hence,

$$\frac{2}{\omega C_2} = 1900$$

and $C_2 = 12\mu\mu fd$

The Q's of L_1 and L_2 were approximately 150 and 600 respectively. The power dissipated, then, by the matching network was calculated to be less than 5 percent of the total power radiated.

When the mercury cups were moved to the antenna axis, the capacitive reactance across the loop terminals was decreased. It was found that to provide a good match the value of C_1 had to be increased about 100μμfd. A small mica capacitor of the appropriate value, strapped in parallel with C_1, eliminated this problem.

Relatively high currents existed in the secondary circuit during operation at full power. Each antenna radiated about 250 watts and the current flowing in the loop (secondary circuit) was about 6 amperes. This current passing through the capacitor C_2 produced a peak voltage across that capacitor in excess of 8000 volts, with the secondary resonated. The high voltages involved made the design of the variable capacitors, C_2, quite critical. They consisted of 3 stator plates and 3 rotor plates, cut from 0.034 inch thick brass plate. The plate area was approximately $\pi/2$ square inches and the spacing between plates was 5/16 inch. The capacitors could be varied from about 17μμfd to 3μμfd. Each capacitor was spark tested using a current limited, high voltage d.c. supply. By polishing smooth all sharp corners and removing burrs and rough spots from the plates, the stand-off voltage of the capacitors was raised to about 10,000 volts over the entire range of adjustment.

To prevent stray coupling between the secondary circuits of the matching networks of each loop, it was necessary to completely shield each capacitor. All interconnections of components were made using RG-8U coaxial line, grounding the outer conductor. Figure 4.16 shows the matching network with the capacitors mounted.

The matching network was adjusted to match the coaxial line by varying C_1 and C_2 while monitoring the input impedance

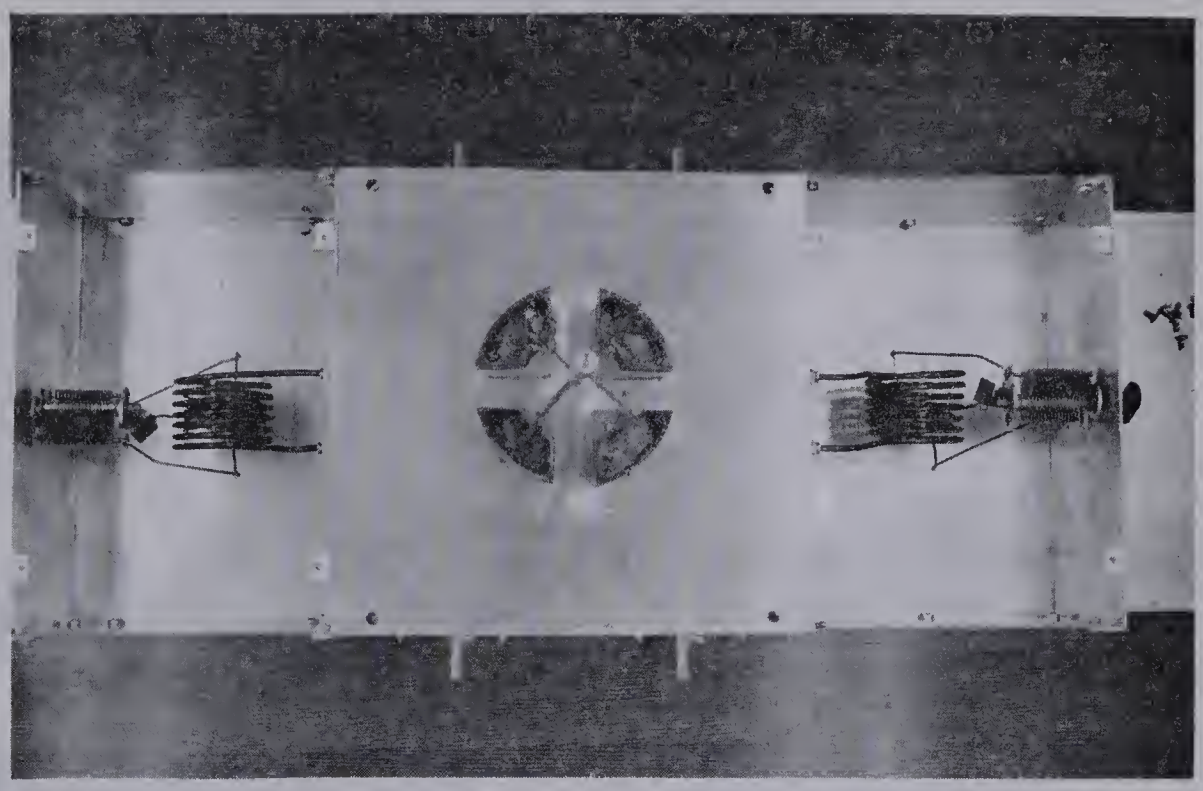

Fig. 4.16 The Matching Network

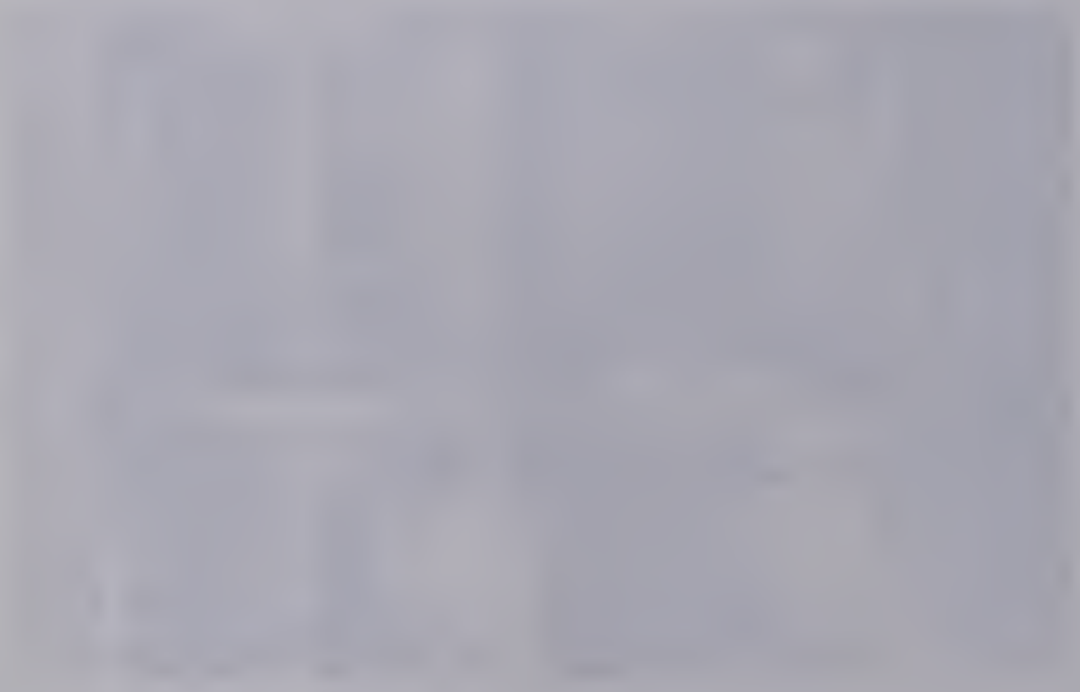

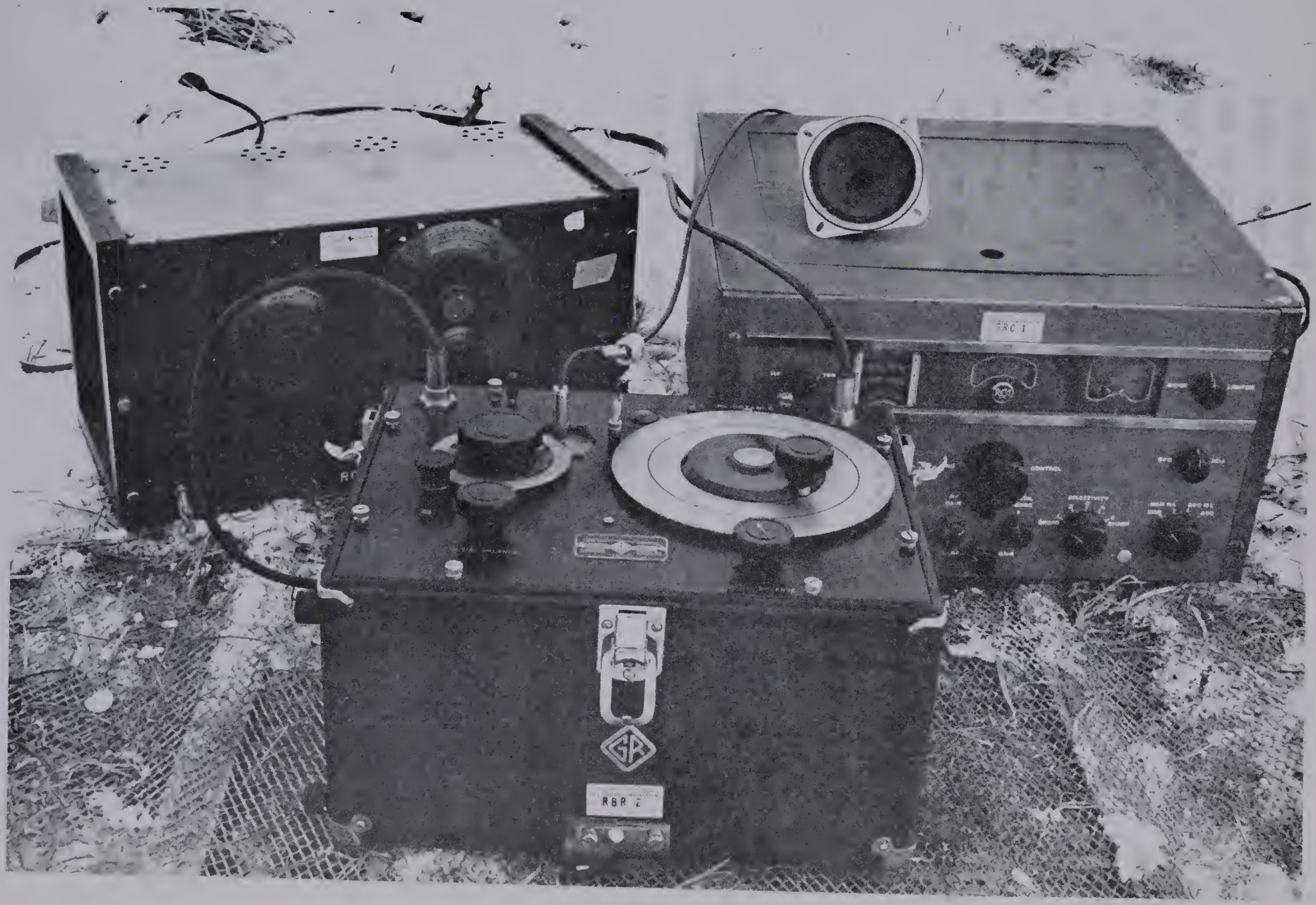

Fig. 4.17 Bridge Measuring Equipment

to the network with a radio frequency bridge (General Radio Type 916A). A standard r-f oscillator was used to drive the bridge and an RCA CR88A Communications Receiver was used as a detector. See Figure 4.17. It was necessary to place the bridge measuring-equipment at least 1/2 wavelength from the antenna to avoid serious detuning and coupling of the loops. The connection from the bridge terminals to the matching network at the antenna was made using a length of RG-58U coaxial cable cut to represent exactly one wavelength. The impedance measured by the bridge was therefore the same as that appearing at the primary of the matching network.

4.6 Phase Shifter and Power Divider

(i) Phase Shifter

The required $\pi/2$ phase shift between the loops forming the torque-antenna was provided by inserting a suitable lumped element T-section in series with one line, as shown in Figure 4.1. Figure 4.18 shows the device schematically. R_{o1} and R_{o2} are, in this case, both equal to 53 ohms.

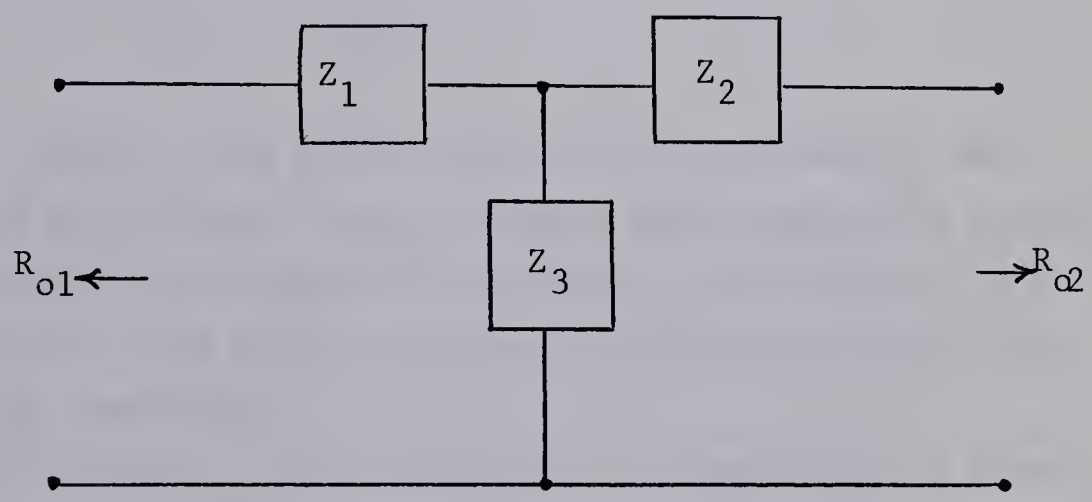

Fig. 4.18 The Phase Shifter

From the theory of 2-port networks:

$$Z_1 = j\left(\frac{-R_{o1}}{\sin\beta}\right)\left(\cos\beta - \frac{\sqrt{R_{o2}}}{R_{o1}}\right)$$

$$Z_2 = j\left(\frac{-R_{o2}}{\sin\beta}\right)\left(\cos\beta - \frac{\sqrt{R_{o1}}}{R_{o2}}\right) \quad \}...4.25$$

$$Z_3 = j\frac{-\sqrt{R_{o1}R_{o2}}}{\sin\beta}$$

where β is the phase shift through the device. β was chosen as -90 degrees. Hence, $\sin\beta = -1$ and,

$$Z_1 = -j53$$

$$Z_2 = -j53$$

$$Z_3 = +j53$$

At 14 Mcs, Z_1 and Z_2 were capacitances of 215μμfd and Z_3 was an inductance of 0.602μh. These elements were mounted in a small metal box provided with coaxial connections. Two sides of the box were replaced with metal screening to permit more efficient cooling of the components.

Experimentally, this device gave a phase shift of about 85 degrees. The phase shift was adjusted to 90 degrees by adding a suitable short length of RG-8U coaxial cable in series with the network. The phase shift was measured using an oscilloscope. Equal signals from the input and output of the network were applied

across the horizontal and vertical deflection plates of the oscilloscope. The resulting Lissajous figure was a measure of the phase difference between the two signals. The pattern was circular for a $\pi/2$ phase shift. In general the pattern is elliptical as shown in Figure 4.19.

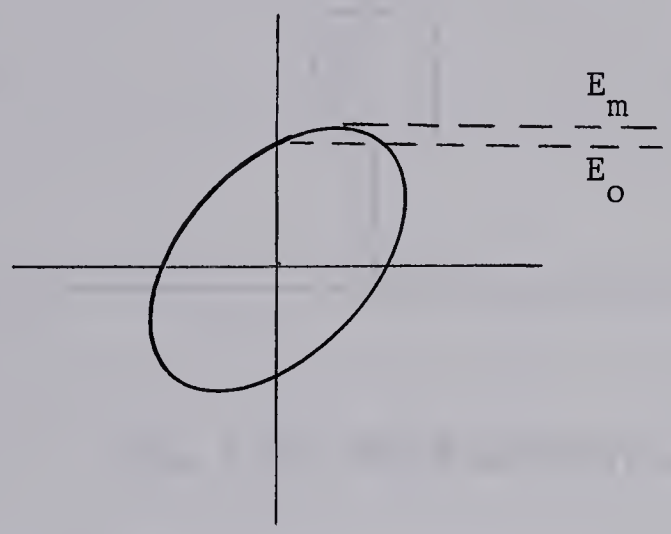

Fig. 4.19 Lissajous Figure for Determining Phase Difference

It can be shown that the phase difference, $\Delta\theta$, is given by,

$$\sin\Delta\theta = \frac{E_o}{E_m} \qquad \ldots 4.26$$

(ii) The Power-Divider

Equal power was delivered to each loop forming the torque-antenna. To accomplish this division the power from the transmitter was fed to the network shown in Figure 4.20. R_{o1} and R_{o2} are respectively 53 and 53/2 ohms. Equations 4.25 can be used to solve for Z_2 and Z_3 by setting Z_1 to zero. Hence,

$$\cos\beta = \frac{\sqrt{R_{o2}}}{R_{o1}}$$

$$= \frac{1}{\sqrt{2}}$$

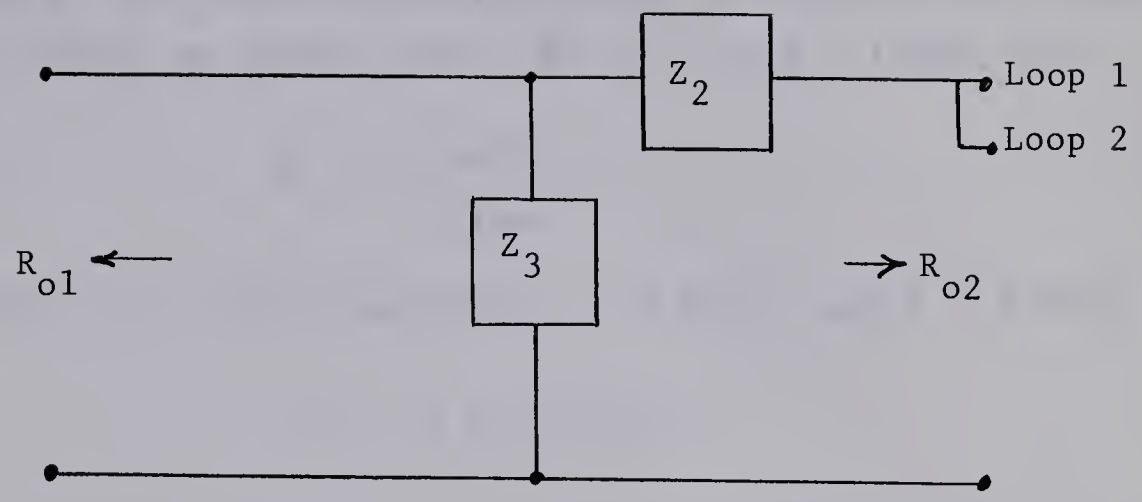

Fig. 4.20 The Power Divider

and $\beta = \pm 45$ degrees. Choosing $\beta = +45$ degrees,

$$Z_2 = j53/2$$

$$Z_3 = -j53$$

At 14 Mcs, Z_2 was an inductance of 0.302μh and Z_3 was a capacitance of 215μμfd. As before these components were mounted in a small metal box with screening to aid in cooling.

4.7 Measurements and Results

(i) Measurement of Radiated Power

The AN/FRT501 was capable of delivering approximately 500 watts to a 50 ohm load. The maximum power actually radiated from the antenna, however, was significantly less than this figure. The 100 feet of coaxial cable from the transmitter to the antenna dissipated about 80 watts. The matching networks, the phase shifter, and the power divider dissipated an additional 40 to 50 watts. Moreover, the plywood shelter and the imperfect ground plane added to the ohmic loss of the system.

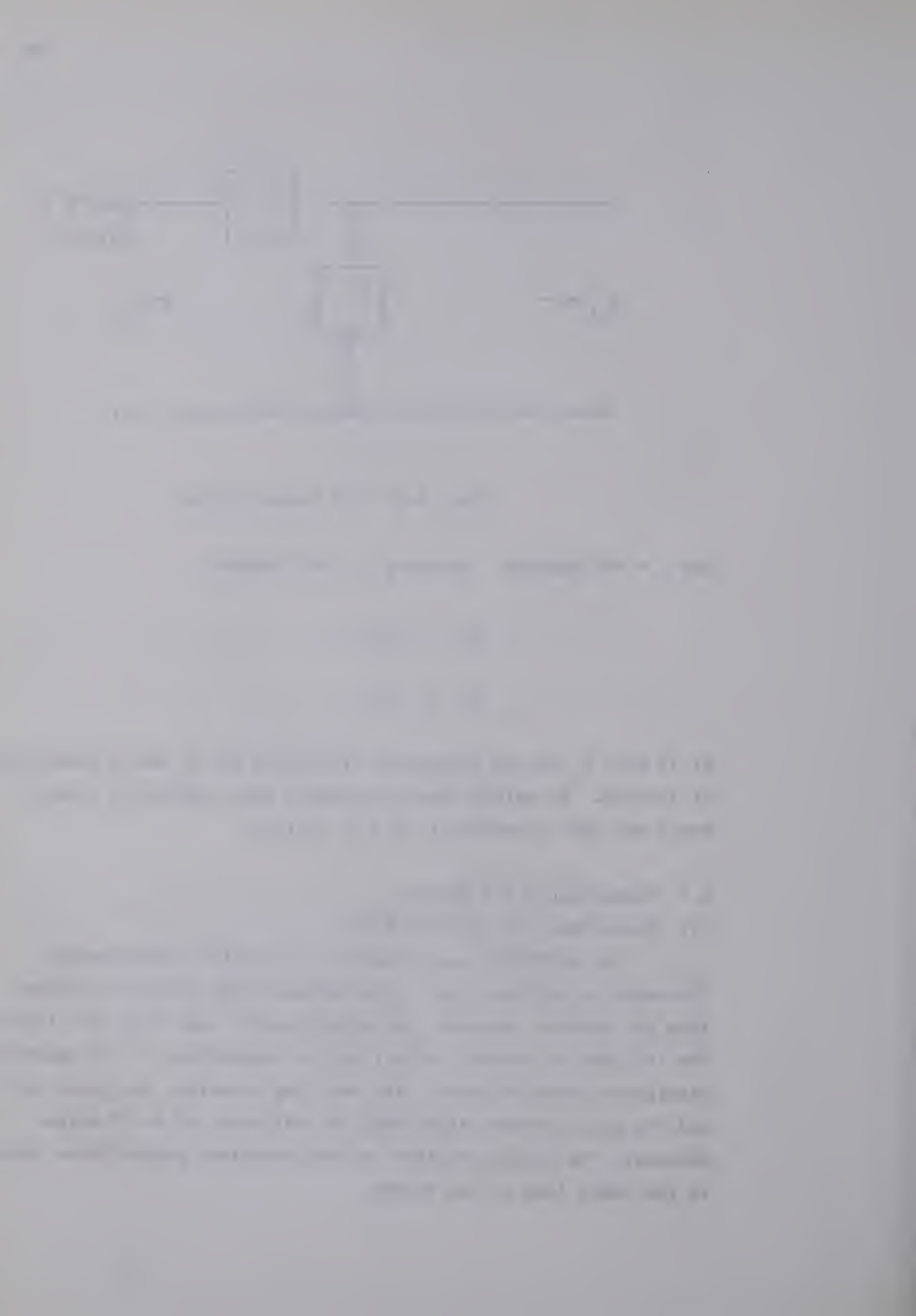

The radiated power can be obtained by making measurements of the electric field strengths at large distances from the antenna. Referring to the field expressions given by equations 4.4, the electric field, at ground level ($\theta = 90^{o}$), for r large, is,

$$E_{\theta} = \frac{-Sk^{3}I_{s}}{2\pi\omega\varepsilon r} \qquad ...4.27$$

In Section 4.4 it was shown that $I_{s} = 0.893I_{o}$, and $P = 2.58I_{o}^{2}$. Hence,

$$P = 0.0123(E_{\theta}r)^{2} \qquad ...4.28$$

Equation 4.29 can be used to calculate the radiated power corresponding to a measured value of E_{θ} by assuming that the imperfect ground plane, consisting of the galvanized iron mesh and the actual earth, does not effect the theoretical E_{θ} radiation pattern. In other words, the only effect of the ground plane is assumed to be the dissipation of a small percentage of the power. Figure 4.21 shows the actual radiation pattern of the electric field at ground level. It can be seen that this pattern deviates negligibly from the theoretically circular pattern.

The field strength measurements were made, at a distance of 5λ from the antenna, with a Ferris Radio Noise and Field Strength Meter (Model 32-D). The instrument was capable of measuring field strengths from 10^{-6} volts per meter to 1 volt per meter, over the frequency range 550Kcs to 25Mcs. In this case,

$$P = 141E_{\theta}^{2} \qquad ...4.29$$

where E_{θ} is measured in volts per meter.

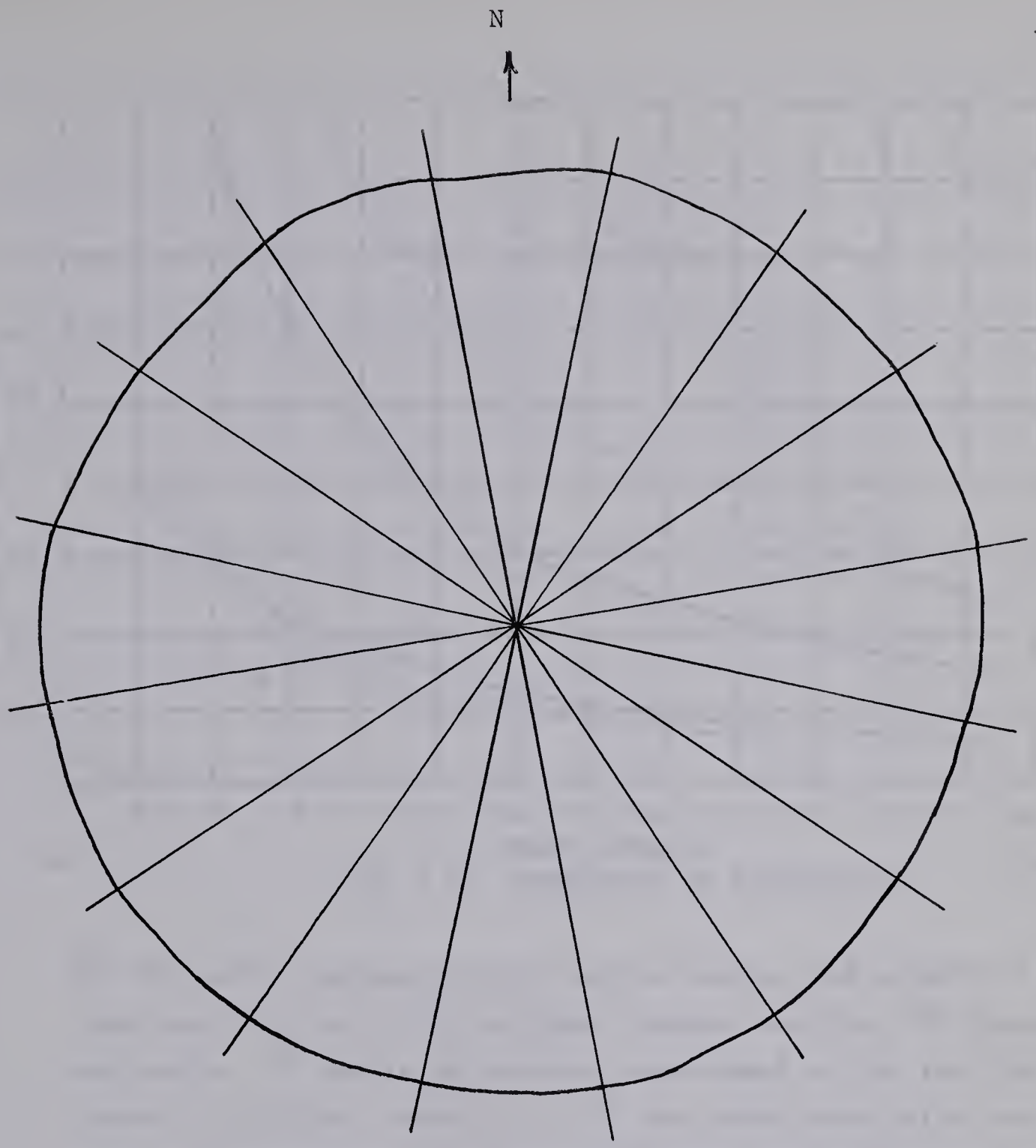

Fig. 4.21 E_θ-Radiation Pattern

(ii) Measurement of Reaction Torque

In order to demonstrate that a torque-antenna could be made to turn by radiating electromagnetic angular momentum, a suspension with relatively small restoring torque was required. Several sizes of nylon and steel line were examined in the laboratory to determine the restoring torque per radian twist as a function of the length of the suspension. Figure 4.22 shows the results.

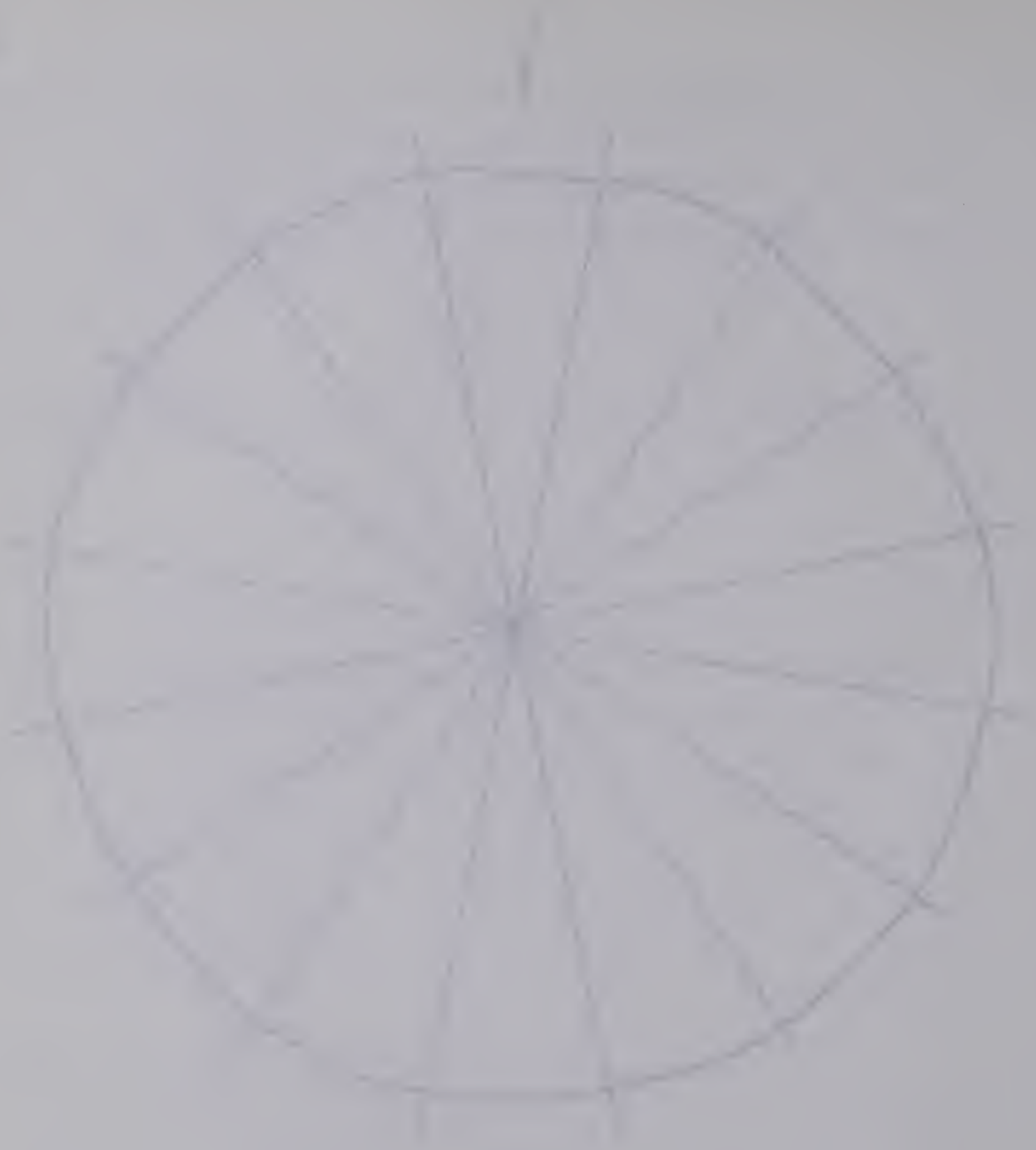

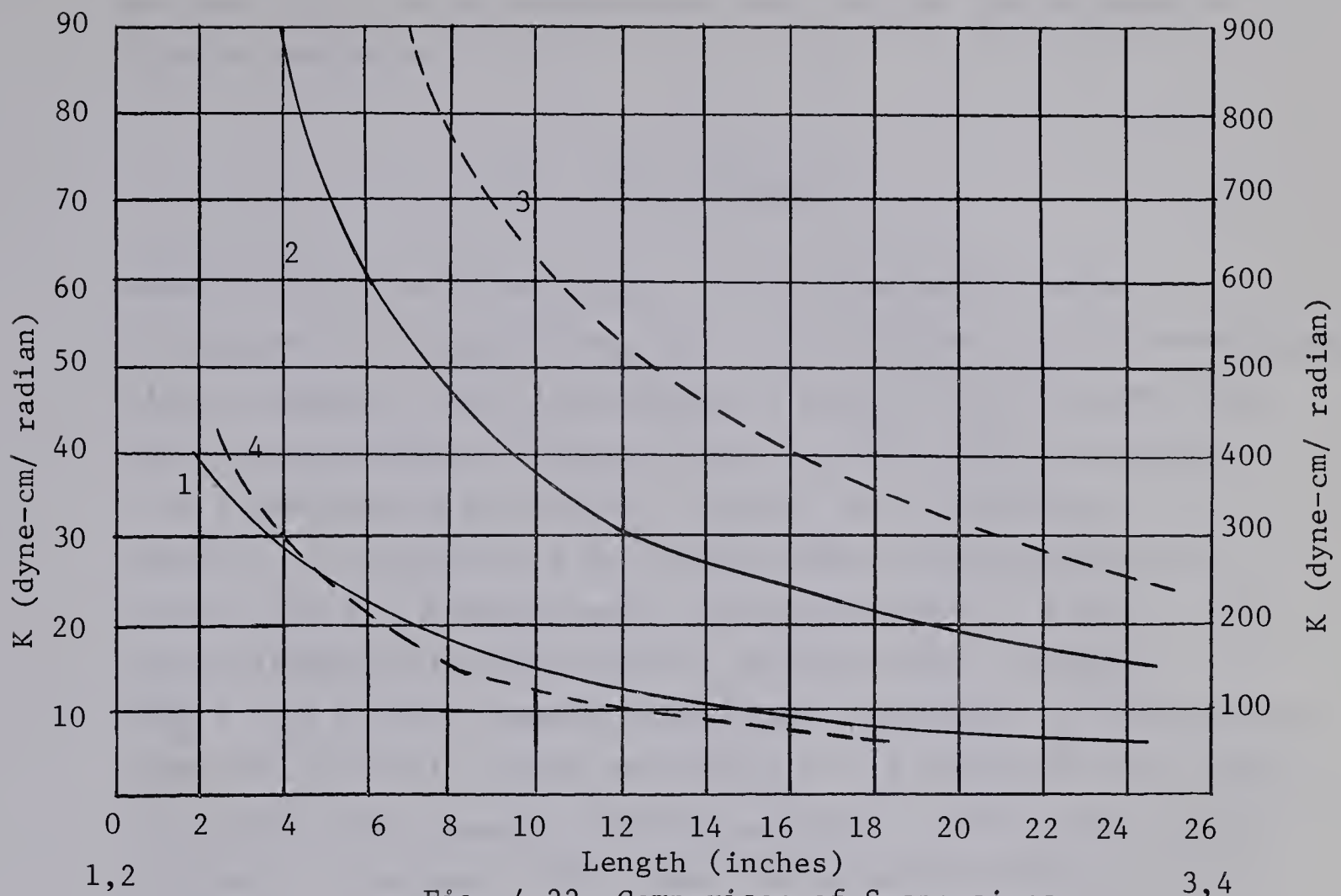

Fig. 4.22 Comparison of Suspensions

For the initial demonstrations various lengths and weights of nylon line were used, all with restoring torques less than 100 dyne-cm per radian. To obtain an accurate measurement of the reaction torque a 3 3/8 inch length of 0.005 inch steel piano wire was used as a suspension. The restoring torque was 348 dyne-cm per radian.

Two ways of measuring the reaction torque were considered, a dynamic method and a static method. In the dynamic method the antenna would be made to oscillate against the suspension. Normally the oscillation would decrease exponentially as the system lost energy. In this case, however, the transmitter would be pulsed at a regular rate, and a steady-state oscillation would be obtained when the power lost per cycle by the system just equaled the work done on the system by the reaction torque. If the transmitter is to be pulsed for half of each cycle it can

be shown that for the steady-state oscillation, the maximum deflection would be,

$$\theta_o = \frac{T}{K}\left(\frac{1}{1 - e^{-2\alpha\tau}}\right)$$

where T is the reaction torque, K is the restoring torque, τ is the period of oscillation, and α is a measure of the non-conservative viscous damping. When the damping is large as would be the case with the experimental torque antenna, $\theta_o \simeq T/K$. For a suspension of K = 200 dyne-cm per radian, τ would be of the order of 10 minutes. From Figure 2.1 a reaction torque of the order of 50 dyne-cm could be expected and, with these values of K and τ, the steady-state oscillation would be approximately 15 degrees. Such a long period, however, would make observation of this deflection very difficult. Even decreasing τ by a factor of three would not significantly improve matters especially since then θ_o would be about 1.5 degrees. This scheme was abandoned because of the relatively small deflections possible for any reasonable response time.

The second method consisted of measuring the angular difference between the equilibrium position with power off and the equilibrium position with power on. The major objection to this scheme was that any static phenomenon could cause serious error in the determination of the equilibrium positions, and hence, in the measurement of the displacement. It was found, however, that for the steel wire suspension the equilibrium point was well defined and this method was selected to measure the reaction torque.

Observations of the rotation of the antenna were made with a telescope placed some 70 feet from the antenna. The telescope was sighted through a 3 inch diameter window in the plywood shelter and focused on the calibrated ring mounted on the top of the antenna. Angular position could be measured to within half a degree quite easily.

(iii) Results

The reaction-torque on the antenna was successfully demonstrated. When a test was performed the antenna and suspension system were first allowed to establish an equilibrium. The power was then applied and the rotation of the antenna monitored with the telescope arrangement. Each time the antenna rotated as far as permitted by the mercury feeding arrangement and each time it returned to the initial starting position with negligible error. For every test the antenna turned in the same direction and at the same rate (for a given suspension). For example, with about 5 inches of 15 pound test nylon line, the antenna turned the first 9 degrees in 3 minutes on each test. Different suspensions were tried (all with restoring torques less than 100 dyne-cm per radian) and each time the antenna responded in the expected manner. With various suspensions, over a period of several days, the torque-antenna was made to turn at will, thus adequately demonstrating the reaction-torque produced by radiating electromagnetic angular momentum.

After the initial series of tests it was decided to make a quantitative measure of the reaction-torque. For this measurement the 3 3/8 inch, 0.005 inch diameter steel wire suspension was used. Before an actual test was made the antenna was forced to oscillate against the suspension by displacing it from its equilibrium position. Each time the antenna returned to the equilibrium position, thus eliminating the possibility of an error, in the measurement of the displacement, due to any static effects. The results of the quantitative test were:

Initial Position	213 degrees
Final Position	219 degrees
Total Displacement	6 degrees
E_θ at 5λ	1.7 volts per meter

From equation 4.30

$$P = 141(1.7)^2$$

$$= 406 \text{ watts}$$

Therefore, since $T = P/\omega$, the theoretical reaction torque to be expected is

$$T = \frac{406 \times 10^{-6}}{14 \times 6.28}$$

$$= 46.2 \text{ dyne-cm} \qquad \ldots 4.30$$

Now, the restoring torque on the suspension was 348 dyne-cm per radian. Hence, for a 6 degree displacement,

$$T = \frac{6}{360} .2\pi .348$$

$$= 36.5 \text{ dyne-cm} \qquad \ldots 4.31$$

Comparing 4.30 and 4.31, there is about 20 percent difference between the experimental torque and the theoretical torque. Considering the approximations involved in determining the fields, and hence, the relationship between E_θ and the radiated power, and considering the errors associated with neglecting the effect of a finitely conducting ground plane the error in measuring the radiated power was probably greater than 10 percent. Moreover, for small displacements, the accuracy with which angular position could be read introduced a considerable error. For the 6 degree displacement above, the error could be as much as 5 percent. Then, in view of the initial series of experiments and the satisfactory agreement of the quantitative results it can be stated that to within experimental error agreement with the theory is complete.

5. CONCLUSIONS

The conservation of electromagnetic momentum was discussed and it was shown that mechanical reactions could be exerted on sources of radiation. The theory of a torque-antenna was developed and applied to several practical antennas. The maximum torque obtainable from a torque-antenna occurred when the dimensions of the radiator were a small portion of a wavelength. In effect radiation efficiency was traded for torque producing efficiency in order to obtain the largest torque per watt for a given antenna. It was shown that all torque-antennas are nearly equivalent and that the final choice between them, as torque producers, depends on the particular application involved.

The discussion in Chapter Three indicated that an electromagnetic torque-antenna could be used to control the attitude of a space vehicle if care was taken to minimize the possible disturbing torques acting on the craft. The torque-antenna would provide a long-life, reliable, relatively simple device, independent of external phenomena, capable of exerting a torque about an arbitrary axis. As increasingly greater powers become available the torque-antenna could provide an attractive alternative to existing stabilization schemes. In any case the electromagnetic reaction-torque must be recognized as a possible disturbing torque on space vehicles radiating circularly polarized radiation.

A torque-antenna was designed and tested, and it was shown that to within experimental error the reaction torque agreed with the theoretical value.

REFERENCES

1. Whittaker, History of the Theories of Aether and Electricity, vol. 1., Thomas Nelson and Sons, 1953

2. de Mairan, J.J., Traité de l'Aurore boréale, p. 370, 1746

3. Bennet, A., Philosophical Transactions, p. 81, 1792

4. Lebedew, P., Astrophysical Journal, vol. 15, p. 60, 1902

5. Nichols, E.F. and Hull, G.F., Physical Review, p. 293, 1901

6. Carrara, N. and Lombardini, P., Nature, vol. 163, p. 171 1949

7. Cullen, A.L., Proc. I.E.E., vol. 99, p. 100, 1952

8. Sadowsky, A., Acta et Comentationes Imp. Universitatis Jurievensis, vol. 7, No. 1-3, 1899

9. Poynting, J.H., Proc. Royal Society, vol. 82, p. 560, 1909

10. Epstein, P.S., Annalen der Physik, vol. 44, p. 593, 1914

11. Beth, R.A., Physical Review, vol. 48, p. 471, 1935

12. Thomson, J.J., Philosophical Magazine, p. 22, 1891, p. 13, 1893, p. 331, 1904

13. Poincaré, Archives Néerland, p. 252, 1900

14. Heitler, W., Quantum Theory of Radiation, p. 401, 1957

15. Stratton, J.A., Electromagnetic Theory, McGraw Hill, 1941

16. Jasik, H., Antenna Engineering Handbook, McGraw Hill, 1961

17. Lynn, G.E; Hurt, J.G.; Harriger, K.A.; "Magnetic Control of Satellite Attitude," I.E.E.E. Trans. Communications and Electronics, vol. 83, p. 570, Sept. 1964

18. Westinghouse Electric Corporation, "Electromagnetic Attitude Control System Study," NASA CR-24 and 25, March, 1964

19. MacLaren, A.P., "A Gas Jet Attitude Control System for Satellites," Control, vol. 8, p. 446, Sept., 1964

20. Robertson, R. E., Farrior, J.S., Progress In Astronautics and Rocketry--Vol. 13--Guidance and Control I, Academic Press, New York, 1962

21. Langford, R.C., and Murdo, C.J., Progress In Astronautics and Rocketry--Vol. 13--Guidance and Control II, Academic Press, New York, 1962

22. Libby, L.L., Proc. I.R.E., vol. 34, p. 641, 1946

ADDITIONAL REFERENCES

Goddard, Physical Review, vol. 4, pp. 99-120, 1914

Roman, National Academy of Sciences, vol. 9, p. 165, 1923

Darwin, C.G., Proc. Royal Society, vol. 136, p. 36, 1932

Page, L., Physical Review, vol. 42, p. 101, 1932

Henriot, E., Compte Rendu, vol. 198, p. 1146, 1934

Halpern, O., Physical Review, vol. 48, p. 431, 1935

Holoborn, A.H.S., Nature, vol. 137, p. 31, 1936

Keller, J.M., American Journal of Physics, vol. 10, p. 302, 1942

Humblet, J., Physica, vol. 10, p. 585, 1943

Humblet, J., Physica, vol. 13, p. 17, 1947

Carrara, N., Il Nuovo Cimento, vol. 5, p. 249, 1948

Slepian, S., Proc. National Academy of Sciences, vol. 36, p. 485, 1950

Dixon, W. R., American Journal of Physics, vol. 19, p. 536, 1951

Iskraut, R.W., Nature, vol. 170, p. 1125, 1952

Ott, Annalen der Physik, vol. 11, pp. 33-44, 1952

Raudorf, W. R., American Journal of Physics, vol. 21, p. 25, 1953

Rhodes, J.E., American Journal of Physics, vol. 21, p. 683, 1953

Balazs, N.L., Physical Review, vol. 91, p. 408, 1953

Marx and Gyorgyi, Acta Phys. Hungar, vol. 3, p. 213, 1954

Rubinowicz, A. Acta Phys. Polon, vol. 14, p. 275, 1955

Dicke, R.H., Physical Review, vol. 97, p. 536, 1955

Schmutzer, Annalen der Physik, vol. 20, p. 349, 1957

Pierce, J.R., Journal of Applied Physics, vol. 30, p. 1341, 1959

Pierce, J.R., Journal of Applied Physics, vol. 32, p. 2580, 1961

Smith, W.E., Australian Journal of Physics, vol. 14, p. 152, 1961

Sturrock, Physical Review, vol. 121, p. 18, 1961

APPENDIX 1

In Section 1.2 the relationship

$$\text{div}\mathbf{M} = \vec{E}\text{div}\vec{D} - \vec{B}\times\text{curl}\vec{H} - \vec{D}\times\text{curl}\vec{E} \qquad \ldots\text{A1.1}$$

was used, where $\text{div}\mathbf{M} = \frac{\partial M_{jk}}{\partial x_k}\vec{i}_j$. Substituting for M,

$$\text{div}\mathbf{M} = \text{div}\vec{\vec{H}\vec{B}} + \text{div}\vec{\vec{E}\vec{D}} - \text{div}\psi\mathbf{U} \qquad \ldots\text{A1.2}$$

where $$\psi = \frac{1}{2}(\vec{E}\cdot\vec{D} + \vec{H}\cdot\vec{B}).$$

From the definition of divM it is easily shown that,

$$\text{div}\vec{\vec{a}\vec{b}} = \vec{a}\text{div}\vec{b} + \vec{b}\cdot\text{grad}\vec{a}$$

$$\text{div}\psi\mathbf{U} = \text{grad}\psi \qquad \ldots\text{A1.3}$$

Therefore,

$$\text{div}\mathbf{M} = \vec{B}\cdot\text{grad}\vec{H} + \vec{D}\cdot\text{grad}\vec{E} + \vec{E}\text{div}\vec{D}$$

$$- \text{grad}\frac{1}{2}(\vec{E}\cdot\vec{D} + \vec{H}\cdot\vec{B}) \qquad \ldots\text{A1.4}$$

But,

$$\text{grad}\psi = \frac{1}{2}(\vec{E}\times\text{curl}\vec{D} + \vec{D}\times\text{curl}\vec{E})$$

$$+ \frac{1}{2}(\vec{H}\times\text{curl}\vec{B} + \vec{B}\times\text{curl}\vec{H})$$

$$+ \frac{1}{2}(\vec{E}\cdot\mathrm{grad}\vec{D} + \vec{D}\cdot\mathrm{grad}\vec{E})$$

$$+ \frac{1}{2}(\vec{H}\cdot\mathrm{grad}\vec{B} + \vec{B}\cdot\mathrm{grad}\vec{H}) \qquad \ldots A1.5$$

Substituting A1.5 in A1.4 gives:

$$\mathrm{divM} = \vec{E}\mathrm{div}\vec{D} - \vec{B}\times\mathrm{curl}\vec{H} - \vec{D}\times\mathrm{curl}\vec{E} \qquad \ldots A1.6$$

which establishes equation A1.1.

APPENDIX 2

In Section 1.2 use was made of the following equation:

$$\int \vec{r}\times\text{div}M\ dv = \int \vec{r}\times M\cdot\vec{n}\ dS \qquad \ldots A2.1$$

In order to establish this relationship consider the integrand on the left hand side of A2.1.

$$\vec{r}\times\text{div}M = \vec{r}\times(\text{div}\vec{H}\vec{B} + \text{div}\vec{E}\vec{D} + \text{div}\psi U)$$

$$= (\vec{r}\times\vec{H})\text{div}\vec{B} + \vec{r}\times(\vec{B}\cdot\text{grad}\vec{H}) + (\vec{r}\times\vec{E})\text{div}\vec{D}$$

$$+ \vec{r}\times(\vec{D}\cdot\text{grad}\vec{E}) + \vec{r}\times\text{div}(\psi\vec{i}_k\vec{i}_k) \qquad \ldots A2.2$$

But,

$$\text{div}(\vec{r}\times\vec{H})\vec{B} = (\vec{r}\times\vec{H})\text{div}\vec{B} + \vec{B}\cdot\text{grad}(\vec{r}\times\vec{H})$$

$$(\vec{r}\times\vec{H})\text{div}\vec{B} + \vec{r}\times(\vec{B}\cdot\text{grad}\vec{H}) + (\vec{B}\cdot\text{grad}\vec{r})\times\vec{H}$$

$$= (\vec{r}\times\vec{H})\text{div}\vec{B} + \vec{r}\times(\vec{B}\cdot\text{grad}\vec{H}) + \vec{B}\times\vec{H} \qquad \ldots A2.3$$

Similarly,

$$\text{div}(\vec{r}\times\vec{E})\vec{D} = (\vec{r}\times\vec{E})\text{div}\vec{D} + \vec{r}\times(\vec{D}\cdot\text{grad}\vec{E}) + \vec{D}\times\vec{E} \qquad \ldots A2.4$$

Also,

$$\begin{aligned} \mathrm{div}(\vec{r}\times\psi\vec{i}_k)\vec{i}_k &= (\vec{r}\times\psi\vec{i}_k)\mathrm{div}\vec{i}_k + \vec{i}_k\cdot\mathrm{grad}(\vec{r}\times\psi\vec{i}_k) \\ &= \vec{r}\times(\vec{i}_k\cdot\mathrm{grad}\psi\vec{i}_k) + (\vec{i}_k\cdot\mathrm{grad}\vec{r})\times\psi\vec{i}_k \\ &= \vec{r}\times\mathrm{grad}\psi + \vec{i}_k\times\vec{i}_k \\ &= \vec{r}\times\mathrm{div}\psi U \end{aligned} \qquad \ldots A2.5$$

Therefore substituting equations A2.3 to A2.5 in equation A2.2,

$$\vec{r}\times\mathrm{div}M = \mathrm{div}(\vec{r}\times\vec{H})\vec{B} + \mathrm{div}(\vec{r}\times\vec{E})\vec{D} + \mathrm{div}(\vec{r}\times\psi\vec{i}_k)\vec{i}_k \qquad \ldots A2.6$$

Integrating both sides of equation A2.6 gives

$$\begin{aligned} \int \vec{r}\times\mathrm{div}M\ dv &= \int \mathrm{div}(\vec{r}\times\vec{H})\vec{B}\ dv + \int \mathrm{div}(\vec{r}\times\vec{E})\vec{D}\ dv + \int \mathrm{div}(\vec{r}\times\psi\vec{i}_k)\vec{i}_k\ dv \\ &= \int (\vec{r}\times\vec{H})\vec{B}\cdot\vec{n}\ dS + \int (\vec{r}\times\vec{E})\vec{D}\cdot\vec{n}\ dS + \int \psi\vec{r}\times\vec{n}\ dS \\ &= \int \vec{r}\times M\cdot\vec{n}\ dS \end{aligned} \qquad \ldots A2.7$$

which is just equation A2.1.

APPENDIX 3

The purpose of this Appendix is to show that, to within some negligible terms, the radial component of Maxwell's Stress Tensor can be replaced by the Poynting vector (with a change in sign) divided by the velocity of light in a vacuum. In other words it will be shown that

$$- M\cdot\vec{i}_r = \frac{\vec{E}\times\vec{H}}{c} \qquad \ldots A3.1$$

To establish this equation, consider the field of a system of localized sources. Then,

$$\vec{E} = \vec{E}_1 + \vec{E}_2 + \vec{E}_3 + O(r^{-3})$$

$$\vec{H} = \vec{H}_1 + \vec{H}_2 + \vec{H}_3 + O(r^{-3}) \qquad \ldots A3.2$$

where $\vec{E}_1$ and $\vec{H}_1$ are the transverse fields varying as r^{-1}, $\vec{E}_2$ and $\vec{H}_2$ are the longitudinal fields varying as r^{-2}, and $\vec{E}_3$ and $\vec{H}_3$ are the transverse fields varying as r^{-2}. $O(r^{-n})$ refers to terms vanishing as $1/r^n$, $1/r^{n+1}$, $1/r^{n+2}$,... as r goes to infinity.

Let $\vec{i}_r$ be a unit vector normal to a spherical surface centered at the origin and directed in the positive r direction. Hence,

$$\vec{E}_1\cdot\vec{i}_r = \vec{E}_3\cdot\vec{i}_r = \vec{H}_1\cdot\vec{i}_r = \vec{H}_3\cdot\vec{i}_r = 0$$

$$\vec{E}_2\cdot\vec{i}_r = \vec{H}_2\cdot\vec{i}_r = 0 \qquad \ldots A3.3$$

$$\vec{E}\cdot\vec{i}_r = \vec{E}_2\cdot\vec{i}_r + O(r^{-3})$$

$$\vec{H}\cdot\vec{i}_r = \vec{H}_2\cdot\vec{i}_r + O(r^{-3})$$

Now,

$$\vec{E}\times\vec{H} = \vec{E}_1\times\vec{H} + (\vec{E}_2 + \vec{E}_3)\times\vec{H} + O(r^{-4})$$

$$= \eta(\vec{H}_1\times\vec{i}_r)\times(\vec{H}_1 + \vec{H}_2 + \vec{H}_3) + \frac{1}{\eta}(\vec{E}_2 + \vec{E}_3)\times(\vec{i}_r\times\vec{E}_1) + O(r^{-4}) \quad \ldots A3.4$$

Therefore,

$$\frac{\vec{E}\times\vec{H}}{c} = \mu(\vec{H}_1\cdot\vec{H}_1 + \vec{H}_1\cdot\vec{H}_3)\vec{i}_r - \mu(\vec{H}_2\cdot\vec{i}_r)\vec{H}_1 - \varepsilon(\vec{E}_2\cdot\vec{i}_r)\vec{E}_1 + \varepsilon(\vec{E}_3\cdot\vec{E}_1)\vec{i}_r + O(r^{-4}) \quad \ldots A3.5$$

Now,

$$\psi = \frac{1}{2}(\mu\vec{H}\cdot\vec{H} + \varepsilon\vec{E}\cdot\vec{E})$$

$$= \frac{1}{2}(\mu\vec{H}_1\cdot\vec{H}_1 + 2\mu\vec{H}_1\cdot\vec{H}_3 + \varepsilon\vec{E}_1\cdot\vec{E}_1 + 2\varepsilon\vec{E}_1\cdot\vec{E}_3) + O(r^{-4})$$

$$= \mu(\vec{H}_1\cdot\vec{H}_1 + \vec{H}_1\cdot\vec{H}_3) + (\vec{E}_1\cdot\vec{E}_3) + O(r^{-4})$$

Hence,

$$\psi\vec{i}_r = \mu(\vec{H}_1\cdot\vec{H}_1 + \vec{H}_1\cdot\vec{H}_3)\vec{i}_r + \varepsilon(\vec{E}_1\cdot\vec{E}_3)\vec{i}_r + O(r^{-4}) \quad \ldots A3.6$$

Therefore,

$$\frac{\vec{E}\times\vec{H}}{c} = \psi\vec{i}_r - \mu(\vec{H}_2\cdot\vec{i}_r)\vec{H}_1 - \varepsilon(\vec{E}_2\cdot\vec{i}_r)\vec{E}_1 + O(r^{-4})$$

Substituting equation A3.3 into the above expression gives:

$$\frac{\vec{E}\times\vec{H}}{c} = \psi\vec{i}_r - \mu(\vec{H}\cdot\vec{i}_r)\vec{H} - \varepsilon(\vec{E}\cdot\vec{i}_r)\vec{E} + O(r^{-4})$$

$$= -M\cdot\vec{i}_r + O(r^{-4}) \qquad \ldots A3.7$$

which establishes equation A3.1

APPENDIX 4

Referring to Figure 2.2 the following relationships are readily apparent:

$$\begin{aligned} \sin\theta\cos\phi &= \sin\theta'\cos\phi' \\ \sin\theta\sin\phi &= \cos\theta' \\ \cos\theta &= -\sin\theta'\sin\phi' \end{aligned} \qquad \ldots A4.1$$

and

$$\begin{aligned} \vec{i}_x &= -\sin\phi\vec{i}_\phi + \sin\theta\vec{i}_r + \cos\theta\cos\phi\vec{i}_\theta \\ &= -\sin\phi'\vec{i}_{\phi'} + \sin\theta'\cos\phi'\vec{i}_{r'} + \cos\theta'\cos\phi'\vec{i}_{\theta'} \end{aligned}$$

$$\begin{aligned} \vec{i}_y &= \sin\theta\sin\phi\vec{i}_r + \cos\theta\sin\phi\vec{i}_\theta + \cos\phi\vec{i}_\phi \\ &= \cos\theta'\vec{i}_{r'} - \sin\theta'\vec{i}_{\theta'} \end{aligned} \qquad \ldots A4.2$$

$$\begin{aligned} \vec{i}_z &= \cos\theta\vec{i}_r - \sin\theta\vec{i}_\theta \\ &= -\sin\theta'\sin\phi'\vec{i}_{r'} - \cos\theta'\sin\phi'\vec{i}_{\theta'} - \cos\phi'\vec{i}_{\phi'} \end{aligned}$$

Similarly,

$$\begin{aligned} \sin\theta\cos\phi &= \cos\theta'' \\ \sin\theta\sin\phi &= \sin\theta''\sin\phi'' \\ \cos\theta &= -\sin\theta''\cos\phi'' \end{aligned} \qquad \ldots A4.3$$

and

$$\begin{aligned} \vec{i}_x &= -\sin\phi\vec{i}_\phi + \sin\theta\cos\phi\vec{i}_r + \cos\theta\cos\phi\vec{i}_\theta \\ &= \cos\theta''\vec{i}_{r''} - \sin\theta''\vec{i}_{\theta''} \end{aligned}$$

$$\begin{aligned} \vec{i}_y &= \sin\theta\sin\phi\vec{i}_r + \cos\theta\sin\phi\vec{i}_\theta + \cos\phi\vec{i}_\phi \\ &= \sin\theta''\sin\phi''\vec{i}_{r''} + \cos\theta''\sin\phi''\vec{i}_{\theta''} + \cos\phi''\vec{i}_{\phi''} \end{aligned} \qquad \ldots A4.4$$

$$\begin{aligned} \vec{i}_z &= \cos\theta\vec{i}_r - \sin\theta\vec{i}_\theta \\ &= \sin\phi''\vec{i}_{\phi''} - \sin\theta''\cos\phi''\vec{i}_{r''} - \cos\theta''\cos\phi''\vec{i}_{\theta''} \end{aligned}$$

In order to express the electric field in terms of the unprimed variables described in Section 2.2, $\sin\theta'\vec{i}_{\phi'}$ and $\sin\theta''\vec{i}_{\phi''}$ must be known in terms of r,θ and ϕ. From equations A4.1 and A4.2,

$$- \sin\theta'\sin\phi'^{2}\vec{i}_{\phi'} + \sin\theta'\cos\theta'\cos\phi'\sin\phi'\vec{i}_{\theta'}$$

$$= - \sin\theta\sin\phi\sin\phi'\vec{i}_{\phi} + \sin\theta'\cos\theta\cos\phi\sin\phi'\vec{i}_{\theta} \quad \ldots A4.5$$

and

$$-\sin\theta'\cos\phi'^{2}\vec{i}_{\phi'} - \sin\theta'\cos\theta'\sin\phi'\cos\phi'\vec{i}_{\theta'}$$

$$= - \sin\theta\sin\theta'\cos\phi'\vec{i}_{\theta} \quad \ldots A4.6$$

Adding A4.5 and A4.6 and using equation A4.1,

$$\sin\theta'\vec{i}_{\phi'} = - \sin\phi\cos\theta\vec{i}_{\phi} + \cos\phi\vec{i}_{\theta} \quad \ldots A4.7$$

Similarly,

$$\sin\theta''\vec{i}_{\phi''} = - \cos\phi\cos\theta\vec{i}_{\phi} - \sin\phi\vec{i}_{\theta} \quad \ldots A4.8$$

APPENDIX 5

Consider the vector magnetic potential, $\vec{A}$, of a small loop of current, I, oriented as shown below. From symetry considerations

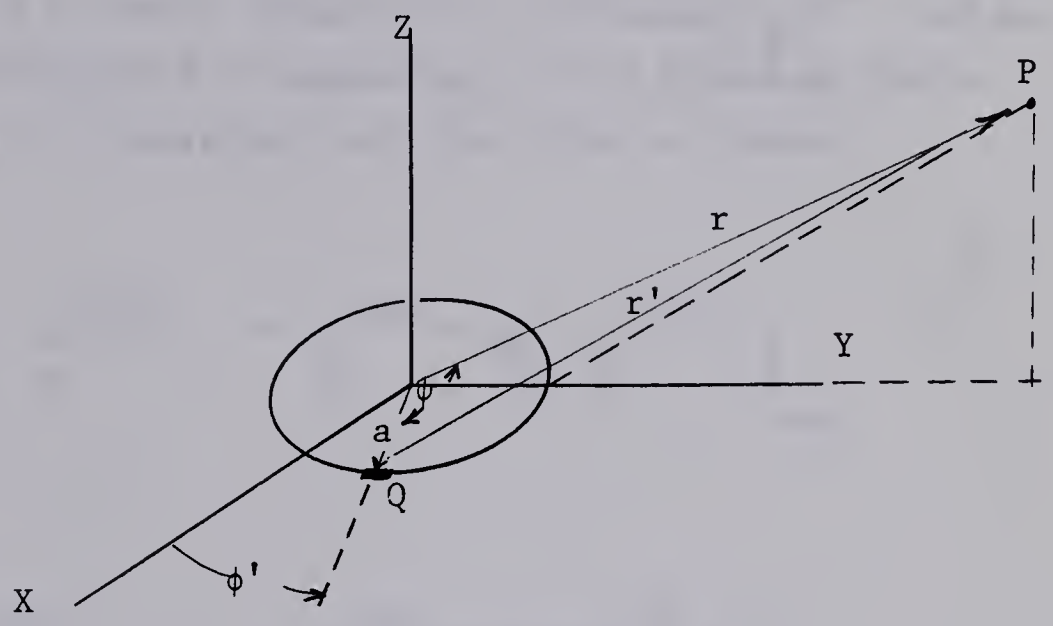

$\vec{A}$ has only an $\vec{i}_\phi$ component and is independent of the angle ϕ. Hence, for convenience, consider the vector potential at a point, P, in the z-y plane. The contribution to the $\vec{i}_\phi$ component by the current element at Q can be expressed as

$$dA_\phi = \mu\frac{Ia}{4\pi}\sin\phi' d\phi' \frac{e^{j(\omega t - kr')}}{r'} \qquad \ldots A5.1$$

from the well known vector potential of a small current element. Then,

$$A_\phi = \mu\frac{Ia}{4\pi}\int_0^{2\pi} \sin\phi' \frac{e^{j(\omega t - kr')}}{r'} d\phi' \qquad \ldots A5.2$$

However r' is a function of ϕ',

$$\begin{aligned} r' &= r^2 + a^2 - 2ra\cos\psi \\ &= r^2 + a^2 - 2ra\sin\theta\sin\phi' \end{aligned} \qquad \ldots A5.3$$

When a is small compared to a wavelength $\frac{e^{-jkr'}}{r'}$ can be adequately represented by expanding it in a McLaurens Series in a about a = 0, retaining only the first two terms,

$$\frac{e^{-jkr'}}{r'} = \frac{e^{-jkr}}{r} + a\frac{\partial}{\partial a}\left(\frac{e^{-jkr'}}{r'}\right)\Bigg|_{a=0} \qquad \ldots A5.4$$

But,

$$\frac{\partial}{\partial a}\left(\frac{e^{-jkr'}}{r'}\right)\Bigg|_{a=0} = e^{-jkr}\sin\theta\sin\phi'\left(\frac{jk}{r} + \frac{1}{r^2}\right) \qquad \ldots A5.5$$

Hence,

$$\frac{e^{-jkr'}}{r'} = \frac{e^{-jkr}}{r} + e^{-jkr}\sin\theta\sin\phi'\left(\frac{jk}{r} + \frac{1}{r^2}\right) \qquad \ldots A5.6$$

Therefore,

$$A_\phi = \frac{\mu Ia}{4\pi}\int_0^{2\pi}\sin\phi'\frac{e^{j(\omega t-kr)}}{r}d\phi' + \frac{\mu Ia}{4\pi}\int_0^{2\pi}a\sin\theta\sin^2\phi' e^{j(\omega t-kr)}\left(\frac{jk}{r}+\frac{1}{r^2}\right)d\phi'$$

and

$$A_\phi = \frac{\mu IS}{4\pi}\sin\theta\left(\frac{jk}{r} + \frac{1}{r^2}\right)e^{j(\omega t-kr)} \qquad \ldots A5.7$$

where $S = \pi a^2$.